Dissertation

Temperature dependent magnetic properties of thin films and bulk ferromagnets
An implementation of the Disordered Local Moment scheme

ausgeführt zum Zwecke der Erlangung des akademischen Grades eines

Doktors der technischen Wissenschaften

unter der Leitung von

Univ.-Prof. Dr. Peter Weinberger

Institutsnummer: E 134

Institut für Allgemeine Physik

eingereicht an der Technischen Universität Wien

Fakultät für Physik

von

Dipl.-Ing. Adam Buruzs

Matrikelnummer: E0527446

A-1200 Wien, Forsthaus gasse 2/2729

Wien, am 21. Mai 2008

Abstract

In the present work an implementation of the relativistic disordered local moment scheme (DLM) within the Screened Korringa-Kohn-Rostoker (KKR) Green's function formalism is presented. This approach is applicable to describe the magnetic properties of ferromagnetic metals and alloy systems at finite temperature. The screened KKR facilitates to treat half infinite systems, such as thin films.

As an application we present a method to calculate the temperature dependent magnetic anisotropy of magnetic thin films, and show an application to $Co_nCu(100)$ thin film structures. We interpret our ab initio results with the help of an anisotropic classical Heisenberg model.

To highlight the importance of a non-unitary Heisenberg exchange we investigate also the magnetic ordering of a Mn monolayer on W surface, and stress the relevance of the so-called Dzyaloshinskii-Moriya interactions.

In the third part of the thesis we apply the DLM formalism to calculate the magnetic part of the electric resistivities. We implement the DLM using the Kubo-Greenwood equation within the KKR framework. This work represents the very first ab initio approach in the literature of this field. As an application we show the results for bulk Fe and Co.

Contents

Chapter 1

Introduction

The history of magnetic data recording is started in 1956. Soon the annual growth rate (AGR) of the storage capacity of magnetic hard disks (HDD) reached the 30%, and lasted until 1992 when the introduction of magneto-resistive (MR) read heads increased the AGR to 60% [1]. The discovery of the giant magneto-resistance (GMR) by Grünberg [2] and Fert [3] rapidly became applied in the industry. The first GMR read heads appeared in 1997 on the market, which contributed to the further increase of the growth rate to 100% per year. Nowadays the magnetic storage density in HDD-s reach the 100 Gbit/inch^2, which is a development of eight order of magnitude, since the first disk drives of the mid 50s. In HDD magnetic recording films the bits are stored in magnetic grains, in which the magnetisation are parallel or perpendicular to the surface. During the shrinking of the bit size the diameter of the magnetic grains became smaller, therefore the total magnetic anisotropy, and the thermal stability decreased. Reaching the so-called superparamagnetic temperature the thermal excitations destroy the parallel alignment of the magnetic grains, i.e., the stored information get lost, however the the grains itself remain ferromagnetic. Nowadays the grain size in magnetic recording media goes under 10 nm. To avoid the superparamagnetic transition materials with large magnetic anisotropy should be used such as Co alloys (CoPtCr, Co, Co$_3$Pt), L1$_0$ ordered ferromagnets (FePd, FePt, CoPt, MnAl) [4]. Nowadays commercially available IBM HDD-s contain antiferromagnetically coupled (AFC) magnetic layers (CoPtCrB), which align parallel to the surface and separated by a $6\mathring{A}$ Ru layer [5]. The thermal stability in AFC HDD-s are provided by the antiferromagnetically coupled underlayer.

As the size of this magnetic structures goes into the nm range, (and they deserve

the denomination of nanostructures) the quantum mechanical effects became more and more important, and ab-inito description can be a promising tool for better understanding of the underlying physical phenomena, and an aid for designing new materials for these applications.

A new and promising method of magnetic storage is the so-called heat assisted magnetic recording [6] [7]. The further decrement of magnetic recording grain size with avoiding of the superparamagnetism can be performed with applying materials with large magnetic anisotropy. However the large anisotropy (large coercitive field) makes the media hard to write. The method of HAMR provide a solution with heating up the magnetic media with a laser beam, thus reducing the magnetic anisotropy just during the write process. The reduced anisotropy makes the writing easier, then after switching off the laser beam, the cooling back increase the anisotropy of the media, therefore stabilize the written bits.

At the beginning of the information technology only magnetic data storage existed, but from the late 1960s the semiconductor memory cells proved to be faster than the magnetic storage, therefore the Random Access Memories (RAM) were built from (field effect FET) transistors. However nowadays strong effort was laid in the development of magnetic RAMs (MRAM), a typical chapter of spintronics. The two main type of MRAM are the one containing magnetic tunnel junctions (MTJ) and the second is using the GMR effect. Both are novel in the way of storing the information in the conductance of parallel or antiparallel magnetized ferromagnetic layers, instead of the conventional semiconductor technologies, i.e. the information is stored in the spin-degree of freedom [8] (therefore this field of research got the denomination of spintronics instead electronics). The first prototypes of MRAM-s are already constructed by the companies IBM and Freescale [9]. The MRAM is a very promising non-volatile memory, which can overcome the existing RAM-s in operation speed and endurance[10].

The understanding of the physical basis of the magnetic data storage devices requires the theoretical description of magnetic anisotropy. The decreasing size of the magnetic data storage devices, and nanostructures makes the ab-initio description usefull for the understanding of the new phenomena in the low dimensional systems. In the CMS the screened Korringa-Kohn-Rostocker (SKKR) method [11] [12] was developed in the last decades, which was successfully applied to describe the

magnetic anisotropy of bulk alloyed magnets [12] [13], magnetic thin films [14] [15] multilayers [16] and with the embedded cluster method finite magnetic clusters [17] [18] [19] at zero temperature. As the magnetic hard disks usually operate on room temperature, and especially in the view of HAMR the theoretical description of the temperature dependent magnetic anisotropy is desirable. In the present dissertation I implemented the so called Disordered Local Moment (DLM) theory (originally proposed by B.L. Gyoörffy et.al.

[20]) to describe the temperature dependent magnetic anisotropy, and resistivity of ferromagnetic bulk materials and thin films. The paramagnetic version of the DLM was used to determine the magnetic properties (such as susceptibility, exchange coupling and Curie temperature) of the paramagnetic state (above the Curie temperature) of ferromagnetic materials [20] [21] [22] [23] [24] [25] . In the present work I implemented the DLM method for ferromagnets below the Curie temperature. I implemented the DLM within the screened-KKR formalism, which enabled the description of surface and thin-film magnetism. As the magneto-crystalline anisotropy is an effect of the spin-orbit interaction [26], in order to access the magnetic anisotropy I implemented the DLM within the relativistic version of the SKKR program.

As the common application of GMR effect in magnetic recording, and the possible application in MRAM-s clearly shows the technological importance of the magnetic resistivity. Better understanding of the magnetoresistive effect is possible with computer simulations. In the last decades in the CMS the linear response theory of Kubo was implemented into the KKR program package [27]. With this tool description of the magnetic resistivity of bulk alloys, thin magnetic films, multilayers spin valve structures became possible [28] [29] [30] and nanocontacts [31] became possible at zero temperature. The former ab initio calculations restricted to zero temperature, however at nonzero temperature new phenomena contribute considerably to the electrical resistivity such as phonon-electron scattering, and scattering of the electrons on magnetic excitations (magnon scattering). However theoretical descriptions are available for the temperature dependence of the magnetic part of the electrical resistivity [32] [33], the ab initio description was still missing. In the present dissertation I give the first attempt for the ab inito description of the temperature dependent magnetic resistivity, with the implementation of the DLM in

the KKR-Kubo formalism.

The thesis is organized such that first the theoretical description, in particular all new formulations are presented, and only then the actual results achieved in terms of these methods are shown. The chapter A deals with the DLM theory, the chapter 3 with the magnetic anisotropy. Chapter 4 is devoted to the application of the DLM to the problem of temperature dependence of electrical transport properties. We show the results of the calculations for the magnetic anisotropy in chapter 5. In Chapter 6 we investigate the effect of the so called Dzyaloshinskii Moriya interaction on the magnetic ordering of a magnetic monolayer. In the appendicies first short reviews of the density functional theory (DFT) A and the KKR scattering theory A are given. In Appendix B we give the derivation of the the special kind of coherent potential approximation (CPA), in Appendix C a derivation of the Onsager reaction field approximation, and finally in Appendix D we give the mean-field solution of the anisotropic Heisenberg model.

Chapter 2

The Disordered Local Moment (DLM) theory

2.1   General framework

The Spin Density Functional Theory (SDFT) (see Appendix A) is regarded to give adequate description of the magnetic ground state of itinerant solids. A straightforward generalization to higher temperatures [34], however fails considerably, giving large Curie temperature by a factor of five, zero magnetic moments and no Curie-Weiss law above the Curie temperature [35]. This model assumes that the magnetic moments point to the same direction at every lattice site, therefore at the Curie temperature the size of the moments disappear. In 1979 Hubbard and Hasegawa introduced [36, 37] a theory, where they allowed the magnetisation direction to vary from unit cell to unit cell. In this Disordered Local Moment (DLM) picture reaching the Curie temperature from below, the size of the magnetic moments avaraged over a unit cell (so called local moments) does not necessarly disappear, nonzero local moments can exist in the paramagnetic phase also, pointing to completely random direction, giving zero macroscopic magnetisation on the average (see Fig.2.1). In 1985 Györffy et. al. [20] published the details of an implementation of the DLM picture in the ab-initio KKR scattering theory (see Appendix A).

The DLM theory is based on the idea that in itinerant metallic magnets, we can find a certain time scale τ, which is small as compared to the characteristic time of spin fluctuations ($\tau_{\text{spinfluct}}$), but longer than the electron hopping times, i.e.,

$$\tau_{\text{hopping}} < \tau < \tau_{\text{spinfluct}} = \frac{1}{\omega_s},$$

where ω_s is the typical spin wave frequency. The typical order of magnitude is $\tau_{\text{hopping}} \sim 10^{-15}s$, and $\tau_{\text{spinfluct}} \sim 10^{-13}s$. Investigating a system on the time scale τ, the spin orientations of the electrons leaving an atomic site are sufficiently correlated with those arriving such that a nonzero magnetization exists when the appropriate quantity is averaged over this time window. If we define

$$\mathbf{M}_\tau(\mathbf{r}) = \frac{1}{\tau} \int_0^\tau \mathbf{M}(\mathbf{r}, t)\,\mathrm{dt}$$

as the average of the magnetizaton in the time window τ, we can define the local moment direction on a specific site by

$$\hat{e}_i = \frac{\int_{V_i} d^3\mathbf{r}\mathbf{M}_\tau(\mathbf{r})}{|\int_{V_i} d^3\mathbf{r}\mathbf{M}_\tau(\mathbf{r})|}, \tag{2.1}$$

where V_i is the volume of the i-th unit cell and

$$\mu_i = \left| \int_{V_i} d^3\mathbf{r}\mathbf{M}_\tau(\mathbf{r}) \right| \tag{2.2}$$

is the size of the local moment. Thus we can associate local moment directions (Eq.2.1) with every lattice site. These directions vary on the time scale $\tau_{spinfluct}$ that is slow compared to τ. DLM includes temperature dependence via the probability distribution of these local moment directions. At zero temperature all the local moments point to a specific direction, while increasing the temperature the local moments can point along other directions also with non-zero probability. Reaching the Curie temperature the local moments will point in any direction with the same probability such that the configurational average of the fluctuating local moments is zero, the total magnetisation disappears, even if the size of the local moments μ_i is non-zero.

The magnetic configuration of the system can be described by a set of $\hat{e}_i$ directions:

$$\{\hat{e}\} = \{\hat{e}_1, \hat{e}_2, \ldots, \hat{e}_N\} \quad , \tag{2.3}$$

where N is the number of sites. The fluctuation of the local moments can be described by a probability distribution, characterised by the probability density function $P^{(\hat{n})}(\{\hat{e}\})$, which depends on the average magnetisation direction $\hat{n}$, and the temperature. At zero temperature all the moments point along the same direction $P^{(\hat{n})}(\{\hat{e}\}) = \prod_i \delta(\hat{e}_i - \hat{n})$. At the Curie temperature this probability is constant
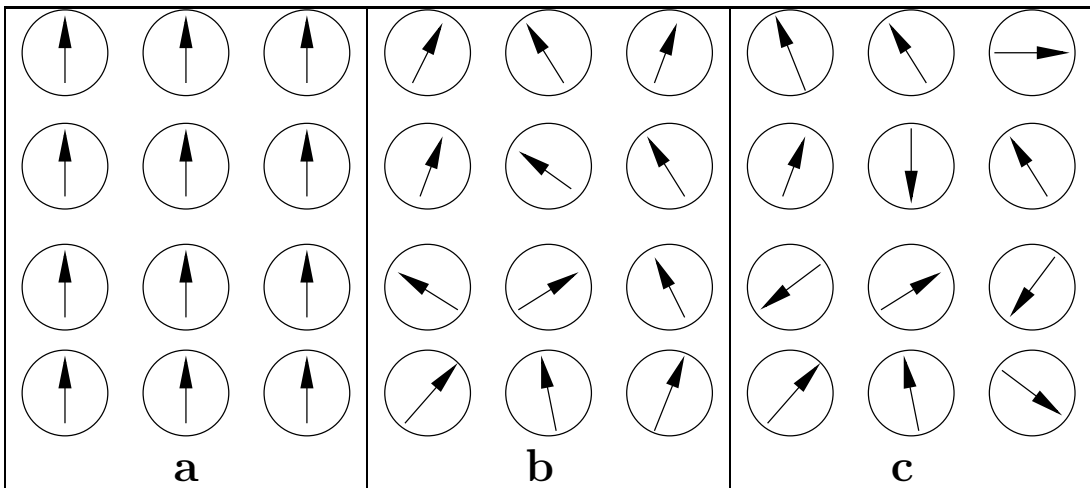
Figure 2.1: The DLM picture. a, $T = 0$ ferromagnetic state. b, A nonzero temperature ferromagnet $0 < T \leq T_C$. c, The paramagnetic state $T_C \leq T$, the average of the magnetic moments is zero.

to all directions: $P^{(\hat{n})}(\{\hat{e}\}) = \prod P(\hat{e}_i)$, with $P(\hat{e}_i) = \frac{1}{4\pi}$. The average of the $\hat{e}_i$ directions:

$$\langle \hat{e}_i \rangle = \int \ldots \int \hat{e}_i P^{(\hat{n})}(\{\hat{e}\}) \, d\hat{e}_1 \ldots d\hat{e}_N = \hat{n} \, |\langle \hat{e}_i \rangle| \, . \tag{2.4}$$

If the Hamiltonian function of the system is $H^{(\hat{n})}(\{\hat{e}\})$, the canonical partition function and the probability function are defined as

$$Z^{(\hat{n})} = \int \ldots \int e^{-\beta H^{(\hat{n})}(\{\hat{e}\})} \, d\hat{e}_1 \ldots d\hat{e}_N \quad , \tag{2.5}$$

and

$$P^{(\hat{n})}(\{\hat{e}\}) = \frac{e^{-\beta H^{(\hat{n})}(\{\hat{e}\})}}{Z^{(\hat{n})}} \quad . \tag{2.6}$$

The free-energy can then be expressed as

$$F^{(\hat{n})} = -\frac{1}{\beta} \ln Z^{(\hat{n})} \quad . \tag{2.7}$$

To calculate these quantities a tractable form of the Hamiltonian is needed. To approximate the energy the Peierls-Feynman [38] inequality can be applied, which states that taking an arbitrary trial Hamiltonian H_0 an upper bound to the system's free-energy can be given as

$$F \leq F_1 = F_0 + \langle H - H_0 \rangle^0 \quad . \tag{2.8}$$

where the free-energy of the trial system is given by

$$F_0 = -\frac{1}{\beta} \ln Z_0 \quad , \quad Z_0 = \int \ldots \int e^{-\beta H_0(\{\hat{e}\})} \, d\hat{e}_1 \ldots d\hat{e}_N.$$

and the $\langle\rangle^0$ denotes the average with respect the probability density

$$P_0\left(\{\hat{e}\}\right) = \frac{e^{-\beta H_0(\{\hat{e}\})}}{Z_0} \quad . \tag{2.9}$$

If we minimize F_1 with respect to the parameters of the trial Hamiltonian H_0, we get the variational upper bound (best approximation) for the free-energy. If we expand H_0 as a sum of terms containing different orders of local-moment interactions,

$$H_0^{(\hat{n})}\left(\{\hat{e}\}\right) = \sum_i h_i^{1^{(\hat{n})}}\left(\hat{e}_i\right) + \frac{1}{2}\sum_{i\neq j} h_{i,j}^{2^{(\hat{n})}}\left(\hat{e}_i, \hat{e}_j\right) + \ldots \quad , \tag{2.10}$$

the best trial free-energy can be obtained from the variational condition:

$$\frac{\delta F_1^{(\hat{n})}}{\delta h_i^{1^{(\hat{n})}}\left(\hat{e}_i\right)} = 0 \quad \frac{\delta F_1^{(\hat{n})}}{\delta h_i^{2^{(\hat{n})}}\left(\hat{e}_i, \hat{e}_j\right)} = 0 \quad \text{etc.}$$

Györffy et al. has showed [20], that this condition is equivalent to the following equalities

$$\left\langle H^{(\hat{n})} \right\rangle_{\hat{e}_i}^0 - \left\langle H^{(\hat{n})} \right\rangle^0 = \left\langle H_0^{(\hat{n})} \right\rangle_{\hat{e}_i}^0 - \left\langle H_0^{(\hat{n})} \right\rangle^0 \quad , \tag{2.11}$$

$$\left\langle H^{(\hat{n})} \right\rangle_{\hat{e}_i,\hat{e}_j}^0 - \left\langle H^{(\hat{n})} \right\rangle^0 = \left\langle H_0^{(\hat{n})} \right\rangle_{\hat{e}_i,\hat{e}_j}^0 - \left\langle H_0^{(\hat{n})} \right\rangle^0 \quad , \quad \text{etc.} \tag{2.12}$$

where $\langle\ \rangle_{\hat{e}_i}$ or $\langle\ \rangle_{\hat{e}_i,\hat{e}_j}$ denote restricted statistical averages with $\hat{e}_i$ or $\hat{e}_i$ and $\hat{e}_j$ kept fixed. For example,

$$\left\langle X^{(\hat{n})} \right\rangle_{\hat{e}_i}^0 = \frac{\int \ldots \int X^{(\hat{n})}\left(\{\hat{e}\}\right) P_0^{(\hat{n})}\left(\{\hat{e}\}\right)\, d\hat{e}_1 \ldots d\hat{e}_{i-1} d\hat{e}_{i+1} \ldots d\hat{e}_N}{P_i^{(\hat{n})}\left(\hat{e}_i\right)}, \tag{2.13}$$

with

$$P_i^{(\hat{n})}\left(\hat{e}_i\right) = \int \ldots \int P_0^{(\hat{n})}\left(\{\hat{e}\}\right)\, d\hat{e}_1 \ldots d\hat{e}_{i-1} d\hat{e}_{i+1} \ldots d\hat{e}_N \quad . \tag{2.14}$$

Obviously with this definition the relationship,

$$\left\langle X^{(\hat{n})} \right\rangle^0 = \int \left\langle X^{(\hat{n})} \right\rangle_{\hat{e}_i} P_i^{(\hat{n})}\left(\hat{e}_i\right) d\hat{e}_i \quad , \tag{2.15}$$

is then satisfied.

2.2 Mean-field theory

In the mean field approximation we terminate the expansion Eq.(2.10) using only the first term:

$$H_0^{(\hat{n})}\left(\{\hat{e}\}\right) = \sum_i h_i^{(\hat{n})}\left(\hat{e}_i\right) \quad . \tag{2.16}$$

which means that we neglect all correlations between neighbouring sites. Therefore the partition function and the configuration probability split up into product of single site terms, implying that the orientations of local moments on the different sites are statistically independent:

$$Z_0^{(\hat{n})} = \int \ldots \int \prod_i e^{-\beta h_i^{(\hat{n})}(\hat{e}_i)} \, d\hat{e}_1 \ldots d\hat{e}_N \quad = \prod_i Z_i^{(\hat{n})} \quad , \quad Z_i^{(\hat{n})} = \int e^{-\beta h_i^{(\hat{n})}(\hat{e}_i)} \, d\hat{e}_i \quad ,$$
(2.17)

$$P_0^{(\hat{n})}(\{\hat{e}\}) = \prod_i P_i^{(\hat{n})}(\hat{e}_i) \quad , \quad P_i^{(\hat{n})}(\hat{e}_i) = \frac{e^{-\beta h_i^{(\hat{n})}(\hat{e}_i)}}{Z_i^{(\hat{n})}} \quad ,$$
(2.18)

and

$$F_0^{(\hat{n})} = -\frac{1}{\beta} \sum_i \ln Z_i^{(\hat{n})} \quad .$$
(2.19)

In order to employ condition (2.11) the following averages have to be evaluated,

$$\left\langle H_0^{(\hat{n})} \right\rangle^0 = \sum_i \prod_j \int h_i^{(\hat{n})}(\hat{e}_i) \, P_j^{(\hat{n})}(\hat{e}_j) \, d\hat{e}_j = \sum_i \int h_i^{(\hat{n})}(\hat{e}_i) \, P_i^{(\hat{n})}(\hat{e}_i) \, d\hat{e}_i \quad , \quad$$
(2.20)

$$\left\langle H_0^{(\hat{n})} \right\rangle_{\hat{e}_i}^0 = h_i^{(\hat{n})}(\hat{e}_i) + \sum_{j \neq i} \int h_j^{(\hat{n})}(\hat{e}_j) \, P_j^{(\hat{n})}(\hat{e}_j) \, d\hat{e}_j \quad ,$$
(2.21)

and consequently,

$$\left\langle H_0^{(\hat{n})} \right\rangle_{\hat{e}_i}^0 - \left\langle H_0^{(\hat{n})} \right\rangle^0 = h_i^{(\hat{n})}(\hat{e}_i) - \int h_i^{(\hat{n})}(\hat{e}_i') \, P_i^{(\hat{n})}(\hat{e}_i') \, d\hat{e}_i' \quad = h_i^{(\hat{n})}(\hat{e}_i) - \left\langle h_i^{(\hat{n})} \right\rangle \quad ,$$
(2.22)

while according to Eq.(2.15)

$$\left\langle H^{(\hat{n})} \right\rangle_{\hat{e}_i}^0 - \left\langle H^{(\hat{n})} \right\rangle^0 = \left\langle H^{(\hat{n})} \right\rangle_{\hat{e}_i}^0 - \int \left\langle H^{(\hat{n})} \right\rangle_{\hat{e}_i'}^0 P_i^{(\hat{n})}(\hat{e}_i') \, d\hat{e}_i' \quad .$$
(2.23)

Eq. (2.11) then implies, that

$$h_i^{(\hat{n})}(\hat{e}_i) - \left\langle H^{(\hat{n})} \right\rangle_{\hat{e}_i}^0 = \int \left(h_i^{(\hat{n})}(\hat{e}_i') - \left\langle H^{(\hat{n})} \right\rangle_{\hat{e}_i'}^0 \right) P_i^{(\hat{n})}(\hat{e}_i') \, d\hat{e}_i' = const. \quad .$$
(2.24)

Thus by adding appropriate constants to the mean-field Hamiltonians, $h_i^{(\hat{n})}(\hat{e}_i)$, which does not affect the probability, $P_i^{(\hat{n})}(\hat{e}_i)$, the below relationship can be obtained

$$h_i^{(\hat{n})}(\hat{e}_i) = \left\langle H^{(\hat{n})} \right\rangle_{\hat{e}_i}^0 \quad .$$
(2.25)

In what follows we shall omit the superscript 0 from the averages.

As a first order approximation we express the trial single site Hamiltonian as

$$h_i^{(\hat{n})}\left(\hat{e}_i\right) = \vec{h}_i^{(\hat{n})} \cdot \hat{e}_i \quad , \tag{2.26}$$

with the Weiss-fields $\vec{h}_i^{(\hat{n})}$. Multiplying Eq. (2.26) with $\hat{e}_i$ from the left and integrating over the unit sphere using

$$\int \hat{e}_i \otimes \hat{e}_i d\hat{e}_i = \frac{4\pi}{3}I_3$$

we get:

$$\vec{h}_i^{(\hat{n})} = \frac{3}{4\pi} \int d\hat{e}_i \, \hat{e}_i \left\langle H^{(\hat{n})}\right\rangle_{\hat{e}_i} \quad . \tag{2.27}$$

The single site partition function is therefore given by

$$Z_i^{(\hat{n})} = \int d\hat{e}_i \exp\left(-\beta \hat{h}_i^{(\hat{n})}\left(\hat{e}_i\right)\right) = \frac{4\pi}{\beta h_i^{(\hat{n})}} \sinh \beta h_i^{(\hat{n})}, \tag{2.28}$$

where $h_i^{(\hat{n})}$ is the magnitude of the Weiss field. In this way the probabilty function Eq. (2.18) reads as

$$P_i^{(\hat{n})}\left(\hat{e}_i\right) = \frac{\beta h_i^{(\hat{n})}}{4\pi \sinh \beta h_i^{(\hat{n})}} \exp\left(-\beta \vec{h}_i^{(\hat{n})} \cdot \hat{e}_i\right) \quad . \tag{2.29}$$

The average of the local moment direction (which we call later magnetisation) is then given by

$$\vec{m}_i^{(\hat{n})} = \langle \hat{e}_i \rangle = \frac{1}{Z_i^{(\hat{n})}} \int \hat{e}_i \exp\left(-\beta \vec{h}_i^{(\hat{n})} \cdot \hat{e}_i\right) d\hat{e}_i \tag{2.30}$$

Here we shouldn't forget, that the local moment has a length μ_i which we consider to be independent from $\hat{e}_i$. This magnetisation, which varies from 0 to 1 describes just the temperature dependent fluctuations of the magnetic moment, which is

$$\vec{M}_i = \vec{m}_i \mu_i. \tag{2.31}$$

From Eq.(2.30) and Eq.(2.26) we get

$$\vec{m}_i^{(\hat{n})} = -L\left(\beta h_i^{(\hat{n})}\right) \hat{h}_i^{(\hat{n})}, \tag{2.32}$$

where L is the Langevin function $L(x) = \frac{1}{x} - \coth(x)$ and $\hat{h}_i^{(\hat{n})}$ is a unit vector pointing in the direction of the Weiss field. The Weiss field points therefore in the direction of the average magnetisation, $\hat{n} = \hat{h}_i^{(\hat{n})}$, i.e. $\vec{h}_i^{(\hat{n})} = h_i^{(\hat{n})}\, \hat{n}$, such that the magnitude of the Weiss field is given by

$$h_i^{(\hat{n})} = \frac{3}{4\pi} \int (\hat{e}_i \cdot \hat{n}) \left\langle H^{(\hat{n})}\right\rangle_{\hat{e}_i} d\hat{e}_i \quad . \tag{2.33}$$

2.3   The coherent potential approximation (CPA)

We used the Korringa-Kohn-Rostoker (KKR) Green's function method to calculate the Weiss-field on an ab initio level. In the KKR formalism the key quantity is the scattering path operator (SPO denoted by τ) (see Appendix A).

The commonly used method for evaluating restricted averages in the KKR method is the coherent potential approximation (CPA) (see Appendix B). Within the *single-site CPA* an effective (coherent), i.e., translational invariant medium is specified by the t-matrices, $\underline{t}_{i,c}^{(\hat{n})}$, that satisfy the CPA condition (Eq. B.9) ,

$$\left\langle \underline{\tau}_{ii}^{(\hat{n})}\left(\{\hat{e}\}\right)\right\rangle = \int \left\langle \underline{\tau}_{ii}^{(\hat{n})}\right\rangle_{\hat{e}_i} P_i^{(\hat{n})}\left(\hat{e}_i\right) d\hat{e}_i = \underline{\tau}_{ii,c}^{(\hat{n})} \quad , \tag{2.34}$$

where the index c refers to the coherent medium, and the site-diagonal matrices of the scattering path operator (SPO denoted by $\underline{\tau}$) are defined as,

$$\left\langle \underline{\tau}_{ii}^{(\hat{n})}\right\rangle_{\hat{e}_i} = \underline{\tau}_{ii,c}^{(\hat{n})}\underline{D}_i^{(\hat{n})}\left(\hat{e}_i\right) \quad , \tag{2.35}$$

with

$$\underline{D}_i^{(\hat{n})}\left(\hat{e}_i\right) = \left[\underline{I} + \left(\underline{m}_i\left(\hat{e}_i\right) - \underline{m}_{i,c}^{(\hat{n})}\right)\underline{\tau}_{ii,c}^{(\hat{n})}\right]^{-1} \quad , \tag{2.36}$$

with $\underline{m}_i\left(\hat{e}_i\right) = \underline{t}_i^{-1}\left(\hat{e}_i\right)$ being the inverse single-site scattering matrix. The coherent SPO is defined as

$$\underline{\underline{\tau}}_c^{(\hat{n})} = \left(\underline{\underline{m}}_c^{(\hat{n})} - \underline{\underline{G}}_0\right)^{-1} \quad . \tag{2.37}$$

In the above equation, double underlines denote matrices in site-angular momentum space, $\underline{\underline{m}}_c^{(\hat{n})}$ is diagonal in site indices, while $\underline{\underline{G}}_0$ stands for the matrix of structure constants (for further details see Appendix A).

By using spherical symmetric potentials , i.e., within the atomic sphere approximation (ASA) for evaluating the $\underline{t}_i\left(\hat{e}_i\right)$ matrices, we can use the similarity transformation of the *single-site t-matrices*,

$$\underline{t}_i\left(\hat{e}_i\right) = \underline{R}\left(\hat{e}_i\right) \underline{t}_i\left(\hat{z}\right) \underline{R}\left(\hat{e}_i\right)^+ \quad , \tag{2.38}$$

where for a given energy (not labeled explicitly) $\underline{t}_i\left(\hat{z}\right)$ stands for the t-matrix with an effective magnetic field pointing along the local z axis and $\underline{R}\left(\hat{e}_i\right)$ is a unitary representation of that $O\left(3\right)$ transformation which rotates the z axis along $\hat{e}_i$. From here, the $\underline{m}_i\left(\hat{e}_i\right)$ matrices can be get by inversion.

The CPA condition Eq. (2.34) can now be rewritten as

$$\int \underline{D}_i^{(\hat{n})}(\hat{e}_i) P_i^{(\hat{n})}(\hat{e}_i) d\hat{e}_i = \underline{1} \quad, \tag{2.39}$$

or by introducing the excess scattering matrices,

$$\underline{X}_i^{(\hat{n})}(\hat{e}_i) = \left[\left(\underline{m}_{i,c}^{(\hat{n})} - \underline{m}_i(\hat{e}_i)\right)^{-1} - \underline{\tau}_{ii,c}^{(\hat{n})}\right]^{-1} = \left(\underline{D}_i^{(\hat{n})}(\hat{e}_i) - \underline{I}\right)\left(\underline{\tau}_{ii,c}^{(\hat{n})}\right)^{-1}, \tag{2.40}$$

as

$$\int \underline{X}_i^{(\hat{n})}(\hat{e}_i) P_i^{(\hat{n})}(\hat{e}_i) d\hat{e}_i = \underline{0} \quad. \tag{2.41}$$

The calculation of the coherent $\underline{t}_{i,c}^{(\hat{n})}$ matrices in the above equation has to be solved self consistently. Starting from a first guess for $\underline{t}_{i,c}^{(\hat{n})}$ the $\underline{\tau}_{ii,c}^{(\hat{n})}$ matrix can be calculated from Eq.(2.37), then the $\underline{X}_i^{(\hat{n})}(\hat{e}_i)$ matrix can be constructed from Eq.(2.40). Using the condition Eq.(2.41) a new guess for the $\underline{t}_{i,c}^{(\hat{n})}$ matrix can be given as proposed by Ginatempo and Staunton [39] [40].

2.4 Paramagnetic DLM

In the nonrelativistic version of the DLM, in the paramagnetic phase, above the Curie temperature, where the probability function of the local moment (Eq.2.29) is simply $1/4\pi$, the CPA condition (Eq.2.39) gets a particularly simple form [20]. In this case the local moment direction dependence of the inverse $t-$matrix is given by [20]

$$t_i^{-1}(\hat{e}_i) = \frac{1}{2}(t_{i+}^{-1} + t_{i-}^{-1})\mathbf{1} + \frac{1}{2}(t_{i+}^{-1} - t_{i-}^{-1})\hat{\sigma}\hat{e}_i, \tag{2.42}$$

instead of Eq.2.39, where t_{i+} and t_{i-} is the scattering $t-$matrix with the local moment pointing in the $\hat{z}$ or $-\hat{z}$ direction respectively, $\hat{\sigma}$ is the vector of the Pauli spin matrices (Eq.A.16) . The D - matrix in Eq.2.39 also can be expressed as

$$D_i(\hat{e}_i) = \frac{1}{2}(D_{i+} + D_{i-})\mathbf{1} + \frac{1}{2}(D_{i+} - D_{i-})\hat{\sigma}\hat{e}_i \tag{2.43}$$

where

$$D_{i\pm} = \left[1 + (t_{i\pm}^{-1} + t_c^{-1})\tau_{c,\text{ii}}\right]^{-1}. \tag{2.44}$$

Calculating the integral in Eq.(2.39) with the paramagnetic probability density function $P(\hat{e}_i) = 1/4\pi$, the term containing $\hat{e}_i$ in Eq.(2.43) gives zero on average, and we get

$$\int D_i(\hat{e}_i)\frac{1}{4\pi}d\hat{e}_i = \frac{1}{2}(D_{i+} + D_{i-}) = 1 \quad, \tag{2.45}$$

i.e. the solution of the DLM-CPA can be interpreted as a CPA for a two component alloy, where 50% of the atoms have an up-spin (+), and 50% down-spin (-). This version of the DLM was commonly used in the literaure to describe the paramagnetic state. The Kohn-Sham potential can easily be calculated self-consistently in this paramagnetic state. Györffy and Staunton et.al. used this DLM scheme to calculate the paramagnetic susceptibilty of Fe and Ni [20] [21]. Later this method was extended to layered structures, and it was used to investigate the Curie temperatures of fcc Fe / Cu(100) and Co / Cu(100) such as bcc Fe /W(100) thin films, and also the influence of a Cu cap layer on the oscillations of the Curie temperature in case of Fe / Cu(100) films was explained [22] [23] [24]. Szunyogh and Udvardi calculated the exchange parameters of the Heisenberg model in the paramagnetic DLM state for Fe, Co and Ni overlayers on Cu(100) substrate [25]. They calculated the Curie temperatures from these paramagnetic exchange parameters by using a mean-field approach.

2.5 Calculation of the Weiss-field

In Section (3.1) we will see that in the spirit of the so-called *magnetic force theorem* it is enough to consider only the single–particle energy (band energy) part of the LSDA total energy, to describe magnetic anisotropy.

$$\Omega^{(\hat{n})}\left(\{\hat{e}\}\right) = -\int d\varepsilon f\left(\varepsilon, \mu\right) N(\varepsilon, \{\hat{e}\}) \tag{2.46}$$

where μ is the chemical potential, $f\left(\varepsilon, \mu\right)$ is the Fermi function, $n(\varepsilon)$ is the density of states (DOS), and $N(\varepsilon) = \int_{-\infty}^{\varepsilon} n(\varepsilon')d\varepsilon'$ is the integrated density of states. The Lloyd formula [41] provides an explicit expression for $N^{(\hat{n})}\left(\varepsilon, \{\hat{e}\}\right)$,

$$N^{(\hat{n})}\left(\varepsilon; \{\hat{e}\}\right) = N_0\left(\varepsilon\right) - \frac{1}{\pi}\text{Im}\,\text{lndet}\left(\underline{\underline{t}}^{(\hat{n})}\left(\varepsilon; \{\hat{e}\}\right)^{-1} - \underline{\underline{G}}_0\left(\varepsilon\right)\right), \tag{2.47}$$

with $N_0\left(\varepsilon\right)$ being the integrated DOS of the free particles and $\underline{t}^{(\hat{n})}$ the site-diagonal single-site scattering matrix. Reformulating the argument on the rhs. as

$$\underline{\underline{t}}^{(\hat{n})}\left(\varepsilon; \{\hat{e}\}\right)^{-1} - \underline{\underline{G}}_0\left(\varepsilon\right) = \left(\underline{\underline{t}}_c^{(\hat{n})}\left(\varepsilon\right)^{-1} - \underline{\underline{G}}_0\left(\varepsilon\right)\right)\left(\left(\underline{\underline{I}} - \underline{\underline{\tau}}_c^{(\hat{n})}\left(\varepsilon\right)\left(\underline{\underline{t}}_c^{(\hat{n})}\left(\varepsilon\right)^{-1} - \underline{\underline{t}}^{(\hat{n})}\left(\varepsilon, \{\hat{e}\}\right)^{-1}\right)\right)\right), \tag{2.48}$$

The integrated density of states can be written as

$$N^{(\hat{n})}\left(\varepsilon; \{\hat{e}\}\right) = N_0\left(\varepsilon\right) + N_c^{(\hat{n})}\left(\varepsilon\right) + \Delta N^{(\hat{n})}\left(\varepsilon, \{\hat{e}\}\right), \tag{2.49}$$

17

where

$$N_c^{(\hat{n})}(\varepsilon) = -\frac{1}{\pi}\mathrm{Im}\,\mathrm{lndet}\,\underline{\underline{\tau}}_c^{(\hat{n})}(\varepsilon) = +\frac{1}{\pi}\mathrm{Im}\,\mathrm{lndet}\left(\underline{\underline{t}}_c^{(\hat{n})}(\varepsilon)^{-1} - \underline{G}_0(\varepsilon)\right)\quad. \qquad (2.50)$$

Furthermore splitting $\underline{\underline{\tau}}_c^{(c)}(\varepsilon)$ matrix into a diagonal and an off-diagonal part $\Delta N = \Delta N_1 + \Delta N_2$ where

$$\Delta N_1 = -\frac{1}{\pi}\sum_i \mathrm{Im}\,\mathrm{lndet}\,\underline{D}_i^{(\hat{n})}(\varepsilon;\hat{e}_i)\,, \qquad (2.51)$$

and

$$\Delta N_2 = -\frac{1}{\pi}\mathrm{Im}\,\mathrm{lndet}\left(\underline{\underline{I}} - \underline{\underline{X}}^{(\hat{n})}(\varepsilon,\{\hat{e}\})\,\underline{\underline{\tau}}_c^{o(\hat{n})}(\varepsilon)\right), \qquad (2.52)$$

and the excess scattering matrices in Eq.(2.52), defined in Eq.(2.40)

$$\underline{\underline{X}}^{(\hat{n})}(\varepsilon;\{\xi\},\{\hat{e}\}) = \left\{\underline{X}_i^{(\hat{n})}(\varepsilon;\hat{e}_i)\;\delta_{ij}\right\}.$$

The ΔN_2 term is neglected in the single-site CPA, because expanding the ln function in Eq.2.52, and taking the ensemble averages, only fourth and higher order terms remain for $\underline{X}_i^{(\hat{n})}$. The restricted average of the grand potential therefore given by

$$\left\langle\Omega^{(\hat{n})}\right\rangle_{\hat{e}_i} = \Omega_0 + \frac{1}{\pi}\mathrm{Im}\int d\varepsilon\,f\left(\varepsilon;\mu^{(\hat{n})}\right)\left(\mathrm{lndet}\,\underline{\underline{\tau}}_c^{(\hat{n})}(\varepsilon) - \mathrm{lndet}\,\underline{D}_i^{(\hat{n})}(\varepsilon;\hat{e}_i) - \quad (2.53)\right.$$

$$\left.\left\langle\sum_{j\neq i}\mathrm{lndet}\,\underline{D}_j^{(\hat{n})}(\varepsilon;\hat{e}_j)\right\rangle\right).$$

and from Eq.(2.33) we get for the Weiss-field:

$$h_i^{(\hat{n})} = -\frac{3}{4\pi^2}\mathrm{Im}\int d\varepsilon\,f\left(\varepsilon;\mu^{(\hat{n})}\right)\left[\int d\hat{e}_i\;(\hat{e}_i\cdot\hat{n})\,\mathrm{lndet}\,\underline{D}_i^{(\hat{n})}(\varepsilon;\hat{e}_i)\right]\quad. \qquad (2.54)$$

2.5.1 Alternative Weiss-field formula

We can also give an alternative formula for the Weiss-field, which is slightly easier to evaluate. Its derivation starts from the assumption, that for a uniaxial ferromagnetic system the orientational dependence of the energy of an impurity at site i, Eq. (2.53), can be written up to second order in $\hat{e}_i = (\sin\vartheta_i\cos\varphi_i, \sin\vartheta_i\sin\varphi_i, \cos\vartheta_i)$ as

$$\left\langle\Omega^{(\hat{n})}\right\rangle_{\hat{e}_i} = \Omega_0 + \Omega^{(\hat{n})} + h_i^{(\hat{n})}\hat{n}\cdot\hat{e}_i + k_{2,i}\cos^2\vartheta_i\quad, \qquad (2.55)$$

with $k_{2,i}$ being the on site anisotropy energy. Choosing the local moment tot to pointing along the $\hat{x}$ axis ($\hat{e}_i = (1,0,0)$), we get:

$$h_i^{(\hat{z})} = -\frac{1}{n_z}\frac{\partial\left\langle\Omega^{(\hat{z})}\right\rangle_{\hat{e}_i=\hat{x}}}{\partial\vartheta_i}. \qquad (2.56)$$

We can now evaluate the derivative of the restricted grand potential using Eq. (2.53),

$$\frac{\partial \left\langle \Omega^{(\hat{n})} \right\rangle_{\hat{e}_i}}{\partial \vartheta_i} = -\frac{1}{\pi} \mathrm{Im} \int d\varepsilon \, f\left(\varepsilon; \mu^{(\hat{n})}\right) \frac{\partial}{\partial \vartheta_i} \mathrm{Tr} \ln \left[\underline{I} + \left(\underline{m}_i \left(\hat{e}_i\right) - \underline{m}_i^{(\hat{n})} \right) \underline{\tau}_{ii,c}^{(\hat{n})} \right] \quad . \quad (2.57)$$

Calculating finally the derivative with respect to the local moment directions, by taking a variation with respect to $\underline{m}_i$, we obtain:

$$\frac{\partial}{\partial \vartheta_i} \mathrm{Tr} \ln \left[\underline{I} + \left(\underline{m}_i \left(\hat{e}_i\right) - \underline{m}_{i,c}^{(\hat{n})} \right) \underline{\tau}_{ii,c}^{(\hat{n})} \right] = -\mathrm{Tr} \left[\frac{\partial \underline{m}_i \left(\hat{e}_i\right)}{\partial \vartheta_i} \underline{\tau}_{ii,c}^{(\hat{n})} \underline{D}_i^{(\hat{n})} \left(\hat{e}_i\right) \right] \quad .$$

The derivative of the Grand potential is therefore given by

$$\frac{\partial \left\langle \Omega^{(\hat{n})} \right\rangle_{\hat{e}_i}}{\partial \vartheta_i} = \frac{1}{\pi} \mathrm{Im} \int d\varepsilon \, f\left(\varepsilon; \mu^{(\hat{n})}\right) \mathrm{Tr} \left[\frac{\partial \underline{m}_i \left(\hat{e}_i\right)}{\partial \vartheta_i} \underline{\tau}_{ii,c}^{(\hat{n})} \underline{D}_i^{(\hat{n})} \left(\hat{e}_i\right) \right] . \quad (2.58)$$

That has to be substituted into Eq.2.56. The derivatives of $\underline{m}_i \left(\hat{e}_i\right)$ can be calculated as described in ref.[42].

2.5.2 Layered systems

In layered systems (surfaces, interfaces, layered bulk materials), translational invariance is present only in 2 dimensions. An effective way of calculating the Green's function in layered systems is the Screened KKR method, which is described in Appendix (A). In this case the physical quantities are 2 dimensional translational invariant, so the dimension of the corresponding matrices reduces, and we can use the layer indices (denoted with p, q) instead of site indices. The layer (p) dependent Weiss-field is defined as

$$h_p^{(\hat{n})} = -\frac{3}{4\pi^2} \mathrm{Im} \int d\varepsilon \, f\left(\varepsilon; \mu^{(\hat{n})}\right) \left[\int d\hat{e}_{\mathrm{pi}} \, \left(\hat{e}_{\mathrm{pi}} \cdot \hat{n}\right) \mathrm{lndet} \, \underline{D}_p^{(\hat{n})} \left(\varepsilon; \hat{e}_{\mathrm{pi}}\right) \right] \quad , \quad (2.59)$$

where similarly to the former definition

$$\underline{D}_p^{(\hat{n})} \left(\varepsilon; \hat{e}_{\mathrm{pi}}\right) = \left[\underline{I} + \left(\underline{t}_p \left(\varepsilon; \hat{e}_{\mathrm{pi}}\right)^{-1} - \underline{t}_p^{c(\hat{n})}(\varepsilon)^{-1} \right) \underline{\tau}_{\mathrm{p0},p0}^{c(\hat{n})}(\varepsilon) \right]^{-1} \quad . \quad (2.60)$$

Chapter 3

Magnetic Anisotropy

The nonrelativistic quantum mechanics leads to a description of the ferromagnetism in which the free energy of the system is independent of the direction of the magnetisation. This is contradiction with the experience, which tells us that the magnetisation generally lies in some preferred directions with respect to the crystalline axes and/or external shape of the body: this property is known as the magnetic anisotropy.

In crystallic solids the lattice symmetry splits the degeneracy of atomic orbitals, a phenomenon which is called as the crystal field effect. Through the spin-orbit interaction this anisotropy also transfered to the magnetic moments, creating preferred directions for the magnetisation in a bulk crystal. This effect is called magneto-crystalline anisotropy. It's worth to mention, that neglecting the spin-orbit interaction, the crystal symmetry, and the magnetisation is not coupled, i.e. no magnetocrystalline anisotropy occurs. In finite pieces of ferromagnetic materials having less than spherical symmetry, the shape of the sample can also produce anisotropy through the magnetic dipole-dipole interaction. This phenomenon is called the shape anisotropy. (The magneto-crystalline and shape anisotropy together is referred to as the magnetic anisotropy).

The Magnetic Anisotropy Energy (MAE) is defined as the difference between the ground state energy of two different orientation of the spontaneous magnetisation $\hat{M}^0$

$$\text{MAE} = E(\hat{M}_1^0) - E(\hat{M}_2^0). \tag{3.1}$$

Due to the time reversal symmetry the free energy has to be invariant under the inversion of the magnetisation direction ($\hat{M}^0 \rightarrow -\hat{M}^0$). Therefore if we expand

the free energy in terms of the components of $\hat{M}^0 = (\alpha_1, \alpha_2, \alpha_3)$ only even powers of the components occur:

$$F(\hat{M}^0) = K_0 + \sum_{i,j} k_{ij}\alpha_i\alpha_j + \sum_{i,j,k,l} k_{ijkl}\alpha_i\alpha_j\alpha_k\alpha_l + \dots \qquad (3.2)$$

Furthermore the symmetry of the crystallic system imply some further restrictions for the form of $F(\alpha_1, \alpha_2, \alpha_3)$, and reduce the number of independent parameters. For cubic system the free energy can be written as

$$F(\hat{M}^0) = K_0 + K_1(\alpha_1^2\alpha_2^2 + \alpha_2^2\alpha_3^2 + \alpha_3^2\alpha_1^2) + K_2\alpha_1^2\alpha_2^2\alpha_3^2 + \dots, \qquad (3.3)$$

where K_1 and K_2 are the so-called fourth and sixth order anisotropy constants, respectively. Expressing the components of the magnetisation with polar-coordinates $\alpha_1 = \sin\vartheta\sin\varphi$, $\alpha_2 = \sin\vartheta\cos\varphi$ and $\alpha_3 = \cos\vartheta$ we get

$$F(\hat{M}^0) = K_0 + K_1(\sin^4\vartheta\sin^2 2\varphi + \sin^2 2\vartheta). \qquad (3.4)$$

Uniaxial systems (such as surfaces or thin films) have lower symmetry, and therefore lower order terms appear in the free energy. E.g. for uniaxial systems with fourfold rotational symmetry around the z axis the expansion will be

$$F(\hat{M}^0) = K_0 + K_1(\alpha_1^2 + \alpha_2^2) + K_2(\alpha_1^2 + \alpha_2^2)^2 + K_2'\alpha_1^2\alpha_2^2 + \dots \qquad (3.5)$$

or in terms of the spherical coordinates (ϑ, φ) $\alpha_1 = \sin\vartheta\cos\varphi$, $\alpha_2 = \sin\vartheta\sin\varphi$

$$F(\vartheta, \varphi) = K_0 + K_1\sin^2\vartheta + K_2\sin^4\vartheta + \frac{1}{4}K_2'\sin^4\vartheta\sin^2(2\varphi). \qquad (3.6)$$

Where now K_1 second order, K_2 and K_2' fourth order anisotropy parameters.

3.1   Magnetic Force Theorem

The typical order of magnitude of the total energy per atom is 10^4 eV. The order of MAE is about 10^{-6} eV/atom for bulk ferromagnets, and 10^{-4} eV / atom for interfaces. Therefore a numerical accuracy of about $10^{-11} - 10^{-8}$ is needed when one wants to calculate the MAE from the total energy, which is a very demanding task. The idea, which helps to overcome this difficulty is the Magnetic Force Theorem, which states that the anisotropy energy can be obtained as the difference between

sums of the eigenvalues of the Dirac equation for different magnetic configurations, which are just order of 10 eV. This method requires much less computational effort for the same numerical accuracy.

Assuming that the direction of the spin moment density is $\hat{M}_0$ the total energy functional within the LSDA can be written as

$$E[n(\mathbf{r}), m(\mathbf{r}), \hat{M}_0] = T^s[n(\mathbf{r}), m(\mathbf{r}), \hat{M}_0] + E_H[n(\mathbf{r})] +$$
$$E_{\mathrm{xc}}[n(\mathbf{r}), m(\mathbf{r})] + \int v_{\mathrm{ext}}(\mathbf{r})n(\mathbf{r})d^3\mathbf{r}.$$

In the ground state the variaton of the energy functional vanishes with respect to the charge and magnetisation density:

$$\frac{\delta E}{\delta n} = \frac{\delta T^s}{\delta n} + \frac{\delta E_H}{\delta n} + \frac{\delta E_{\mathrm{xc}}}{\delta n} + v_{\mathrm{ext}} = 0, \tag{3.7}$$

$$\frac{\delta E}{\delta m} = \frac{\delta T^s}{\delta m} + \frac{\delta E_{\mathrm{xc}}}{\delta m} = 0, \tag{3.8}$$

such that the total variation of the energy in the ground state can be expressed as

$$\Delta E = \frac{\delta E}{\delta n}\Delta n + \frac{\delta E}{\delta m}\Delta m + \frac{\delta E}{\delta \hat{M}_0}\Delta \hat{M}_0 = \frac{\delta E}{\delta \hat{M}_0}\Delta \hat{M}_0.$$

The orientation dependence of the total energy thus

$$\frac{\mathrm{dE}}{d\hat{M}_0} = \frac{\partial E}{\partial \hat{M}_0} = \frac{\partial T^s}{\partial \hat{M}_0}. \tag{3.9}$$

The non-interacting kinetic energy term is defined as

$$T^s = \sum_{\mathrm{occ}} d^3\mathbf{r}\bar{\psi}_n(\mathbf{r}) \left(\frac{\hbar c}{i}\alpha\nabla + \beta\,\mathrm{mc}^2\right)\psi_n(\mathbf{r}) = \tag{3.10}$$
$$\sum_{\mathrm{occ}} d^3\mathbf{r}\bar{\psi}_n(\mathbf{r}) \left(\varepsilon_n - \mathrm{ev}_{\mathrm{eff}}(\mathbf{r}) - \mu_B B_{\mathrm{eff}}(\mathbf{r})\hat{B}_0\beta\Sigma\right)\psi_n(\mathbf{r}),$$

where we used the Kohn-Sham Dirac equation. The total derivative of the kinetic energy

$$\Delta T^s = \frac{\delta T^s}{\delta n}\Delta n + \frac{\delta T^s}{\delta m}\Delta m + \frac{\delta T^s}{\delta \hat{M}_0}\Delta \hat{M}_0, \tag{3.11}$$

can be given from Eq.(3.11) as

$$\Delta T^s = -e \int v_{\mathrm{eff}}(\mathbf{r})\Delta n(\mathbf{r})d^3\mathbf{r} - \mu_B \int B_{\mathrm{eff}}(\mathbf{r})\Delta m(\mathbf{r})d^3\mathbf{r} + \Delta\sum_{\mathrm{occ}}\varepsilon_n. \tag{3.12}$$

Comparing the two last equation, using Eq.(3.7) and (3.8), and assuming that $\hat{B}_0 = \hat{M}_0$, we get [43]:

$$\frac{\partial T^s}{\partial \hat{M}_0} = \frac{\partial}{\partial \hat{M}_0} \sum_{\text{occ}} \varepsilon_n. \tag{3.13}$$

Together with Eq.(3.9) the Magnetic Force Theorem is retained

$$\frac{dE}{d\hat{M}_0} = \frac{\partial}{\partial \hat{M}_0} \left(\sum_{\text{occ}} \varepsilon_n \right). \tag{3.14}$$

Although this theorem exactly stands only in this differential form with $\hat{M}_0$ pointing along some easy axis, it is commonly used in an integral form, where the energy difference is taken between two different directions of the magnetisation,

$$\text{MAE} = \sum_{\text{occ}} \varepsilon_n|_{\hat{M}_1} - \sum_{\text{occ}} \varepsilon_n|_{\hat{M}_2}. \tag{3.15}$$

This approximation is well tried [44][15]. Since in this approximation only explicit dependence of the Hamiltonian on $\hat{M}_0$ is considered, the potential and effective fields are regarded to be the same for the two different magnetization directions (frozen-potential approximation). The band energy is calculated from the electron density of states, and the MAE is written as

$$\text{MAE} = E_b^1 - E_b^2 \quad \text{where} \quad E_b^i = \int_{\varepsilon_B}^{\varepsilon_F} (\varepsilon - \varepsilon_F) n(\varepsilon, \hat{M}_i) d\varepsilon. \tag{3.16}$$

3.2 Torque based formula for the magnetic anisotropy

For calculating the MCA energy we used the torque method [45] originally proposed by Wang et. al. In Eq.(3.6) the free-energy with respect to the angle between the rotational axis, and the average magnetization (ϑ) was expressed. Reindexing the anisotropy parameters, and neglecting the sixth and higher order terms we get

$$F(\vartheta) = F_0 + K_2 \sin^2 \vartheta + K_4 \sin^4 \vartheta. \tag{3.17}$$

The magnetic torque is defined as the following derivative

$$T = \frac{dF(\vartheta)}{d\vartheta}.$$

It easily can be seen, that for the special angle:

$$T(\vartheta = \frac{\pi}{4}) = \frac{dF(\vartheta)}{d\vartheta}\bigg|_{\vartheta=\pi/4} = \frac{d\langle\Omega^{(\hat{n})}\rangle}{d\vartheta}\bigg|_{\vartheta=\pi/4} = K_2 + K_4 = K. \qquad (3.18)$$

Note that for $K > 0$ (< 0) the system is magnetized parallel (perpendicular) to the symmetry axis. In our work we investigated thin films on semi-infinite bulk structures. In this case the symmetry axis is perpendicular to the plane of the thin film, therefore positive K means out-of-plane preferred magnetic orientation. In the above equation we replaced the derivative of the free energy with respect of the magnetization angle by the corresponding derivative of the grand potential which follows from an approximation of removing the dependence of $h_p^{(\hat{n})}$ on $\hat{n}$, $h_p^{(\hat{n})} = h_p$, which in turn implies that the spin–entropy term in the free energy is also independent from $\hat{n}$.

Neglecting the contribution of the entropy to the anisotropy (which is equivalent of the assumption of direction independent Weiss-fields), the free-energy can be replaced by the grand-potential. The grand potential from the restricted average by definition can be expressed as

$$\langle\Omega^{(\hat{n})}\rangle = \int d\hat{e}_i \, \langle\Omega^{(\hat{n})}\rangle_{\hat{e}_i} \, P_i^{(\hat{n})}(\hat{e}_i).$$

Using the Magnetic Force Theorem (Eq.(2.53)) we get for the derivative

$$\begin{aligned}\frac{\partial\Omega^{(\hat{n})}(\vartheta)}{\partial\vartheta} &= \frac{1}{\pi}\text{Im}\int d\varepsilon \, f(\varepsilon;\mu) \, \frac{\partial}{\partial\vartheta}\left\{\text{Indet}\,\underline{\underline{\tau}}_c^{(\hat{n})}(\varepsilon)\right.\\ &\left. + \sum_i \int d\hat{e}_i P_i^{(\hat{n})}(\hat{e}_i)\,\text{Indet}\,\underline{\hat{D}}_i^{(\hat{n})}(\varepsilon;\hat{e}_i)\right\} \quad,\end{aligned}$$

here by evaluating the second integral it is worth to use a local frame of reference fixed to the average magnetization direction ($\hat{n}$). In this local frame the probability function doesn't have $\hat{n}$ dependence:

$$P_i^{(\hat{n})\,\text{loc}}(\hat{e}_i) == \frac{\beta h_i}{4\pi\sinh\beta h_i}\exp\left(-\beta h_i\hat{e}_i^z\right)$$

and

$$\underline{\hat{D}}_i^{(\hat{n})}(\varepsilon;\hat{e}_i) = \left[\underline{I} + \left(\underline{m}_i^{(\hat{n})}(\varepsilon;\hat{e}_i) - \underline{m}_{i,c}^{(\hat{n})}(\varepsilon)\right)\underline{\tau}_{ii,c}^{(\hat{n})}(\varepsilon)\right]^{-1} \quad,$$

with

$$\underline{m}_i^{(\hat{n})}(\varepsilon;\hat{e}_i) = \underline{R}(\hat{n})\,\underline{m}_i(\varepsilon;\hat{e}_i)\,\underline{R}(\hat{n})^+ = \underline{R}(\hat{n})\,\underline{R}(\hat{e}_i)\,\underline{m}_i(\varepsilon;\hat{z})\,\underline{R}^+(\hat{e}_i)\,\underline{R}(\hat{n})^+ \qquad (3.19)$$

24

here the rotation matrix $\underline{R}(\hat{n})$ rotates the $\hat{n}$ axis along the $\hat{z}$ axis, $\underline{R}(\hat{e}_i)$ the $\hat{e}_i$ axis into the $\hat{z}$ axis, and $\underline{m}_i(\varepsilon; \hat{z}) = \underline{t}_i^{-1}(\varepsilon; \hat{z})$ is the inverse scattering t-matrix if the magnetization point to the z axis. We can then expand the derivatives as

$$\frac{\partial \ln\det \underline{\underline{\tau}}_c^{(\hat{n})}(\varepsilon)}{\partial \vartheta} = \sum_k \frac{\delta \ln\det \underline{\underline{\tau}}_c^{(\hat{n})}(\varepsilon)}{\delta \underline{m}_{k,c}^{(\hat{n})}(\varepsilon)} \cdot \frac{\partial \underline{m}_{k,c}^{(\hat{n})}(\varepsilon)}{\partial \vartheta} \quad , \tag{3.20}$$

$$\frac{\partial ln\det \underline{\hat{D}}_i^{(\hat{n})}(\varepsilon; \hat{e}_i)}{\partial \vartheta} = \frac{\delta ln\det \underline{\hat{D}}_i^{(\hat{n})}(\varepsilon; \hat{e}_i)}{\delta \underline{m}_{i,c}^{(\hat{n})}(\varepsilon)} \cdot \frac{\partial \underline{m}_{i,c}^{(\hat{n})}(\varepsilon)}{\partial \vartheta} \tag{3.21}$$

$$+ \frac{\delta ln\det \underline{\hat{D}}_i^{(\hat{n})}(\varepsilon; \hat{e}_i)}{\delta \underline{m}_i^{(\hat{n})}(\varepsilon; \hat{e}_i)} \cdot \frac{\partial \underline{m}_i^{(\hat{n})}(\varepsilon; \hat{e}_i)}{\partial \vartheta} \quad . \tag{3.22}$$

It is well-known [46] that the CPA integrated DOS is stationary with respect to a small variation of the coherent $t-$matix, i.e.:

$$\frac{\delta \ln\det \underline{\underline{\tau}}_c^{(\hat{n})}(\varepsilon)}{\delta \underline{m}_{k,c}^{(\hat{n})}(\varepsilon)} + \sum_i \int d\hat{e}_{i\alpha} P_i^{(\hat{n})loc}(\hat{e}_i) \frac{\delta \ln\det \underline{\hat{D}}_i^{(\hat{n})}(\varepsilon; \hat{e}_i)}{\delta \underline{m}_{k,c}^{(\hat{n})}(\varepsilon)} =$$

$$= \frac{\delta \ln\det \underline{\underline{\tau}}_c^{(\hat{n})}(\varepsilon)}{\delta \underline{m}_{k,c}^{(\hat{n})}(\varepsilon)} + \sum_i \int d\hat{e}_i P_i^{(\hat{n})}(\hat{e}_i) \frac{\delta \ln\det \underline{D}_i^{(\hat{n})}(\varepsilon; \hat{e}_i)}{\delta \underline{m}_{k,c}^{(\hat{n})}(\varepsilon)} = 0 \quad ,$$

which in turn implies that

$$\frac{\partial F^{(\hat{n})}(\vartheta)}{\partial \vartheta} = \frac{1}{\pi} \sum_i \mathrm{Im} \int d\varepsilon \, f\left(\varepsilon; \mu^{(\hat{n})}\right) \int d\hat{e}_i P_i^{(\hat{n})loc}(\hat{e}_i) \times$$

$$\times \frac{\delta \ln\det \underline{\hat{D}}_i^{(\hat{n})}(\varepsilon; \hat{e}_i)}{\delta \underline{m}_i^{(\hat{n})}(\varepsilon; \hat{e}_i)} \cdot \frac{\partial \underline{m}_i^{(\hat{n})}(\varepsilon; \hat{e}_i)}{\partial \vartheta} \quad .$$

Moreover, for a small variation of $\underline{m}_{i\alpha}^{(\hat{n})}(\varepsilon; \hat{e}_i)$,

$$\mathrm{Tr}ln\underline{\hat{D}}_i^{'(\hat{n})}(\varepsilon; \hat{e}_i) = -\mathrm{Tr}ln\left(\underline{I} + \left(\delta\underline{m}_i^{(\hat{n})}(\varepsilon; \hat{e}_i) + \underline{m}_i^{(\hat{n})}(\varepsilon; \hat{e}_i) - \underline{m}_{i,c}^{(\hat{n})}(\varepsilon)\right) \underline{\tau}_{i*i,c}^{(\hat{n})}(\varepsilon)\right) \tag{3.23}$$

$$= -\mathrm{Tr}ln\left(\underline{I} + \left(\underline{m}_i^{(\hat{n})}(\varepsilon; \hat{e}_i) - \underline{m}_{i,c}^{(\hat{n})}(\varepsilon)\right) \underline{\tau}_{i*i,c}^{(\hat{n})}(\varepsilon) + \delta\underline{m}_i^{(\hat{n})}(\varepsilon; \hat{e}_i) \underline{\tau}_{i*i,c}^{(\hat{n})}(\varepsilon)\right) \tag{3.24}$$

$$= \mathrm{Tr}ln\underline{\hat{D}}_i^{(\hat{n})}(\varepsilon; \hat{e}_i) - \mathrm{Tr}ln\left(\underline{I} + \delta\underline{m}_i^{(\hat{n})}(\varepsilon; \hat{e}_i) \underline{\tau}_{i*i,c}^{(\hat{n})}(\varepsilon) \underline{\hat{D}}_i^{(\hat{n})}(\varepsilon; \hat{e}_i)\right) \tag{3.25}$$

$$\simeq \mathrm{Tr}ln\underline{\hat{D}}_i^{(\hat{n})}(\varepsilon; \hat{e}_i) - \mathrm{Tr}\left(\delta\underline{m}_i^{(\hat{n})}(\varepsilon; \hat{e}_i) \underline{\tau}_{i*i,c}^{(\hat{n})}(\varepsilon) \underline{\hat{D}}_i^{(\hat{n})}(\varepsilon; \hat{e}_i)\right) \quad . \tag{3.26}$$

We therefore get for the derivative:

$$\frac{\delta \ln\det \hat{\underline{D}}_i^{(\hat{n})}(\varepsilon;\hat{e}_i)}{\delta \underline{m}_i^{(\hat{n})}(\varepsilon;\hat{e}_i)} \circ \frac{\partial \underline{m}_i^{(\hat{n})}(\varepsilon;\hat{e}_i)}{\partial \vartheta} = -\mathrm{Tr}\left(\frac{\partial \underline{m}_i^{(\hat{n})}(\varepsilon;\hat{e}_i)}{\partial \hat{n}} \underline{\mathcal{T}}_{ii,c}^{(c,\hat{n})}(\varepsilon)\,\hat{\underline{D}}_i^{(\hat{n})}(\varepsilon;\hat{e}_i)\right) \quad .$$

where from Eq.(3.19)

$$\frac{\partial \underline{m}_i^{(\hat{n})}(\varepsilon;\hat{e}_i)}{\partial \vartheta} = \frac{\partial \underline{R}(\hat{n})}{\partial \vartheta}\,\underline{m}_i(\varepsilon;\hat{e}_i)\,\underline{R}(\hat{n})^+ + \underline{R}(\hat{n})\,\underline{m}_i(\varepsilon;\hat{e}_i)\,\frac{\partial \underline{R}^+(\hat{n})}{\partial \vartheta} \quad . \tag{3.27}$$

In using these results in Eq.3.18 we get the LSDA contribution to the magnetic anisotropy constant, usually termed as the band energy part, K_b, which in a layered system can be given as a sum of layer resolved contributions, $K_{b,p}$,

$$K_b = \sum_p K_{b,p} \quad , \tag{3.28}$$

where

$$K_{b,p} = \frac{1}{\pi}\mathrm{Im}\int d\varepsilon\,f(\varepsilon;\mu)\,\int d\hat{e}_{pi*}\,P_p^{(z)}(\hat{e}_{p*i}) \times \tag{3.29}$$

$$\mathrm{Tr}\left[\left(\frac{\partial \underline{R}(\hat{n})}{\partial \vartheta}\,\underline{t}_p(\varepsilon;\hat{e}_{pi})^{-1}\,\underline{R}(\hat{n})^+ + \underline{R}(\hat{n})\,\underline{t}_p(\varepsilon;\hat{e}_{pi})^{-1}\,\frac{\partial \underline{R}^+(\hat{n})}{\partial \vartheta}\right)\times\right. \tag{3.30}$$

$$\left. \times \underline{\mathcal{T}}_{pi,pi}^{c(\hat{n})}(\varepsilon)\,\hat{\underline{D}}_p^{(\hat{n})}(\varepsilon;\hat{e}_{pi})\right]_{\vartheta=\pi/4,\varphi=0}. \tag{3.31}$$

Note that for an accurate calculation of $K_{b,p}$ in terms of Eq. (3.29) the CPA condition has to be satisfied with a high precision.

3.3 The magnetic dipole-dipole anisotropy term

The total magnetic anisotropy energy also consists of a contribution arising from the classical magnetic dipole-dipole energy (E_{dd}) which can be approximated by means of the magnetisation m_i at site i as

$$E_{\mathrm{dd}} = \sum_{i\neq j}\frac{1}{r_{\mathrm{ij}}^3}\left(m_i m_j - 3\frac{(r_{\mathrm{ij}}\cdot m_i)(r_{\mathrm{ij}}\cdot m_j)}{r_{\mathrm{ij}}^2}\right). \tag{3.32}$$

In the case of completely ordered ($T = 0$ K) ferromagnetic layered systems this equation can be expressed further as [13][15]

$$E_{dd}^{(\hat{n})} = \sum_{pq}\frac{M_p M_q}{c^2}\,\hat{n}\,\underline{D}_{pq}^{dd}\,\hat{n} \quad , \tag{3.33}$$

where c ($= 274.072$) is the speed of light in atomic (Rydberg) units and the $\underline{D}_{pq}^{dd}$ are the dipole-dipole Madelung matrices, and the averaged magnetic moment in layer p is M_p. The corresponding contribution to the uniaxial MAE is then defined as

$$K_{dd} = E_{dd}^{(\hat{x})} - E_{dd}^{(\hat{z})} \quad , \tag{3.34}$$

while the total MA constant is given by the sum of band energy and dipole-dipole contributions

$$K = K_b + K_{dd} \quad . \tag{3.35}$$

In the present work for disordered magnetic systems as an approximation we calculate the average dipole-dipole interaction energy substituting the configurational average of the magnetisation (see also Eq. (2.31))

$$M_p(T) = \mu_p(0)\, m_p(T), \tag{3.36}$$

into Eq.(3.33). With this formulation the dipole-dipole anisotropy can be get from Eq.(3.34).

Chapter 4

Spin-disorder part of electrical resistivity

4.1 History of temperature dependent electrical conductivity calculations

In a ferromagnetic metal in principle there are three main sources of the electrical resistivity. The first one is scattering of itinerant electrons on impurities, the second is the scattering caused by the lattice vibrations (phonons), and the third one arises from the spin-dependent scattering, i.e., interaction with the magnetic spin system (spin waves). In case of nonmagnetic impurity the first one causes a temperature independent contribution to the resistivity, magnetic impurities are responsible for the Kondo effect [47], i.e., for the resistivity minimum at a specific temperature. For a pure metal we can disregard this contribution. The resistivity due to the phonon-electron interaction can be well described by the Bloch-Grüneisen formula [48],

$$\varrho(T) = K \left(\frac{T}{\Theta_D} \right)^5 J \left(\frac{\Theta_D}{T} \right), \tag{4.1}$$

where Θ_D is the Debye temperature, K is a constant, and

$$J(x) = \int_0^x \frac{\xi^5 d\xi}{(e^\xi - 1)(1 - e^{-\xi})} \approx \left\{ \begin{array}{ll} \frac{1}{4} x^4 & x \ll 1 \\ 124,43 & x \gg 1 \end{array} \right. .$$

The magnetic part of the resistivity often called as spin disorder resistivity poses a challenging a subject of solid state physics since decades. One of the mostly referred theoretical papers on the temperature dependent magnetic resistivity of magnetic metals is the one of Goodings [32], in which he introduces a theoretical model calculation for the magnetic part of the resistivity for pure crystalline Fe, Co, Ni and Gd.

He describes the magnetic scattering with a simple s-d Hamiltonian,

$$H_{\text{sd}} = -2 \sum_{n} J(\mathbf{r} - \mathbf{R}_n)\mathbf{s}\mathbf{S}_n, \tag{4.2}$$

where $\mathbf{s}$ is the (classical) spin operator of itinerant electrons and $\mathbf{S}_n$ the one for those localised at $\mathbf{R}_n$. The itinerant electrons can be either in an s or in a d band, so they can be described with a wave number ($\mathbf{k}$), an s or d band index ($\alpha = s, d$) and a spin ($\pm$). The localized moments form a spin-wave eigenstate, which in turn can be described by $n(\mathbf{q})$, i.e., the number of magnons with wave number $\mathbf{q}$. The transition probability can then be given as the square of the Hamiltonian matrix element,

$$P(\mathbf{k}\alpha\mp \to \mathbf{k}'\alpha'\pm) = \frac{2\pi}{\hbar} |\langle \mathbf{k}'\alpha'\pm, n(\mathbf{q}) \pm 1 | H_{\text{sd}} | \mathbf{k}\alpha\mp, n(\mathbf{q})\rangle|^2 = \tag{4.3}$$

$$= \frac{2\pi}{\hbar} \frac{2S}{N} \left[n(\mathbf{q}) + \frac{1}{2} \pm \frac{1}{2} \right] |J_{\alpha\alpha'}(\mathbf{k} - \mathbf{k}')|^2 \delta_{\mathbf{k}',\mathbf{k}\mp\mathbf{q}}.$$

According to the Boltzmann theory of transport the time derivative of the distribution function is given by

$$\frac{\partial f}{\partial t}(\mathbf{k}\alpha\pm)]_{\text{collision}} = \sum_{q} \sum_{\mathbf{k}'\alpha'} f(\mathbf{k}'\alpha')(1 - f(\mathbf{k}\alpha))P(\mathbf{k}'\alpha' \to \mathbf{k}\alpha) -$$

$$-f(\mathbf{k}\alpha)(1 - f(\mathbf{k}'\alpha'))P(\mathbf{k}\alpha \to \mathbf{k}'\alpha'), \tag{4.4}$$

where the collision term corresponds to the scattering caused by the electric field,

$$\frac{\partial f}{\partial t}(\mathbf{k}\alpha\pm)]_{\text{collision}} = -\frac{\partial f}{\partial t}(\mathbf{k}\alpha\pm)]_{\text{field}} = \mathbf{v}(\mathbf{k}\alpha)e\mathbf{E}\frac{\partial f(\mathbf{k}\alpha\pm)}{\partial E(\mathbf{k}\alpha\pm)}, \tag{4.5}$$

where $\mathbf{v}(\mathbf{k}\alpha)$ being the electron group velocity, $\mathbf{E}$ the electric field, and E is the energy of the electron. In terms of these quantities the electric current density can be expressed as

$$\mathbf{j} = e\varrho \sum_{k\alpha} \left[\mathbf{v}(\mathbf{k}\alpha+)f(\mathbf{k}\alpha+) + \mathbf{v}(\mathbf{k}\alpha-)f(\mathbf{k}\alpha-) \right],$$

such that from

$$\mathbf{j} = \sigma\mathbf{E}$$

the conductivity σ can be obtained. Goodings calculated this conductivity with the help of the variational method, using several approximations such as spherical energy bands, neglecting the spin-wave umklapp processes, $\mathbf{k}$ independence of $J_{\alpha\alpha'}(\mathbf{k})$

(i.e., representing the s-d interaction by a δ function), and the variational method itself. In spite of all these approximations he got quite a complicated temperature dependence for the electric resistivity. In particular, he stressed the importance of the s-d scattering for Fe for temperatures above about 20 K. Below 20 K the s-s scattering gives the main contribution such that he reproduced the old results of a quadratic temperature dependence

$$\varrho_{\text{magn}} \propto T^2 \quad \text{for small } T.$$

The parameters $J_{\alpha\alpha'}$, effective masses or Fermi wave numbers $\mathbf{k}_{F\alpha}$ were taken from experimental data. The results for Fe (Fig.4.1) underestimates the experimental curves, however, Goodings took no attempt to exclude the phonon contribution from the experimental results.
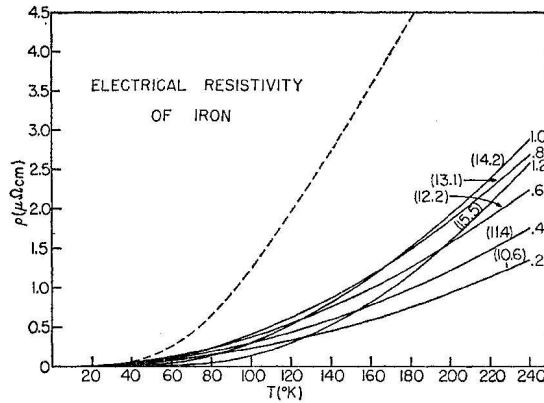

Figure 4.1: Theoretical predictions of Goodings [32]. Calculated ϱ_{magn} magnetic resistivity of Fe with different values of $(\mathbf{k}_{F1} - \mathbf{k}_{F2})a$ shown an the right side of each curve. The numbers in brackets are the effective mass ratios m_2/m_1. The dashed line refers to the experimental total resistivity [49].

The model of Goodings was extended lately by Raquet et.al [33][50], in order to explain high field magnetoresistance data. They took into account the magnetic field dependence of the spin wave spectra such as the temperature dependence by a magnon mass renormalization (i.e., temperature dependent spin wave stiffness). They evaluated and also measured the magnetoresistance

$$\Delta\varrho(T,B) = \varrho(T,B) - \varrho(T,B=0) \approx \Delta\varrho_{\text{magn}}(T,B) \tag{4.6}$$

which mainly originates from the magnetic part of the resistivity. They used similar experimental parameters as Goodings. In addition they fitted the temperature

dependent magnon stiffness to reproduce the experimental $\Delta \varrho(T, B)$ magnetore-sistence data for Fe,Co and Ni. With these parameters they predicted the magnetic part of the resistivity $(\varrho_{\mathrm{magn}}(T, B = 0))$ from their model. In Fig.4.2 their results can be seen. The results of their calculations for the magnetic part of the resistivity in these metals is an order of magnitude smaller than the total experimental resistivity. We have to stress that this model starts from a simple s-d Hamiltonian, and that they used the same approximations as Goodings (e.g., neglecting the umklapp processes).
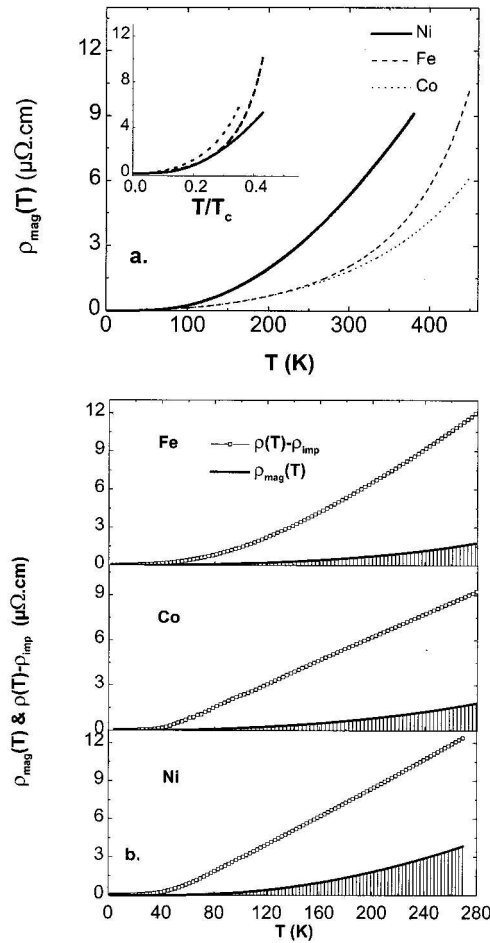

Figure 4.2: a, The magnetic part of the resistivity for Fe, Co, and Ni according to the calculations of Raquet et.al. [33] b: comparison of the magnetic part with the total resistivity $\varrho(T)$.

The other early theoretical approach for the temperature dependent resistivity of Fe and Ni alloys was based on the so-called two current model, proposed by Albert Fert et.al. [51][52][53]. The two-current model of ferromagnetic materials

assumes, that the electrons can be grouped into two class, one with spin up ($\uparrow$) electrons, and the other with spin down ($\downarrow$). In the electron scatterings the spin conservation was assumed to dominate, at least at low temperature. In addition, to the spin conserving processes Fert et.al. included a temperature dependent spin-flip scattering term described by the parameter $\varrho_{\uparrow\downarrow}(T)$. Thus the total resistivity was of the form:

$$\varrho = \frac{\varrho_\uparrow \varrho_\downarrow + \varrho_{\uparrow\downarrow}(\varrho_\uparrow + \varrho_\downarrow)}{\varrho_\uparrow + \varrho_\downarrow + 4\varrho_{\uparrow\downarrow}}, \tag{4.7}$$

where the parameters $\varrho_\uparrow, \varrho_\downarrow$ are formulated within the Boltzmann theory. By vanishing spin-flip scattering ($\varrho_{\uparrow\downarrow} = 0$) the equation gives the resistivity of parallelly connected $\uparrow$ and $\downarrow$ spin channels. Fert et.al. used the below form for the temperature dependent resistivities

$$\varrho_\sigma = \varrho_{0\sigma} + \varrho_\sigma(T).$$

Detaching thus the residual resistivity ($\varrho_{0\sigma}$) with $\sigma = \uparrow, \downarrow$. The $\varrho_{\uparrow\downarrow}$ scattering arises from spin wave scattering, thus it is negligible at $T = 0K$. Using these assumptions they obtained the following expression:

$$\varrho_T(T) = \varrho(T) - \varrho_0 = \left(1 + \frac{(\alpha - \mu)^2}{(1 + \alpha)^2 \mu}\right) \varrho_i(T) + \frac{(\alpha - 1)^2}{(\alpha + 1)^2} \varrho_{\uparrow\downarrow}(T), \tag{4.8}$$

where

$$\alpha = \varrho_{0\downarrow}/\varrho_{0\uparrow}, \quad \mu = \varrho_\downarrow(T)/\varrho_\uparrow(T),$$

and

$$\varrho_i(T) = \frac{\varrho_\uparrow(T)\varrho_\downarrow(T)}{\varrho_\uparrow(T) + \varrho_\downarrow(T)}.$$

They fitted the parameters α, μ to the experimental results, as well as parameters c_1 and c_2 to the temperature dependent resistivity

$$\varrho_i(T) = c_1 T^2 + c_2 T^4.$$

They also fitted the resistivity $\varrho_{\uparrow\downarrow}(T)$. However, they tried to give [54][55] an analytical expression for $\varrho_{\uparrow\downarrow}(T)$ starting from an $s - d$ Hamiltonian (similar to Eq.4.2) and calculating the relaxation time within the Boltzmann theory. They succeeded to give the qualitative dependence of $\varrho_{\uparrow\downarrow}(T)$, which however, for Fe differed quantitatively from the experiments by a factor of 2 [54]. Later they fitted the $\varrho_{\uparrow\downarrow}(T)$ to the experiments and obtained results for $\varrho(T)$ (Eq.4.7) in fair agreement with the

experiments for Fe and Ni alloys [55], but the large number of fitting parameters weakened the predictive force of their theory. Later on the two current model was criticized by A. Vernes et.al. [56], who showed that the two current model fails two orders of magnitude for the resistivity of Co-Ni alloys when compared to results based on calculations using a fully relativistic Kubo-Greenwood formalism. According to their argument, the difference arises from the dominance of the spin-orbit coupling induced spin-flip scatterings.

For dilute magnetic alloys a widespread description of the electrical conductivity in the literature given in terms of spin-spin correlation functions, first proposed by de Gennes and Friedel [57]. Their theory starts from a similar s-d interaction perturbation as in Eq.(4.2), where the $\mathbf{s}$ denotes the conduction electron spin, $\mathbf{S}_i$ a localized spin on site i, and I an assumed site-independent interaction,

$$V = I \sum_i \mathbf{s}_i \mathbf{S}_i. \tag{4.9}$$

Expressing the transition matrix element in the Born approximation [1]

$$P(\mathbf{k}\alpha\gamma \to \mathbf{k}'\alpha'\gamma') = \frac{2\pi}{\hbar} \left| \langle \mathbf{k}'\alpha'\gamma' \left| V \right| \mathbf{k}\alpha\gamma \rangle \right|^2, \tag{4.10}$$

in which the delocalised electrons are described by the wave function $|\mathbf{k}\rangle = c_{\mathbf{k}} e^{i\mathbf{k}\mathbf{r}}$, α is the spin quantum number of the delocalised electron, γ is the same for the localised moment. One easily obtains

$$P(\mathbf{k}\alpha\gamma \to \mathbf{k}'\alpha'\gamma') = \frac{2\pi}{\hbar} \left| I \sum_i \sigma_{\alpha\alpha'} \langle \gamma \left| \mathbf{S}_i \right| \gamma' \rangle e^{i(\mathbf{k}-\mathbf{k}')\mathbf{R}_i} \right|^2 = \tag{4.11}$$

$$= \frac{2\pi}{\hbar} I^2 \sum_{ij} |\sigma_{\alpha\alpha'}| \langle \gamma \left| \mathbf{S}_i \right| \gamma' \rangle \langle \gamma' \left| \mathbf{S}_j \right| \gamma \rangle e^{i(\mathbf{k}-\mathbf{k}')(\mathbf{R}_i - \mathbf{R}_j)}.$$

When used in Eq.(4.4) we have to sum up over all the local moment states

$$\frac{\partial f}{\partial t}(\mathbf{k}\alpha)]_{\text{collision}} = \sum_{\gamma\gamma'} \sum_{\mathbf{k}'\alpha'} f(\mathbf{k}'\alpha')(1 - f(\mathbf{k}\alpha))w_{\gamma'}P(\mathbf{k}'\alpha'\gamma' \to \mathbf{k}\alpha\gamma) -$$

$$- f(\mathbf{k}\alpha)(1 - f(\mathbf{k}'\alpha'))w_\gamma P(\mathbf{k}\alpha\gamma \to \mathbf{k}'\alpha'\gamma'), \tag{4.12}$$

___
[1]Indeed here we neglect higher order scattering terms (i.e. electron scatterings through intermediate states), which can lead to the Kondo effect.

where w_γ is the occupation of state γ. From Eq.(4.11) one obtains

$$W(\mathbf{k}\alpha \to \mathbf{k}'\alpha') = \sum_{\gamma\gamma'} w_\gamma P(\mathbf{k}\alpha\gamma \to \mathbf{k}'\alpha'\gamma') = \frac{2\pi}{\hbar} I^2 \sum_{ij} \langle \mathbf{S}_i \cdot \mathbf{S}_j \rangle \, e^{i(\mathbf{k}-\mathbf{k}')\cdot(\mathbf{R}_i-\mathbf{R}_j)}.$$

(4.13)

In the relaxation-time approximation to the Boltzmann equation the relaxation time can be given by [48]

$$\frac{1}{\tau(\mathbf{k})} = \int \frac{d\mathbf{k}'}{(2\pi)^3} \sum_{\alpha'} W(\mathbf{k}\alpha \to \mathbf{k}'\alpha')[1 - \cos(\mathbf{k}, \mathbf{k}')],$$

(4.14)

from which the resistivity follows as

$$\varrho = \frac{m^*}{\mathrm{n}e^2\,\tau(\varepsilon_F)},$$

(4.15)

with m^* being the effective mass. Introducing the spin-spin correlation function

$$\chi_{ij} = \langle \mathbf{S}_i \cdot \mathbf{S}_j \rangle - \langle \mathbf{S}_i \rangle \cdot \langle \mathbf{S}_j \rangle,$$

it can be seen that in the case of a bulk translation invariant material $\langle \mathbf{S}_i \rangle = S$, therefore the term

$$\sum_{ij} \langle \mathbf{S}_i \rangle \langle \mathbf{S}_j \rangle \, e^{i(\mathbf{k}-\mathbf{k}')(\mathbf{R}_i-\mathbf{R}_j)} = N^2 S^2 \delta_{\mathbf{k},\mathbf{k}'}$$

doesn't give contribution to Eq.(4.14). Therefore the resistivity can be expressed in terms of the spin-susceptibility:

$$\varrho = \frac{2\pi m^*}{\hbar\,\mathrm{n}e^2} I^2 N \int \frac{d\mathbf{k}'}{(2\pi)^3} \chi(\mathbf{k} - \mathbf{k}')[1 - \cos(\mathbf{k}, \mathbf{k}')],$$

(4.16)

where

$$\chi(\mathbf{q}) = \sum_j \chi_{0j} e^{-i\mathbf{q}\mathbf{R}_j}.$$

(4.17)

With similar (but more detailed) calculations the peak in the temperature derivative of the resistivity in Ni around the Curie temperature was explained in the 60-ies [58][59], and the role of the short range order in the resistivity was stressed. A similar theory was given by Haas [60] for magnetic semiconductors , who found a maximum in the resistivity at the Curie temperature. This resistivity peak was measured for magnetic alloys (e.g. $(\mathrm{Fe}_{1-x}\,M_x)_3\,\mathrm{Si}$ [61]) and dilute semiconductors (e.g. (Ga,Mn)As [62] [63]) . A more recent parametric model calculation for the resistivity peak using a similar s-d Hamiltonian can be found in Ref [64].

4.2 Magnetic part of electrical conductivity

For our electrical conductivity calculations we used the linear-response theory of Kubo [65]. In this approximation the static ($\mathbf{q} = 0$, $\omega = 0$) electrical conductivity is given by [66]:

$$\sigma_{\mu\mu} = \frac{\pi\hbar}{NV_{at}}\left\langle \sum_{m,n} J_{mn}^\mu J_{nm}^\mu \delta\left(\varepsilon_F - \varepsilon_m\right)\delta\left(\varepsilon_F - \varepsilon_n\right)\right\rangle, \tag{4.18}$$

where $\mu = \{x, y, z\}$ refers to the direction, N is the number of atoms, V_{at} is the atomic volume, $\langle\ldots\rangle$ refers to the average over spin configurations, and J_{mn}^μ is the current operator matrix element,

$$J_{mn}^\mu = \langle m|J^\mu|n\rangle$$

in the basis of the eigenstates $|n\rangle$ of the unperturbed Hamiltonian, where the current operator is given by

$$\vec{J}(\mathbf{r}) = \begin{cases} \frac{e\hbar}{2\,\mathrm{mi}}\psi^+(\mathbf{r})(\overrightarrow{\nabla} - \overleftarrow{\nabla})\psi(\mathbf{r}), & \text{in non-relativistic case} \\ \mathrm{ec}\,\psi^+(\mathbf{r})\,\overrightarrow{\alpha}\,\psi(\mathbf{r}), & \text{in relativistic case} \end{cases}. \tag{4.19}$$

In the Green's function formalism:

$$\sum_n |n\rangle\langle n|\,\delta\left(\varepsilon - \varepsilon_n\right) = -\frac{1}{\pi}\,\mathrm{ImG}^+(\varepsilon) = -\frac{1}{2\pi i}[G^+(\varepsilon) - G^-(\varepsilon)], \tag{4.20}$$

with the notation

$$\lim_{\eta\to\pm 0} G(\varepsilon + i\eta) = G^\pm(\varepsilon). \tag{4.21}$$

The δ functions in Eq.(4.18) can be replaced such that

$$\sigma_{\mu\mu} = \frac{\pi\hbar}{NV_{at}}Tr\left\langle J^\mu\,\mathrm{ImG}^+(\varepsilon_F)J^\mu\,\mathrm{ImG}^+(\varepsilon_F)\right\rangle. \tag{4.22}$$

Using the notation

$$\lim_{\eta\to\pm 0}\varepsilon + i\eta = \varepsilon^\pm,$$

we can further express Eq.(4.22) as

$$\sigma_{\mu\mu} = \frac{1}{4}\{\tilde{\sigma}_{\mu\mu}(\varepsilon^+, \varepsilon^+) + \tilde{\sigma}_{\mu\mu}(\varepsilon^-, \varepsilon^-) - \tilde{\sigma}_{\mu\mu}(\varepsilon^+, \varepsilon^-) - \tilde{\sigma}_{\mu\mu}(\varepsilon^-, \varepsilon^+)\}, \tag{4.23}$$

where

$$\tilde{\sigma}_{\mu\mu}(\varepsilon_1, \varepsilon_2) = \frac{\pi\hbar}{NV_{at}} Tr \left\langle J^\mu \operatorname{ImG}^+(\varepsilon_1) J^\mu \operatorname{ImG}^+(\varepsilon_2) \right\rangle,$$

$$(\varepsilon_i \in \{\varepsilon^+, \varepsilon^-\} \quad ; \quad i = 1, 2).$$

Using Eq.(A.27) the Green's function can be expressed in terms of the KKR quantities. We calculate the resistivity of a region consisting of n intermediate atomic layers, and surrounded by two semi-infinite systems of the same material. If n tends to infinity, the resistivity converges to the bulk value. It can be shown that the second term on rhs of Eq.(A.27) is real [67] [2], so it doesn't contribute to Eq.(4.22). The term containing the SPO gives [27]:

$$\tilde{\sigma}_{\mu\mu}(\varepsilon_1, \varepsilon_2) = \frac{C}{n} \sum_{p=1}^{n} \sum_{i \in I(L_2)} \sum_{q=1}^{n} \sum_{j \in I(L_2)} \operatorname{tr} \left\langle \underline{J}_\mu^{\mathrm{pi}}(\varepsilon_2, \varepsilon_1) \underline{\tau}^{\mathrm{pi,qj}}(\varepsilon_1) \underline{J}_\mu^{\mathrm{qj}}(\varepsilon_1, \varepsilon_2) \underline{\tau}^{\mathrm{qj,pi}}(\varepsilon_2) \right\rangle,$$

(4.24)

where we have to sum up for the pair of sites $\{i, j\}$ which can be situated in every possible layers $0 < p, q \leq n$. C contains all the constants, and $I(L_2)$ contains all the indices belonging to a simple two-dimensional lattice L_2 .

In the basis of regular scattering solutions $(Z_\Lambda^p(\mathbf{r}_{p0}, \epsilon))$ the matrix elements of the current operator (Eq.(4.19)) are given by:

$$J_{\mu,\Lambda\Lambda'}^p(\varepsilon_1, \varepsilon_2) = \frac{e\hbar}{\mathrm{im}} \int_{\mathrm{WS}} Z_\Lambda^p(\mathbf{r}_{p0}, \varepsilon_1)^+ \frac{\partial}{\partial \mathbf{r}_{p0,\mu}} Z_{\Lambda'}^p(\mathbf{r}_{p0}, \varepsilon_2) d^3\mathbf{r}_{p0},$$

(4.25)

with $\Lambda = (\mathrm{lm})$, in the nonrelativistic case, and

$$J_{\mu,\Lambda\Lambda'}^p(\varepsilon_1, \varepsilon_2) = \mathrm{ec} \int_{\mathrm{WS}} Z_\Lambda^p(\mathbf{r}_{p0}, \varepsilon_1)^+ \alpha_\mu Z_{\Lambda'}^p(\mathbf{r}_{p0}, \varepsilon_2) d^3\mathbf{r}_{p0},$$

(4.26)

with $\Lambda = (\kappa\mu)$, in the relativistic case. Provided that two-dimensional invariance applies in all layers under consideration we can make use of the fact that

$$J_\mu^p(\varepsilon_1, \varepsilon_2) = J_\mu^{p0}(\varepsilon_1, \varepsilon_2) = J_\mu^{\mathrm{pi}}(\varepsilon_1, \varepsilon_2) \quad \forall i \in I(L_2),$$

(4.27)

and from which one easily can see that for each layer p the sum over $i \in I(L_2)$ gives N times the same contribution, therefore

$$\tilde{\sigma}_{\mu\mu}(\varepsilon_1, \varepsilon_2) = \frac{C}{n} \sum_{p=1}^{n} \sum_{q=1}^{n} \left(\sum_{j \in I(L_2)} \operatorname{tr} \left\langle \underline{J}_\mu^p(\varepsilon_2, \varepsilon_1) \underline{\tau}^{p0,\mathrm{qj}}(\varepsilon_1) \underline{J}_\mu^q(\varepsilon_1, \varepsilon_2) \underline{\tau}^{\mathrm{qj},p0}(\varepsilon_2) \right\rangle \right).$$

(4.28)

---

[2]In the relativistic case the proof is more complicated.

Neglecting the so-called vertex corrections [67] we can calculate the conductivity as:

$$\tilde{\sigma}_{\mu\mu}(\varepsilon_1, \varepsilon_2) = \frac{C}{n} \sum_{p=1}^{n} \sum_{q=1}^{n} \sum_{j \in I(L_2)} \int d\hat{e}_0 d\hat{e}_j P(\{\hat{e}_0, \hat{e}_j\}) \times \qquad (4.29)$$

$$\times \text{tr} \left(\underline{J}_{\mu}^{p}(\varepsilon_2, \varepsilon_1, \hat{e}_0) \left\langle \underline{\tau}^{p0,qj}(\varepsilon_1) \right\rangle_{p0\hat{e}_0, qj\,\hat{e}_j} \underline{J}_{\mu}^{q}(\varepsilon_1, \varepsilon_2, \hat{e}_j) \left\langle \underline{\tau}^{qj,p0}(\varepsilon_2) \right\rangle_{qj\,\hat{e}_j, p0\hat{e}_0} \right),$$

where the restricted averages $\left\langle \underline{\tau}^{p0,qj}(\varepsilon_1) \right\rangle_{p0\hat{e}_0, qj\,\hat{e}_j}$ we are obtained by fixing the local moment directions in site 0 and j, and average over all the other lattice sites. Notice that the current matrix is direction dependent, from the transformation of Eq.(4.26)

$$J_{\mu,\Lambda\Lambda'}^{p}(\varepsilon_1, \varepsilon_2, \hat{e}) = \sum_{\Gamma\Gamma'} \sum_{\nu=1,3} O_{\Lambda\Gamma}^{*} R_{\mu\nu} J_{\nu,\Gamma\Gamma'}^{p}(\varepsilon_1, \varepsilon_2) O_{\Gamma'\Lambda'} \qquad (4.30)$$

where $J_{\mu,\Gamma\Gamma'}^{p}(\varepsilon_1, \varepsilon_2)$ is the current matrix if the local moment points along the $\hat{z}$ axis, $O_{\Lambda\Gamma}$ and $R_{\mu\nu}$ are the representations of the rotation which takes the $\hat{z}$ axis into the $\hat{e}$ axis in angular momentum and in real space, respectively.

We can calculate the thermal average of the SPO-s using the coherent potential approximation. The sum in Eq.(4.29) can be split up into a site-diagonal and an off-diagonal term:

$$\tilde{\sigma}_{\mu\mu}(\varepsilon_1, \varepsilon_2) = \tilde{\sigma}_{\mu\mu}^{0}(\varepsilon_1, \varepsilon_2) + \tilde{\sigma}_{\mu\mu}^{1}(\varepsilon_1, \varepsilon_2), \qquad (4.31)$$

where the diagonal part will be:

$$\tilde{\sigma}_{\mu\mu}^{0}(\varepsilon_1, \varepsilon_2) = \frac{C}{n} \sum_{p=1}^{n} \int d\hat{e} P_p(\hat{e}) \, \text{tr} \left(\underline{J}_{\mu}^{p}(\varepsilon_2, \varepsilon_1, \hat{e}) \left\langle \underline{\tau}^{pp}(\varepsilon_1) \right\rangle_{p0\hat{e}} \underline{J}_{\mu}^{p}(\varepsilon_1, \varepsilon_2, \hat{e}) \left\langle \underline{\tau}^{pp}(\varepsilon_2) \right\rangle_{p0\hat{e}} \right).$$
$$(4.32)$$

By employing the CPA the restricted SPO-s can be expressed from Eq.(B.11), and we get

$$\tilde{\sigma}_{\mu\mu}^{0}(\varepsilon_1, \varepsilon_2) = \frac{C}{n} \sum_{p=1}^{n} \int d\hat{e} P(\hat{e}) \, \text{tr} \left[\underline{J}_{\mu}^{p}(\varepsilon_2, \varepsilon_1, \hat{e}) \underline{\tau}_{c}^{pp}(\varepsilon_1) \times \qquad (4.33) \right.$$
$$\left. \times \underline{D}^{p}(\varepsilon_1, \hat{e}) \underline{J}_{\mu}^{p}(\varepsilon_1, \varepsilon_2, \hat{e}) \underline{\tau}_{c}^{pp}(\varepsilon_2) \underline{D}^{p}(\varepsilon_2, \hat{e}) \right],$$

where we used the underlying two-dimensional translational invariance,

$$\underline{\tau}_{c}^{pipi}(\varepsilon_1) = \underline{\tau}_{c}^{pp}(\varepsilon_1) \quad \forall i \in I(L_2). \qquad (4.34)$$

The site off-diagonal part can further be decomposed into two terms,

$$\tilde{\sigma}_{\mu\mu}^{1}(\varepsilon_1, \varepsilon_2) = \tilde{\sigma}_{\mu\mu}^{2}(\varepsilon_1, \varepsilon_2) + \tilde{\sigma}_{\mu\mu}^{3}(\varepsilon_1, \varepsilon_2), \qquad (4.35)$$

where

$$\tilde{\sigma}_{\mu\mu}^{2}(\varepsilon_1, \varepsilon_2) = \frac{C}{n} \sum_{p=1}^{n} \sum_{q=1}^{n} (1 - \delta_{pq}) \sum_{j \in I(L_2)} \mathrm{tr} \left\langle \underline{J}_{\mu}^{p}(\varepsilon_2, \varepsilon_1) \underline{\tau}^{p0,qj}(\varepsilon_1) \underline{J}_{\mu}^{q}(\varepsilon_1, \varepsilon_2) \underline{\tau}^{qj,p0}(\varepsilon_2) \right\rangle,$$

(4.36)

$$\tilde{\sigma}_{\mu\mu}^{3}(\varepsilon_1, \varepsilon_2) = \frac{C}{n} \sum_{p=1}^{n} \sum_{q=1}^{n} \delta_{pq} \sum_{(j \neq 0) \in I(L_2)} \mathrm{tr} \left\langle \underline{J}_{\mu}^{p}(\varepsilon_2, \varepsilon_1) \underline{\tau}^{p0,qj}(\varepsilon_1) \underline{J}_{\mu}^{q}(\varepsilon_1, \varepsilon_2) \underline{\tau}^{qj,p0}(\varepsilon_2) \right\rangle.$$

(4.37)

As one can see $\tilde{\sigma}_{\mu\mu}^{2}$ arises from sites located in different layers, while $\tilde{\sigma}_{\mu\mu}^{3}$ refers to sites in one and the same layer. Using again the CPA for the restricted averaged SPO (Eq.B.12) and neglecting the vertex corrections we get for $\tilde{\sigma}_{\mu\mu}^{2}$:

$$\tilde{\sigma}_{\mu\mu}^{2}(\varepsilon_1, \varepsilon_2) = \frac{C}{n} \sum_{p=1}^{n} \sum_{q=1}^{n} (1 - \delta_{pq}) \sum_{j \in I(L_2)} \int \int d\hat{e}_i d\hat{e}_j P_p(\hat{e}_i) P_q(\hat{e}_j) \times$$

$$\times \mathrm{tr} \left\{ \underline{J}_{\mu}^{p}(\varepsilon_2, \varepsilon_1, \hat{e}_i) \underline{\tilde{D}}^{p}(\varepsilon_1, \hat{e}_i) \underline{\tau}_{c}^{p0,qj}(\varepsilon_1) \underline{D}^{q}(\varepsilon_1, \hat{e}_j) \times \right.$$

$$\left. \times \underline{J}_{\mu}^{q}(\varepsilon_1, \varepsilon_2) \underline{\tilde{D}}^{q}(\varepsilon_2, \hat{e}_j) \underline{\tau}_{c}^{qj,p0}(\varepsilon_2) \underline{D}^{p}(\varepsilon_2, \hat{e}_i) \right\},$$

(4.38)

with

$$\underline{\tilde{D}}^{p}(\varepsilon_1, \hat{e}) = [I + \underline{\tau}_{c}^{pp}(\varepsilon_1)(\underline{m}_p(\varepsilon_1, \hat{e}) - \underline{m}_{c,p}(\varepsilon_1))]^{-1}.$$

Or, using the below quantity

$$\underline{\tilde{J}}_{\mu}^{p,\mathrm{av}}(\varepsilon_2, \varepsilon_1) = \int d\hat{e}_i P(\hat{e}_i) \underline{D}^{p}(\varepsilon_2, \hat{e}_i) \underline{J}_{\mu}^{p}(\varepsilon_2, \varepsilon_1, \hat{e}_i) \underline{\tilde{D}}^{p}(\varepsilon_1, \hat{e}_i),$$

(4.39)

Eq.(4.38) can be reformulated as

$$\tilde{\sigma}_{\mu\mu}^{2}(\varepsilon_1, \varepsilon_2) = \frac{C}{n} \sum_{p=1}^{n} \sum_{q=1}^{n} (1 - \delta_{pq}) \sum_{j \in I(L_2)} \mathrm{tr} \left\{ \underline{\tilde{J}}_{\mu}^{p,\mathrm{av}}(\varepsilon_2, \varepsilon_1) \underline{\tau}_{c}^{p0,qj}(\varepsilon_1) \underline{\tilde{J}}_{\mu}^{q,\mathrm{av}}(\varepsilon_1, \varepsilon_2) \underline{\tau}_{c}^{qj,p0}(\varepsilon_2) \right\}.$$

From the Fourier transformed form:

$$\underline{\tau}_{c}^{p0,qj}(\varepsilon) = \frac{1}{\Omega_{\mathrm{SBZ}}} \int e^{i\vec{k}\vec{R}_j} \underline{\tau}_{c}^{pq}(\vec{k}, \varepsilon) d^2k,$$

and using the orthogonality relations

$$\sum_{j \in I(L_2)} \underline{\tau}_{c}^{p0,qj}(\varepsilon_1) \underline{\tau}_{c}^{qj,p0}(\varepsilon_2) = \frac{1}{\Omega_{\mathrm{SBZ}}} \int \underline{\tau}_{c}^{pq}(\vec{k}, \varepsilon_1) \underline{\tau}_{c}^{qp}(\vec{k}, \varepsilon_2) d^2k$$

we get for $\tilde{\sigma}_{\mu\mu}^2(\varepsilon_1, \varepsilon_2)$,

$$\tilde{\sigma}_{\mu\mu}^2(\varepsilon_1, \varepsilon_2) = \frac{C}{n\Omega_{\text{SBZ}}} \sum_{p=1}^{n} \sum_{q=1}^{n} (1 - \delta_{\text{pq}}) \times \qquad (4.40)$$

$$\int \text{tr}\left\{ \underline{\tilde{J}}_\mu^{p,\text{av}}(\varepsilon_2, \varepsilon_1) \underline{\mathcal{T}}_c^{\text{pq}}(\vec{k}, \varepsilon_1) \underline{\tilde{J}}_\mu^{q,\text{av}}(\varepsilon_1, \varepsilon_2) \underline{\mathcal{T}}_c^{\text{qp}}(\vec{k}, \varepsilon_2) \right\} d^2k.$$

Similarly, for $\tilde{\sigma}^3$ we obtain:

$$\tilde{\sigma}_{\mu\mu}^3(\varepsilon_1, \varepsilon_2) = \frac{C}{n\Omega_{\text{SBZ}}} \times$$

$$\times \sum_{p=1}^{n} \int \text{tr}\left\{ \underline{\tilde{J}}_\mu^{p,\text{av}}(\varepsilon_2, \varepsilon_1) \underline{\mathcal{T}}_c^{\text{pp}}(\vec{k}, \varepsilon_1) \underline{\tilde{J}}_\mu^{p,\text{av}}(\varepsilon_1, \varepsilon_2) \underline{\mathcal{T}}_c^{\text{pp}}(\vec{k}, \varepsilon_2) \right\} d^2k + \tilde{\sigma}_{\mu\mu}^{3\,\text{corr}}(\varepsilon_1, \varepsilon_2) \quad (4.41)$$

with

$$\tilde{\sigma}_{\mu\mu}^{3\,\text{corr}}(\varepsilon_1, \varepsilon_2) = -\frac{C}{n} \sum_{p=1}^{n} \int \int d\hat{e}_i d\hat{e}_j P_p(\hat{e}_i) P_q(\hat{e}_j) \times$$

$$\times \text{tr}\left\{ \underline{J}_\mu^p(\varepsilon_2, \varepsilon_1, \hat{e}_i) \underline{\tilde{D}}^p(\varepsilon_1, \hat{e}_i) \underline{\mathcal{T}}_c^{\text{pp}}(\varepsilon_1) \underline{D}^p(\varepsilon_1, \hat{e}_j) \underline{J}_\mu^p(\varepsilon_1, \varepsilon_2) \underline{\tilde{D}}^p(\varepsilon_2, \hat{e}_j) \underline{\mathcal{T}}_c^{\text{pp}}(\varepsilon_2) \underline{D}^p(\varepsilon_2, \hat{e}_i) \right\} =$$

$$= -\frac{C}{n} \sum_{p=1}^{n} \text{tr}\left\{ \underline{\tilde{J}}_\mu^{p,\text{av}}(\varepsilon_2, \varepsilon_1) \underline{\mathcal{T}}_c^{\text{pp}}(\varepsilon_1) \underline{\tilde{J}}_\mu^{p,\text{av}}(\varepsilon_1, \varepsilon_2) \underline{\mathcal{T}}_c^{\text{pp}}(\varepsilon_2) \right\}. \qquad (4.42)$$

Collecting all the terms, the electrical conductivity obtained from Eq.(4.23) is of the form

$$\tilde{\sigma}_{\mu\mu}(\varepsilon_1, \varepsilon_2) =$$

$$= \frac{C}{n} \sum_{p=1}^{n} \left\{ \int d\hat{e} P(\hat{e}) \, \text{tr}\left(\underline{J}_\mu^{p0}(\varepsilon_2, \varepsilon_1, \hat{e}) \underline{\mathcal{T}}_c^{\text{pp}}(\varepsilon_1) \underline{D}^p(\varepsilon_1, \hat{e}) \underline{J}_\mu^{p0}(\varepsilon_1, \varepsilon_2, \hat{e}) \underline{\mathcal{T}}_c^{\text{pp}}(\varepsilon_2) \underline{D}^p(\varepsilon_2, \hat{e}) \right) - \right.$$

$$- \text{tr}\left(\underline{\tilde{J}}_\mu^{p,\text{av}}(\varepsilon_2, \varepsilon_1) \underline{\mathcal{T}}_c^{\text{pp}}(\varepsilon_1) \underline{\tilde{J}}_\mu^{p,\text{av}}(\varepsilon_1, \varepsilon_2) \underline{\mathcal{T}}_c^{\text{pp}}(\varepsilon_2) \right) +$$

$$\left. + \frac{1}{\Omega_{\text{SBZ}}} \sum_{q=1}^{n} \int \text{tr}\left\{ \underline{\tilde{J}}_\mu^{p,\text{av}}(\varepsilon_2, \varepsilon_1) \underline{\mathcal{T}}_c^{\text{pq}}(\vec{k}, \varepsilon_1) \underline{\tilde{J}}_\mu^{q,\text{av}}(\varepsilon_1, \varepsilon_2) \underline{\mathcal{T}}_c^{\text{qp}}(\vec{k}, \varepsilon_2) \right\} d^2k \right\}. \qquad (4.43)$$

Chapter 5

Magnetic anisotropy results

5.1   Callen-Callen single-ion anisotropy

The results of Callen and Callen [68] for a single-ion anisotropy was the only theory
for the temperature dependent magnetic anisotropy until the 90s, and was used
frequently in the literature. This theory assumes that the anisotropy is confined to
a single-ion anisotropy, i.e., just the second term on the rhs. of Eq.(D.1) contains
anisotropy, assuming the exchange matrix to be isotropic. In this case the free-
energy can be written in the form [68]

$$F = F_0 + \sum_l \kappa_l \left\langle g_l(\mathbf{S}) \right\rangle,$$ (5.1)

where coefficients κ_l are regarded to be temperature independent, and $g_l(\mathbf{S})$ are l-th
order polynomials in the direction of the spin orientation $\mathbf{S}$. The g_l are defined by
the symmetry of the system, and $\langle \ldots \rangle$ refer to thermal averaging. These $g_l(\hat{n})$ can
be further expressed in terms of the spherical harmonic expansion,

$$F = F_0 + \sum_l \kappa_l \sum_m a_l^m \left\langle Y_l^m(\mathbf{S}) \right\rangle,$$ (5.2)

where $\mathbf{S}$ is the direction of the spin orientation. Choosing a frame of reference fixed
to the average magnetization direction $\hat{n}$, this can be further expressed [68] as

$$F = F_0 + \sum_l \kappa_l \left\langle Y_l^0(\mathbf{S}') \right\rangle g_l(\hat{n}),$$ (5.3)

where $\mathbf{S}'$ is the spin orientation in the frame fixed to $\hat{n}$. From this equation, it easily
can be seen that the temperature dependent anisotropy coefficients are given by

$$K_l(T) = \kappa_l \left\langle Y_l^0(\mathbf{S}') \right\rangle,$$ (5.4)

and therefore,

$$\frac{K_l(T)}{K_l(0)} = \frac{\langle Y_l^0(\mathbf{S}')\rangle_T}{\langle Y_l^0(\mathbf{S}')\rangle_0}. \tag{5.5}$$

Note that the magnetisation is the $l = 1$ case of the rhs,

$$m(T) = \frac{\langle Y_1^0(\mathbf{S}')\rangle_T}{\langle Y_1^0(\mathbf{S}')\rangle_0}. \tag{5.6}$$

Eq. 5.5 can be expressed in terms of $m(T)$ in two limiting case as was shown in Ref. [68]. For small temperatures $(m(T) \simeq 1)$

$$\frac{K_l(T)}{K_l(0)} \smile [m(T)]^{\frac{l(l+1)}{2}} \quad \text{for small } T, \tag{5.7}$$

whereas for large temperatures, close to the Curie temperature, where $m(T) \to 0$:

$$\frac{K_l(T)}{K_l(0)} \smile [m(T)]^l \quad \text{for } T \to T_c. \tag{5.8}$$

In uniaxial systems the lowest order invariant polynomial is second order, i.e., the first non-vanishing coefficient belongs to $l = 2$. Therefore the magnetic anisotropy $K(T) \propto m(T)^3$ for large m (small T), and $K(T) \propto m(T)^2$ for small m (large T).

In cubic bulk systems the lowest order invariant polynomial is of fourth order, therefore $K(T) \propto m(T)^{10}$ for large m (small T), and $K(T) \propto m(T)^4$ for small m (large T).

5.2 Computational details

The present Chapter address the calculation of the magnetic anisotropy of bulk ferromagnets, and magnetic thin films in an ab initio level. As described in Chapter (2) and (3) we implemented the DLM theory in the KKR formalism. To test the theory, we performed realistic calculations for bulk FePt, FePd and CoCu(100) thin films. The calculations were performed by using the relativistic version of the Screened KKR method (as described in appendix A) within the LSDA as parametrized by Vosko et al. [69] and the atomic sphere approximation (ASA). Self-consistent potentials were calculated both for the ferromagnetic ground state and for the paramagnetic state; these potentials then were used for the DLM calculations at finite temperatures (see below). The experimental lattice constant of bulk Cu $(a = 6.83\,a_0)$ was used, i.e., no attempt was made to include geometrical relaxations of an fcc(001) parent lattice.

For a fixed orientation of the average magnetization $\hat{n}$ and at a given temperature T, our strategy for determining the layer (denoted by p) dependent effective t–matrices $\underline{t}_p^{c(\hat{n})}$ and Weiss fields $h_p^{(\hat{n})}$ simultaneously, is as follows:

1. Choose an initial (usually uniform) set of $h_p^{(\hat{n})}$.

2. Solve the CPA condition (as described in section 2.3), with the corresponding probabilities, $P_p^{(\hat{n})}(\hat{e}_{pi})$, Eq. (2.29).

For this step we employed the method proposed by Ginatempo and Staunton [39], while we performed the integral over orientations (Eq.2.41) in terms of a cascade adaptive sampling. This turned out to be numerically very efficient when using a local frame of reference with the z axis fixed parallel to the average magnetization direction, since in that case $P_p^{(\hat{n})}(\hat{e}_{pi})$ depends just on ϑ_{pi}. The CPA loop was iterated up to a relative accuracy of 10^{-4} for $\underline{t}_p^{c(\hat{n})}$.

3. Calculate a new set of $h_p^{(\hat{n})}$ from Eq. (2.33) or (2.56).

An asymmetric sampling of 16 points on a semi–circular contour in the upper complex semi–plane was sufficient for the corresponding energy integration to achieve a relative accuracy of 10^{-4} for $h_p^{(\hat{n})}$. In order to keep this accuracy, the BZ integration of the scattering path operator ($\underline{\tau}_{pp}^{c(\hat{n})}(\mathbf{k})$) was performed by using a variable k-mesh with a maximum of 465 k-points in the irreducible (1/8) wedge of the BZ for energies close to the Fermi level.

4. Repeat steps 2 and 3 until convergence of $h_p^{(\hat{n})}$ is achieved.

By using Broyden's second modified method [70] we needed just 5–10 iterations in order to reach the above mentioned accuracy.

After having obtained well converged Weiss fields and effective t-matrices the band energy part of the magnetic anisotropy (MA) constant K_b, see Eq. (3.28), was calculated using Eq. (3.29). It turned out, however, that unlike the local moments the MA constant is very sensitive to the self-consistent potentials used. Clearly, a self-consistent calculation of the effective potentials and fields at each temperature would complete the R-DLM scheme described above. To mimic the temperature dependence of the potentials and the exchange fields, here we used an approximate procedure which at least recovers the limiting cases, i.e., $T = 0$ and $T \geq T_C$, correctly. At $T = 0$ the ferromagnetic ground state of the system is described by the self-consistent potentials and exchange fields, V_{FM}^p and B_{FM}^p, while above

the Curie temperature the system is in the paramagnetic DLM state (see section 2.4), specified by V_{PM}^p and B_{PM}^p, respectively. The temperature dependence of the potentials was then approximated by

$$V^p(T) = m_p(T)V_{FM}^p + (1 - m_p(T)) V_{PM}^p \quad , \tag{5.9}$$

and similarly for the effective fields, with $m_p(T)$ being the layer dependent average magnetization at a given temperature T, see Eq. (2.32). The parameters for the energy– and the BZ–integrations used for the Weiss fields were sufficient to achieve a relative numerical accuracy of 5 % for K_b.

5.3 Bulk anisotropy results

The relativistic version of the DLM (R-DLM) to describe ferromagnetism and magnetic anisotropy below the Curie temperature was first implemented by Julie Staunton et.al. in 2004 [71]. They investigated the $L1_0$-ordered FePt. This is a layered bulk ferromagnet, where the Fe layers provide large magnetic moments, while the Pt are non-magnetic, but exhibits large spin-orbit coupling. The exchange field of the Fe moments induce magnetic moments on the Pt atoms giving rise to a large magnetic anisotropy, because of the large spin-orbit coupling of the Pt atoms [72]. This large magnetic anisotropy made FePt to be one of the most promising material in the magnetic recording industry [4]. Staunton first determined the magnetisation-temperature curve and got 935 K for the Curie temperature in reasonable agreement with the experimental value of 750 K [73]. She calculated the magnetic anisotropy energy as the free-energy difference,

$$\text{MAE} = F^{(001)} - F^{(100)}. \tag{5.10}$$

The results plotted versus the magnetisation squared can be seen in Fig. (5.1). As can be seen from the figure apart from $0.9 < M(T)/M(0) < 1$ the results show a $K(T) \propto [M(T)]^2$ behavior in good agreement with the experiment[73], and in contrast to the Callen-Callen model, which is also shown in Fig.(5.1).

Later on we [74] investigated $L1_0 - $ FePd and got similar results as for FePt (see Fig. (5.2)). The calculated anisotropy results fit again to a $K_0[M(T)/M(0)]^2$ curve. The calculated value for the zero temperature anisotropy of $0.335\,\text{meV}$ agree well
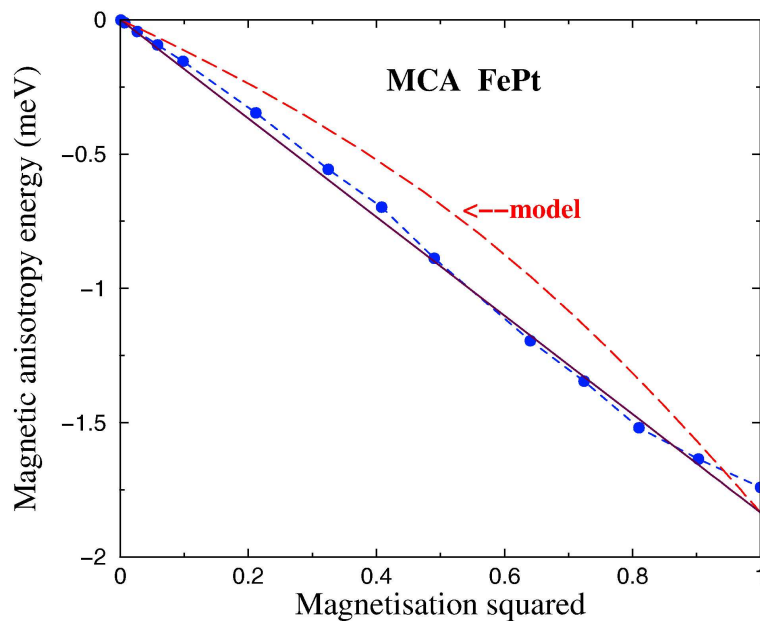
Figure 5.1: Magnetic anisotropy of $L1_0-$FePt as a function of the squared magnetisation from Ref. [71]. The filled circles are the results of R-DLM calculations, the full line refers to $K_0[M(T)/M(0)]^2$, the dashed line to the single ion model function $K_0\left\langle Y_2^0(\mathbf{S}')\right\rangle_T / \left\langle Y_2^0(\mathbf{S}')\right\rangle_0$ (see Eq.5.5) with $K_0 = -1.835\,\mathrm{meV}$.

with the experimental result of 0.373 meV [75], exhibiting an out-of-plane preferred magnetization direction. We also calculated the second and fourth order anisotropy parameters (see Eq.3.17), from the magnetic torque in two different orientation. For $\vartheta_1 = \pi/4, \varphi_1 = 0$ the torque (Eq.3.18) $T_\vartheta = -(K_2 + K_4)$, while for $\vartheta_1 = \pi/3, \varphi_1 = 0$ we obtain $T_\vartheta = -\frac{\sqrt{3}}{2}(K_2 + \frac{3}{2}K_4)$. The gained results show that K_4 is an order of magnitude smaller than K_2, which agrees with the general theory that the anisotropy constants tends to zero with increasing order [76]. The deviation from the Callen-Callen single ion model results were explained in terms of anisotropic exchange interactions.

Lowering the chemical order in $L1_0$-FePt (randomly interchanging Fe and Pt atoms) cause a decrease in the magnetic anisotropy. The totally disordered $Fe_{50}Pt_{50}$ solid solution has an order of magnitude smaller anisotropy than the ordered $L1_0$ phase. Indeed, the disordered $Fe_{50}Pt_{50}$ has cubic symmetry, i.e., fourth order anisotropy. The anisotropy coefficient K_1 in Eq.(3.4) can be determined using the DLM from the torque

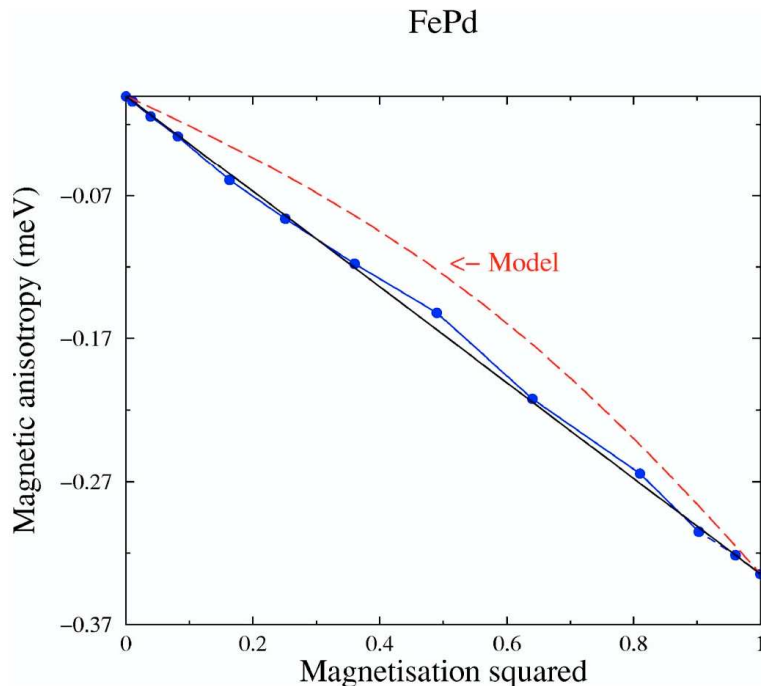$$T_\varphi(\vartheta = \pi/2, \varphi = \pi/8) = \frac{K_1}{2}. \tag{5.11}$$

44

FePd

Figure 5.2: Magnetic anisotropy of $L1_0-$FePd as a function of squared magnetisation from Ref. [74]. The filled circles denote the results of R-DLM calculations, the full line refers to $K_0[M(T)/M(0)]^2$, and the dashed line depicts the function proposed by the single ion model function $K_0 \langle Y_2^0(\mathbf{S'}) \rangle_T / \langle Y_2^0(\mathbf{S'}) \rangle_0$ (see Eq.5.5) with $K_0 = -0.335 meV$.

The results for K_1 are shown in Fig.(5.3). The Callen-Callen model predicts $K(T) \propto m^4$ for small m, and $K(T) \propto m^{10}$ for $m \to 1$. Quite contradictory the R-DLM results give $K(T) \propto m^4$ for small m and vary as m^7 for large m. Fig.(5.3) also shows for comparison the behavior of both the single ion anisotropy model with an anisotropy energy-term $k \sum_i \left(e_{x,i}^2 e_{y,i}^2 + e_{y,i}^2 e_{z,i}^2 + e_{z,i}^2 e_{x,i}^2 \right)$ and an anisotropic exchange model $1/2 \Delta J \sum_{i,j} \left(e_{x,i}^2 e_{y,j}^2 + e_{y,i}^2 e_{z,j}^2 + e_{z,i}^2 e_{x,j}^2 \right)$ with $k = \Delta J = 8.4 \mu$ eV . As can be seen from the figure, the ab initio results can be understood from an interpretation based on a predominantly anisotropic exchange interactions.

5.4 Application to Co films on Cu(001)

Ferromagnetic Co films are known to grow epitaxially on Cu(100) due to the small lattice mismatch and show a strong in-plane magnetic anisotropy [77][78]. As this system is experimentally and theoretically well–studied it is most suitable for an application of the relativistic-DLM (R-DLM) scheme for layered systems. We per-
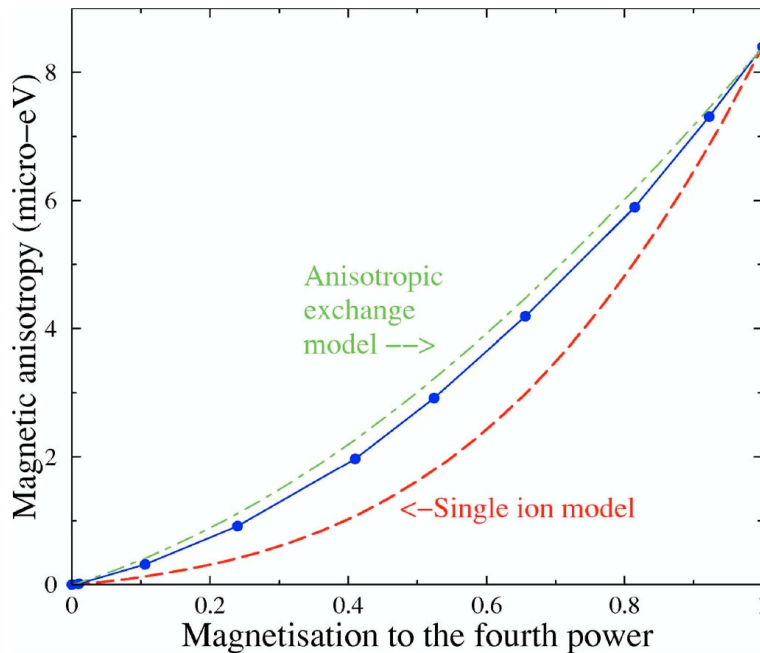
Figure 5.3: The magnetic anisotropy constant of the cubic magnet chemically disordered $Fe_{50}Pt_{50}$, as a function of fourth power of the magnetisation from Ref. [74]. The filled circles show the result of the ab initio theory, the dashed line the single ion anisotropy model, and dotted-dashed line is the solution of an anisotropic exchange model.

formed calculations for film thicknesses of $n=1$ to 6 monolayers.

In Figure 5.4 the calculated layer dependent magnetizations are shown as a function of the temperature for the case of the Co_4 film. As can be inferred from this figure the magnetization in all layers vanishes at $T_C=960$ K. Interestingly, however, the shape of the curves differs from layer to layer: the largest overall magnetization corresponds to the surface layer (S), the lowest to the interface layer $(S-3)$. This behavior can be attributed to a well known tendency of enhanced ferromagnetism [25][79] (i.e., enhanced Weiss fields) at the surface due to the reduced coordination of the Co atoms, while at the interface a weakening of the magnetic interactions is expected due to hybridization between the electronic states of the Co and Cu atoms.

This reasoning can be justified by comparing the DLM results with the mean–field solution of a classical Heisenberg spin model. Supposing isotropic exchange interactions, J_{pq}, the mean–field energy is of simple form,

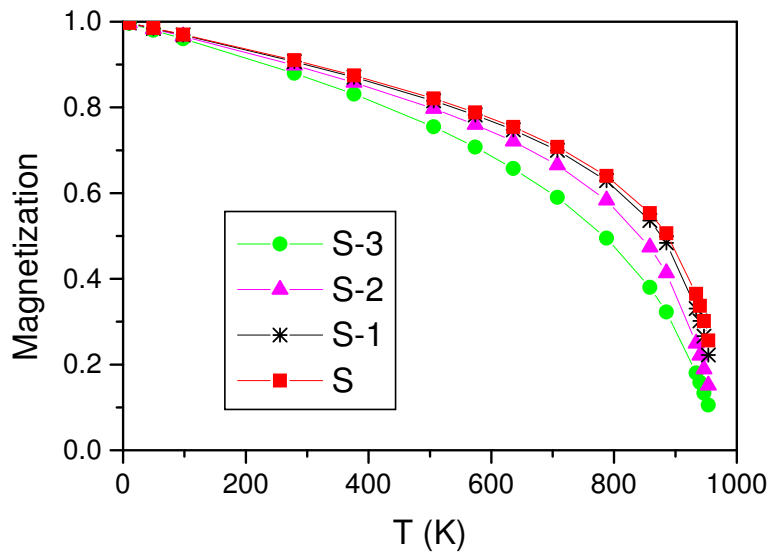$$H_{MF} = -\frac{1}{2}\sum_{pq} m_p\, J_{pq}\, m_q \quad , \tag{5.12}$$

Figure 5.4: Average magnetizations, m_p, see Eq. (2.32), versus temperature for $Co_4/Cu(100)$ as obtained from the R-DLM calculations. The label S refers to the surface Co layer, while $S - n$ ($n = 1, 2, 3$) to the n-th Co layer under the surface.

while the corresponding Weiss-field,

$$h_p = \sum_q J_{pq}\, m_q \quad , \tag{5.13}$$

can be used together with Eq. (2.32) to determine the average magnetizations, m_p, as a function of the temperature. Fig. 5.5 shows that the corresponding results with parameters J_{11}=155 meV, J_{22}=90 meV, J_{33}=70 meV , J_{44}=115 meV, J_{12}=J_{34}=100 meV, and J_{23}=70 meV (labels 1, 2-3, 4 indexing the surface layer, the in between layers and the layer adjacent to the substrate, respectively) fit well to the results obtained from the DLM calculations. From this model study it obviously turned out that the asymmetry of the exchange parameters, in particular, $J_{11} > J_{44}$, and $J_{22} > J_{33}$, is the main source of the asymmetry of the magnetizations, since by choosing $J_{11} = J_{44}$, and $J_{22} = J_{33}$ this asymmetry is completely removed.

From Fig.(5.5) it is obvious that the magnetisation, correspondingly, also the Weiss-fields vanish at about 950 K. This temperature is clearly associated with the Curie temperature of the $Co_4Cu(100)$ film. In Fig 5.6 we plotted the Curie temperatures calculated for different Co layer thicknesses. These values are consistent with those of Szunyogh and Udvardi [25] obtained from a mean field solution of a Heisenberg-model containing exchange parameters as calculated in the paramagnetic DLM state. Razee et al. [23] derived the Curie temperature of $Co_n/Cu(100)$
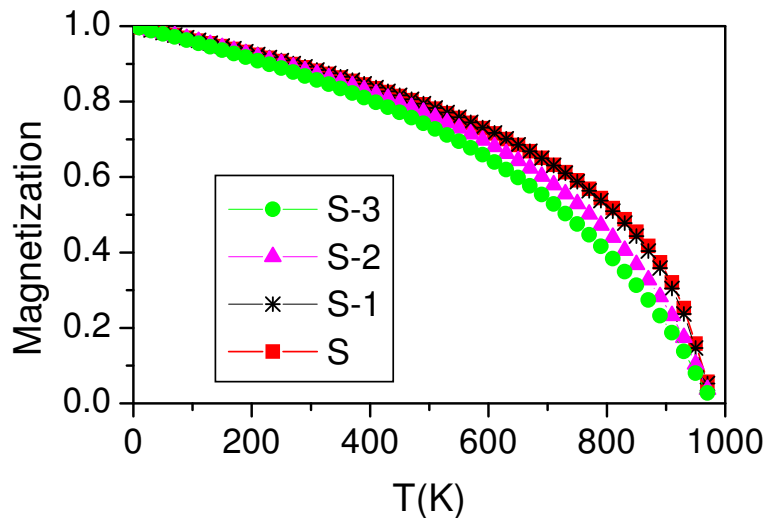
47

Figure 5.5: Average magnetizations, m_p, see Eq. (2.32), versus temperature for $Co_4/Cu(100)$ as obtained from a mean–field solution of an isotropic Heisenberg model (see text for the exchange parameters used). The label S refers to the surface Co layer, while $S - n$ ($n = 1, 2, 3, 4$) to the n-th Co layer below the surface.

by directly evaluating the spin-susceptibility from the paramagnetic DLM state. Although a smaller Curie temperature for the monolayer case was reported, for thicker layers they obtained roughly the same results as here.

Experimentally much smaller Curie temperatures were measured, in particular, for very thin layers, while T_C increased with increasing film thickness according to a power law [77][78]. The reason for the disagreement with respect to experiment can be attributed either to the mean-field approximation used in the ab-initio DLM theories that is most critical for very thin layers, or to incomplete layer growth in the experimental studies, again most critical for thin layers. The experimental value of about 950 K for large thicknesses of Co (Ref. [78]) is, however, in good agreement with our present results. Experimentally the investigation of sharp surfaces was possible only until 3-4 monolayer thickness, because of the Co-Cu intermixing on the phase boundary at higher temperatures.

In terms of a spin-wave theory and by using estimated bulk parameters for the magnetization and the exchange field, Bruno [81] obtained about 200 K for T_C of the $Co_1/Cu(001)$ system. Pajda et al. [82] performed first-principles calculations for the exchange parameters, J_{ij}, in the ferromagnetic ground-state of $Co_1/Cu(001)$ and showed that by solving the Heisenberg spin-model within the Random Phase
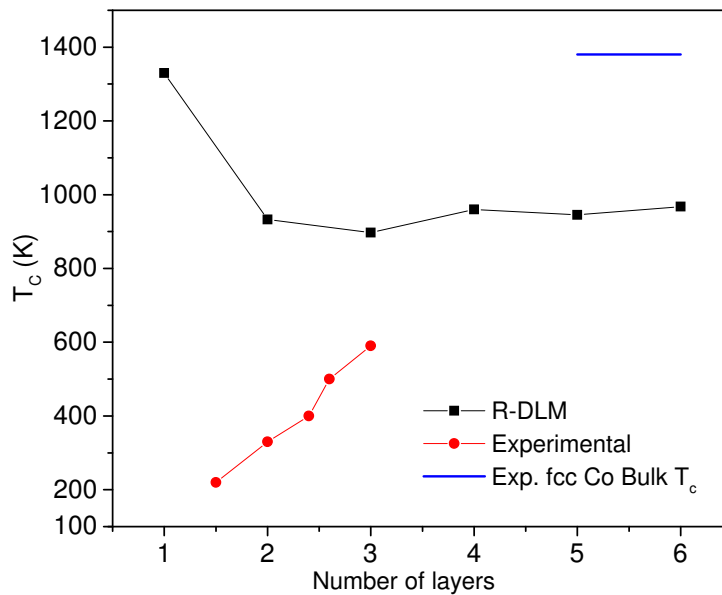
Figure 5.6: Curie temperature versus Co layer thickness on Cu(100) surface. The experimental results from Ref [80][78]. The blue line shows the experimental bulk Co Curie temperature.

Approximation (RPA) reduces the calculated T_C to 426 K as compared to a value of 1043 K predicted by the mean-field theory. In a recent review [83]} Jensen and Bennemann showed that a strong enhancement of the exchange coupling in the surface layer can lead to a considerable deviation from the power scaling law for T_C and can result even in an enhancement for very thin magnetic layers. This observation qualitatively explains the trend to be seen in Fig.5.6 .

In Fig. 5.7 the calculated band energy contributions of the magnetic anisotropy energy, K_b, are plotted as a function of temperature. The corresponding values near $T=0$ are consistent with previous calculations of Szunyogh et.al. for the ground state in terms of the relativistic Screened KKR method showing quite large fluctuations with respect to the layer thickness (see Fig. 1 of Ref. [16]). Similar to the bulk systems studied before [71][74] the MA constant decreases in the monolayer case almost monotonically in magnitude with increasing temperature. For thicker films, however, $K_b(T)$ shows a non-monotonic temperature behavior with a more or less pronounced maximum. In addition, for the cases of $n \geq 3$, $K_b(T)$ also changes sign at a given temperature. This kind of behavior did not show up in early studies based on the Callen-Callen model or in ab-initio calculations [71][74][72] of $K_b(T)$.
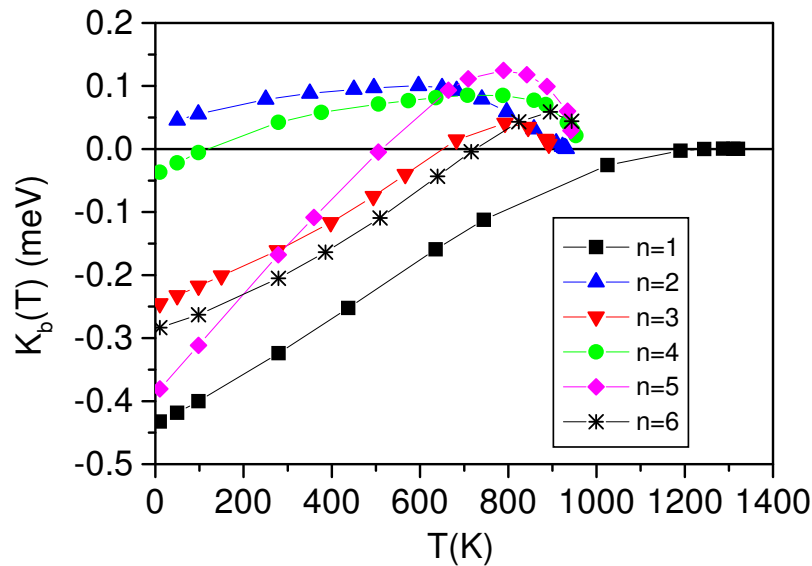
Figure 5.7: Band energy part of the magnetic anisotropy constant $K_b(T)$ for $Co_n/Cu(100)$

In order to explain this unusual result we again used a classical Heisenberg spin model, which includes terms arising from relativistic (spin-orbit coupling) effects to describe magnetic anisotropy. These include not only on-site anisotropies, K_p, but also anisotropic exchange interactions, $J_{pq}^{xx} \neq J_{pq}^{zz}$. As shown in Appendix D the anisotropy of the mean–field free–energy is given by

$$K = F^x - F^z = -\frac{1}{2} \sum_{pq} m_p \left(J_{pq}^{xx} - J_{pq}^{zz} \right) m_q + \sum_p K_p \left(\frac{3}{\beta h_p} m_p + 1 \right) \quad . \quad (5.14)$$

This equation was used to fit the exchange anisotropies, $\Delta J_{pq} = J_{pq}^{zz} - J_{pq}^{xx}$, and the on-site anisotropies, K_p, to the $K_b(T)$ values obtained from the R-DLM calculations. Note that in order to reduce the number of fitting parameters, unlike the interpretation of the layer dependent magnetizations, in here we restricted ourselves to exchange parameters being symmetric with respect to layers. Indeed, from our tests, we found the moderate asymmetry of the magnetizations, see Fig. 5.5, to have only a very little effect on the MA constants obtained from the spin model. Furthermore, for some cases we also checked our results by comparing them with a full solution within the mean–field theory [84], i.e., by using the canonical partition function with an exact account of the on-site anisotropies and of the orientational dependence of the magnetizations, and obtained a nearly perfect agreement between the two approaches.

The fitted parameters are listed in Table 5.1, while in Fig. 5.8 the corresponding magnetic anisotropies, Eq. (5.14), are shown. As can be seen, the MA constants obtained from the spin model compare qualitatively well with the DLM results, Fig. 5.7. Inferring the parameters in Table 5.1 it is obvious that the exchange anisotropies, ΔJ_{pq}, are of the same order of magnitude as the on-site anisotropy energies, K_p, but of opposite sign. Clearly from Eq.5.14 the exchange anisotropy part of the MAE is proportional to m^2 while the on-site anisotropy term follows the Callen-Callen behavior, i.e., $K \propto m^2$ for small m, and $K \propto m^3$ for large m. Thus, an interplay of these two terms in an itinerant electron system can lead to a thermal reorientation transition.

n	Parameters
1	$J_{11}^z = 336$, $\Delta J_{11} = 0.36$, $K_1 = -0.615$
2	$J_{11}^z = J_{22}^z = 136$, $\Delta J_{11} = 0.36$, $J_{12}^z = 100$, $\Delta J_{12} = 0.64$, $K_1 = -0.37$, $K_2 = -0.615$
3	$J_{11}^z = J_{33}^z = 136$, $\Delta J_{11} = \Delta J_{33} = 0.36$, $J_{22}^z = 60$, $\Delta J_{22} = 0$, $J_{12}^z = J_{23}^z = 100$, $\Delta J_{12} = \Delta J_{23} = 0.4$, $K_1 = -0.37$, $K_2 = -0.425$, $K_3 = -0.615$
4	$J_{11}^z = J_{44}^z = 136$, $\Delta J_{11} = \Delta J_{44} = 0.36$, $J_{22}^z = J_{33}^z = 60$, $\Delta J_{22} = \Delta J_{33} = 0$, $J_{12}^z = J_{34}^z = 100$, $\Delta J_{12} = \Delta J_{34} = 0.23$, $J_{23}^z = 60$, $\Delta J_{23} = 0$, $K_1 = -0.37$, $K_2 = 0$, $K_3 = -0.37$, $K_4 = -0.615$
5	$J_{11}^z = J_{55}^z = 136$, $\Delta J_{11} = \Delta J_{55} = 0.36$, $J_{22}^z = J_{33}^z = J_{44}^z = 60$, $\Delta J_{22} = \Delta J_{33} = \Delta J_{44} = 0$, $J_{12}^z = J_{45}^z = 100$, $\Delta J_{12} = \Delta J_{45} = 0.8$, $J_{23} = J_{34} = 60$, $\Delta J_{23} = \Delta J_{34} = 0$, $K_1 = -0.37$, $K_2 = -0.37$, $K_3 = -0.37$, $K_4 = -0.615$, $K_5 = -0.615$,
6	$J_{11}^z = J_{66}^z = 136$, $\Delta J_{11} = \Delta J_{66} = 0.36$, $J_{22}^z = J_{55}^z = 60$, $\Delta J_{22} = \Delta J_{55} = 0$, $J_{33}^z = J_{44}^z = 20$, $\Delta J_{33} = \Delta J_{44} = 0$, $J_{12}^z = J_{56}^z = 100$, $\Delta J_{12} = \Delta J_{56} = 0.36$, $J_{23}^z = J_{34}^z = J_{45} = 60$, $\Delta J_{23} = \Delta J_{34} = \Delta J_{45} = 0$, $K_1 = -0.37$, $K_2 = 0$, $K_3 = 0$, $K_4 = 0$, $K_5 = -0.4$, $K_6 = -0.615$

Table 5.1: Model parameters, J_{pq}, $\Delta J_{pq} = J_{pq}^{zz} - J_{pq}^{xx}$, and K_p, see Eqs. (5.13) and (5.14), fitted to the temperature dependent MA constants of the $Co_n/Cu(100)$ films as obtained from the R-DLM calculations. All parameters are given in units of meV.

In order to demonstrate this effect we performed model calculations for the MA constants of the $Co_3/Cu(100)$ system by uniformly scaling the exchange anisotropies, $\Delta J_{pq} = x\Delta J_{pq}^{fit}$, and the on-site anisotropies, $K_p = yK_p^{fit}$, with ΔJ_{pq}^{fit} and K_p^{fit} taken from Table 5.1. As a constraint we kept the MA constant at $T=0$ fixed, from which the scaling factors y can uniquely be determined as a function of x. The corresponding MA constant vs. T curves are plotted for selected x values in Fig. 5.9. As can be seen in this figure, by decreasing the exchange anisotropy the MA constant gradually decreases and the reorientation transition completely disappears below
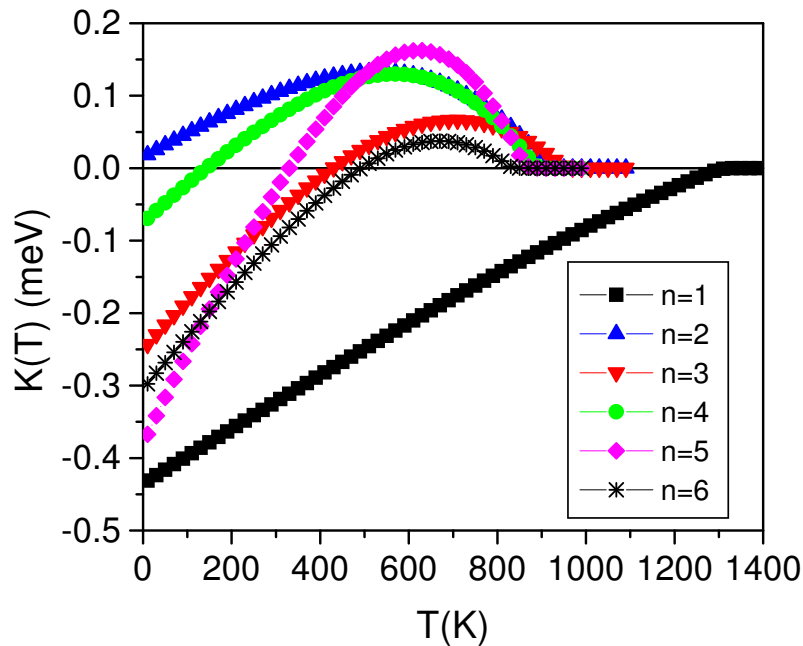
Figure 5.8: Magnetic anisotropy constants vs. temperature obtained from a mean-field approach of the Heisenberg model, Eq. (5.14), with the fitted parameters listed in Table 5.1.

about $x=0.5$. For vanishing exchange anisotropy, $x=0$, the Callen-Callen behavior is recovered. In the case of $\Delta J_{pq} = -0.2 \Delta J_{pq}^{fit}$, similar to the $L1_0$-FePt and FePd systems [74]. a nearly $K \propto m^2$ dependence over the whole temperature regime is obtained. Thus the remarkably different behavior of $K(T)$ for different itinerant metallic magnets, i.e., $L1_0$-FePt and FePd vs. Co_n/Cu(100), can be interpreted as an effect of different magnitudes and, in particular, of different signs of the exchange anisotropies with respect to the corresponding on-site anisotropies.

As mentioned in Chapter 3 the total magnetic anisotropy energy is obtained by adding the magnetic dipole-dipole contribution, see Eq. (3.34), to the band energy part, $K_b(T)$. The corresponding results can been seen in Fig. 5.10. Since for layered systems $K_{dd}(T)$ is always negative, favouring thus an in-plane magnetization, except in the two-monolayer case, the total MA constants are shifted to negative values over almost the entire temperature range. Since, however, $K_{dd}(T)$ is proportional to $M(T)^2$ which goes to zero very rapidly at T_C, and since as shown above $K_b(T)$ exhibits a maximum, $K(T)$ slightly overshoots to positive values near T_C. This behavior is most pronounced for $n = 2$, where $K(T) > 0$ between 350 K and T_C (=933 K).
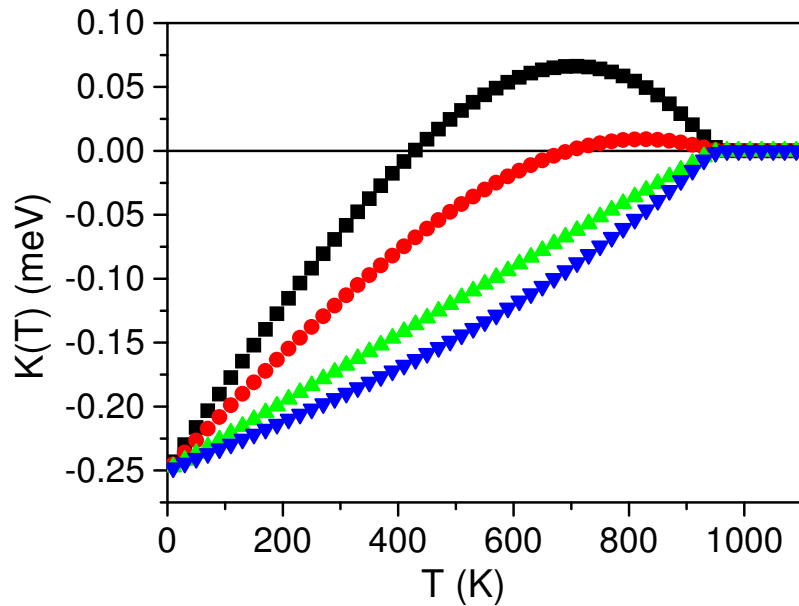
Figure 5.9: Magnetic anisotropy constant of the $Co_3/Cu(100)$ system vs. temperature obtained from a mean-field approach to the Heisenberg model and scaling the exchange anisotropies, $\Delta J_{pq}=x\Delta J_{pq}^{fit}$, with ΔJ_{pq}^{fit} from Table 5.1 and the on-site anisotropies accordingly (see text), Black squares: $x=1$, red circles: $x=0.5$, green up-triangles: $x=0.0$, blue down-triangles: $x = -0.2$.

Theoretically, such a temperature dependence of the MA constant implies a reorientation transition from an in-plane orientation to an out-of-plane orientation of the magnetization. However, as can bee seen in Fig. 5.10 the positive values of $K(T)$ are very small and might be reduced by quite a few circumstances such as growth conditions, interface mixing, surface relaxations and stresses, or domain formation, which in turn make it difficult to relate this prediction to experiments. Indeed, so far such an inverse reorientation has not been found for Co films on Cu(001).
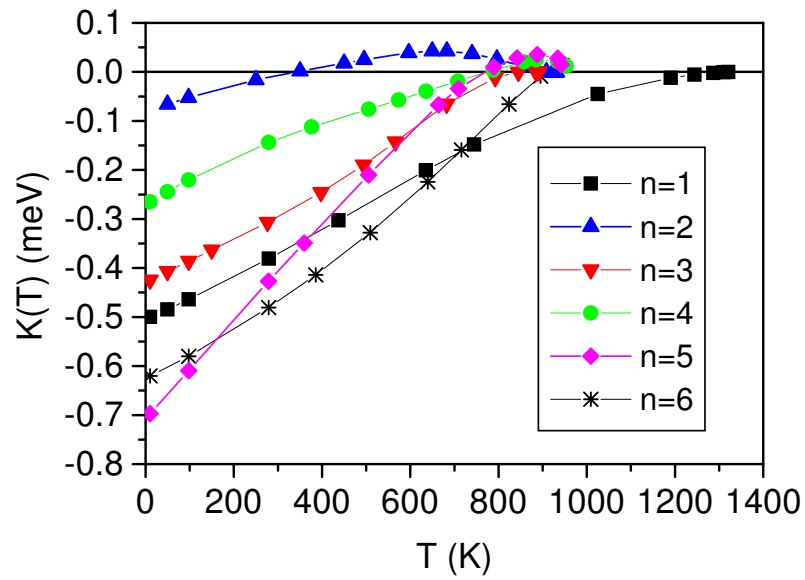
Figure 5.10: Calculated total magnetic anisotropy constant, $K(T) = K_b(T) + K_{dd}(T)$, as a function of temperature for $Co_n/Cu(100)$.

Chapter 6

Magnetic pattern formation in magnetic monolayers

We have seen in the former chapter that the exchange interaction is not necessarily isotropic, and an anisotropic exchange interaction can lead to an unusual temperature dependence of the magnetic anisotropy. The exchange matrix can have not only symmetric but also antisymmetric terms, which gives rise to the so-called Dzyaloshinskii-Moriya [85][86] interaction. We investigated the effect of this interaction on the magnetic ordering of a Mn monolayer on a W surface. It should be noted that for this structure a spin-spiral ground state was observed experimentally [87] .

6.1   The Dzyaloshinskii-Moriya interaction

In general a second order classical spin Hamiltonian can be written as

$$H = \sum_i \mathbf{s_i} K_{ij} \mathbf{s}_j + \frac{1}{2} \sum_{i \neq j} \mathbf{s}_i \mathfrak{J}_{ij} \mathbf{s}_j, \qquad (6.1)$$

where K_{ij} stands for the on-site anisotropy matrix, and $\mathfrak{J}_{ij}$ are 3×3 exchange matrices. It is evident, that the exchange matrices can be chosen such that

$$\mathfrak{J}_{ij} = \mathfrak{J}_{ji}^t, \qquad (6.2)$$

where t index refers to the transposed matrix. The exchange matrix can be further decomposed as

$$\mathfrak{J}_{ij} = J_{ij} \underline{I} + \mathfrak{J}_{ij}^S + \mathfrak{J}_{ij}^A , \qquad (6.3)$$

where $\underline{I}$ is the unit matrix,

$$J_{ij} = \frac{1}{3} \operatorname{Tr}(\mathfrak{J}_{ij}) , \tag{6.4}$$

the symmetric traceless part is defined by

$$\mathfrak{J}_{ij}^{S} = \frac{1}{2} \left(\mathfrak{J}_{ij} + \mathfrak{J}_{ij}^{t} \right) - J_{ij}\underline{I} , \tag{6.5}$$

while the antisymmetric part of $\mathfrak{J}_{ij}$, $\mathfrak{J}_{ij}^{A}$ is

$$\mathfrak{J}_{ij}^{A} = \frac{1}{2} \left(\mathfrak{J}_{ij} - \mathfrak{J}_{ij}^{t} \right) . \tag{6.6}$$

Since a multiplication with a 3×3 antisymmetric matrix can always be written as a vector cross-product, the second term on the rhs. of Eq.(6.1) can therefore reformulated as

$$\mathbf{s}_i\mathfrak{J}_{ij}\mathbf{s}_j = J_{ij}\mathbf{s}_i\mathbf{s}_j + \mathbf{s}_i\mathfrak{J}_{ij}^{S}\mathbf{s}_j + \mathbf{D}_{ij}(\mathbf{s}_i \times \mathbf{s}_j). \tag{6.7}$$

In here the $\mathbf{D}_{ij}$ are the so called Dzyaloshinskii-Moriya vectors,

$$\mathbf{D}_{ij}^{x} = \frac{1}{2} \left(\mathfrak{J}_{ij}^{yz} - \mathfrak{J}_{ij}^{zy} \right) , \quad \mathbf{D}_{ij}^{y} = \frac{1}{2} \left(\mathfrak{J}_{ij}^{xz} - \mathfrak{J}_{ij}^{zx} \right) , \quad \mathbf{D}_{ij}^{z} = \frac{1}{2} \left(\mathfrak{J}_{ij}^{xy} - \mathfrak{J}_{ij}^{yx} \right) . \tag{6.8}$$

The last term of the exchange interaction

$$H_{\mathrm{DM}} = \sum_{ij} \mathbf{D}_{ij}(\mathbf{s}_i \times \mathbf{s}_j), \tag{6.9}$$

first introduced by Dzyaloshinskii [85], and Moriya [86].

It can be seen from Eq.(6.7) and Eq.(6.1) that the symmetric isotropic part of the exchange interaction J_{ij} prefers a parallel orientation of neighboring spins, namely a ferromagnetic or an antiparallel (antiferromagnetic) alignment depending on the sign of J_{ij}, but without preference of any global direction. The $\mathfrak{J}_{ij}^{S}$ is responsible for the magnetic anisotropy, preferring some crystalline orientation of the magnetic moments. The Dzyaloshinskii-Moriya (DM) interaction (Eq.6.9) tends to rotate the spins because this term is minimal for perpendicular spins. The ground state of the actual system is determined by the competition between all these three terms, which therefore in many cases can lead to noncollinear spin-structure. The DM interaction arises from spin-orbit coupling, and varies linear with it [88]. In bulk crystals the inversion symmetry implies a symmetrical exchange matrix, i.e., in systems with inversion symmetry there is no DM interaction. In case of thin films or surfaces the

inversion symmetry no longer is present and therefore might gives rise to large DM interactions.

The parameters of the Hamiltonian Eq.(6.7) i.e. the on-site anisotropy parameters and the elements of the $\mathfrak{J}_{ij}$ exchange matrices can be obtained from ab initio KKR calculations, as described in details by Udvardi et. al [42]. This authors used the torque method[89], i.e., calculated the derivatives of the free-energy with respect to the rotation of two specific spins. The corresponding derivatives can be calculated within the KKR theory. From these derivatives the whole exchange matrix $\mathfrak{J}_{ij}$, and the on-site anisotropy parameters can be obtained[42].

6.2 Mn monolayer on W surface

6.2.1 Experimental results

As was already mentioned the DM interaction arises in systems with low symmetry. A good candidate for such a system is a Mn monolayer on a bcc W (110) surface. The magnetic ground state of this system was studied experimentally by Bode et.al. [87], who used spin-polarized scanning tunneling microscopy (SP-STM) to study the magnetic properties of the surface, which showed a periodic modulation with a wavelength of 12 nm, i.e., the Mn layer is not in the usual antiferromagnetic (AFM) state. By varying the orientation of the magnetic moment of the Fe STM-tip, they could distinguish between the spin density wave state, where all the magnetic moments are parallel, and just the magnitude of the moments is modulated, and a so called spin spiral structure, where the direction of the magnetic moments varies periodically (see Fig (6.1)). The spin spirals that are confined to a plane perpendicular or parallel to the propagation direction are called as helical spirals (h-SS) or cycloidal spirals (c-SS), respectively.

6.2.2 Multiscale modeling

We investigated the magnetism of a Mn monolayer on W(100) and W(110) surface theoretically by means of Monte Carlo (MC) simulations. First the parameters appearing in a model Hamiltonian are determined by first principles calculations.
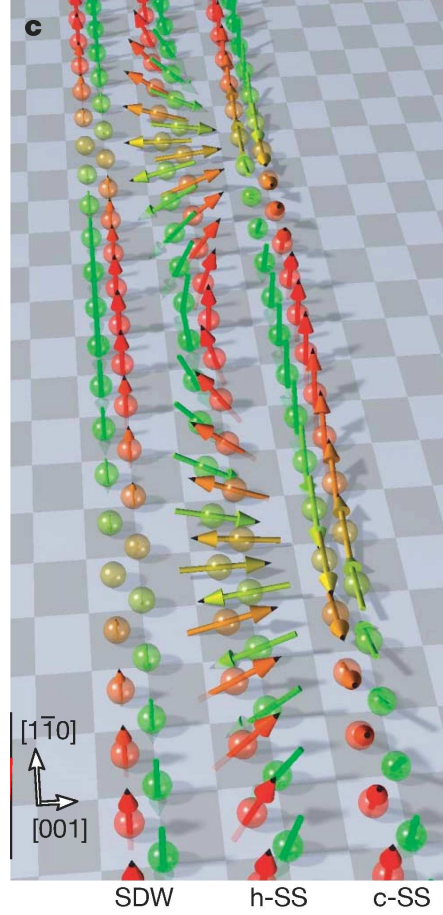
Figure 6.1: The view of the spin-structures from Ref.[87]: spin density wave (SDW), helical spiral (h-SS) and cycloidal spiral (c-SS)

The classical Heisenberg Hamiltonian, Eq.(6.1), now takes the form

$$H = \frac{1}{2} \sum_{i \neq j} \mathbf{s}_i \mathfrak{J}_{\mathrm{ij}} \mathbf{s}_j + \sum_i \left(K_x s_{\mathrm{ix}}^2 + K_y s_{\mathrm{iy}}^2 \right), \tag{6.10}$$

where K_x and K_y are the bi-axial on-site anisotropy constants. Quite clearly, for a bcc(001) surface $K_x = K_y$. In the case of a bcc(110) surface the x and y in-plane directions correspond to the $(1\bar{1}0)$ and the (001) crystal axes and, in general, $K_x \neq K_y$.

We calculated the parameters entering the Hamiltonian (6.10) in terms of the relativistic spin-polarized Screened Korringa-Kohn-Rostoker (SKKR) method (see Appendix A). In particular, the $\mathcal{J}_{ij}$ have been obtained by using the torque method as described above. From a decomposition of the tensorial exchange it turned out that the most relevant parts are the isotropic exchange interactions, J_{ij}, and the

58

DM interactions.

Using the Hamiltonian (6.10) we performed MC simulations on a 32×32 two-dimensional lattice with periodic boundary conditions. The low-temperature spin-state of the system has been searched in terms of simulated annealing starting from the completely disordered state at high temperatures.

Results Subsequent to a self-consistent determination of the effective potentials and exchange fields we calculated the exchange interactions for a large number of atomic pairs of the Mn monolayer. The experimental lattice constant of bcc W was used, i.e., no attempts were made to account for lattice relaxations. Note that the first nearest neighbor (1NN) distance of the Mn atoms is 0.32 nm. The isotropic exchange interactions and the lengths of DM vectors for the first few NN's are listed in Table 6.1. Excluding the effect of the DM interactions, due to the dominating negative 1NN exchange interactions the ground-state of Mn/W(001) is ferromagnetic, see also Eq. (6.10). Because of the positive on-site anisotropy constant, $K_x = K_y$=0.047 mRyd, we obtained the magnetic moments in this state to be aligned normal-to-plane for Mn/W(001). In the case of Mn/W(110), the strong antiferromagnetic 1NN interactions give rise to a chequerboard c(2×2) antiferromagnetic structure and the calculated anisotropy constants, K_x=-0.047 mRyd and K_y=-0.037 mRyd, imply that the magnetic moments are parallel to the (1$\overline{1}$0) axis.

Table 6.1: Calculated isotropic exchange interactions, J_{ij}, and magnitudes of the DM vectors, D_{ij} (all in mRyd), for the first few nearest neighbors (NN) of a Mn monolayer on W(001) and on W(110) .

System	Mn/W(001)			Mn/W(110)				
NN	1	2	3	1	2	3	4	5
J_{ij}	-3.91	1.10	0.12	7.30	-3.84	-0.85	2.17	-1.38
D_{ij}	0.57	0.04	0.24	0.09	0.22	0.03	0.23	0.20

Inspecting Table (6.1) it is obvious that some of the DM vectors are almost by an order of magnitude larger than the corresponding anisotropy energies and only by an order of magnitude smaller than the largest isotropic exchange interactions. This is, however, not surprising since in terms of perturbation theory the DM inter-

actions and the uniaxial anisotropy appear in first and second order of the spin-orbit coupling strength, respectively.

Because of the twofold rotational symmetry around the z axis that applies for all the pair of sites for both the square and primitive rectangular 2-dimensional lattices the z component of the DM vectors disappears. The DM vectors, all being parallel to the plane, are depicted in Fig. (6.2). As is obvious, in the case of Mn/W(001) the DM vectors referring to atomic pairs along a given direction ($\pm x$ or $\pm y$) are parallel to each other, thus their effect to misalign the spins is enhanced. On the contrary, due to the reduced symmetry the DM vectors exhibit a higher complexity for Mn/W(110) as their spatial distribution shows an apparent asymmetry.

By using the above parameters, including also the antisymmetric DM interactions in Hamiltonian (6.10), we performed MC simulations for both systems. The magnetic patterns we obtained for a sufficiently low temperature, $k_B T = 0.02|J|$ ($J = \sum_j J_{ij}$), are shown in Fig. 6.3. In the case of Mn/W(001) we find that the ferromagnetic order is nearly maintained along the (110) direction, whereas a spin-spiral propagating along the ($1\bar{1}0$) direction evolves with a wavelength of about 2.2 nm. The formation of this spin-spiral is the consequence of the large and competing DM vectors between NN's along the x and y axes.

In the case of Mn/W(110), the large asymmetry of the DM interactions seen in Fig. 6.2 gives rise to a cycloidal spin-spiral along the ($1\bar{1}0$) direction that modulates the underlying antiferromagnetic arrangement. The estimated wavelength of this spin-spiral is about 7.2 nm. Although one half of this wavelength should be compared with the periodicity of about 6 nm seen recently for the same monolayer system in SP-STM images [87], the agreement between our simulations and the experiment is quite satisfactory. In addition, a different theoretical approach used in Ref. [87] predicted a wavelength of 8 nm for this spin-spiral rather close to our value.

6.2.3 Analytical calculation

Using the parameters of table 6.1 we can try to write up a model classical spin Hamiltonian of the magnetic layer, using only interactions between first and second nearest neighbour sites, neglecting the interactions between sites far from each other. Determining the minimum point of this Hamiltonian we get the wave length of the ground state spin spiral. For simplicity we deal just with the MnW(100)
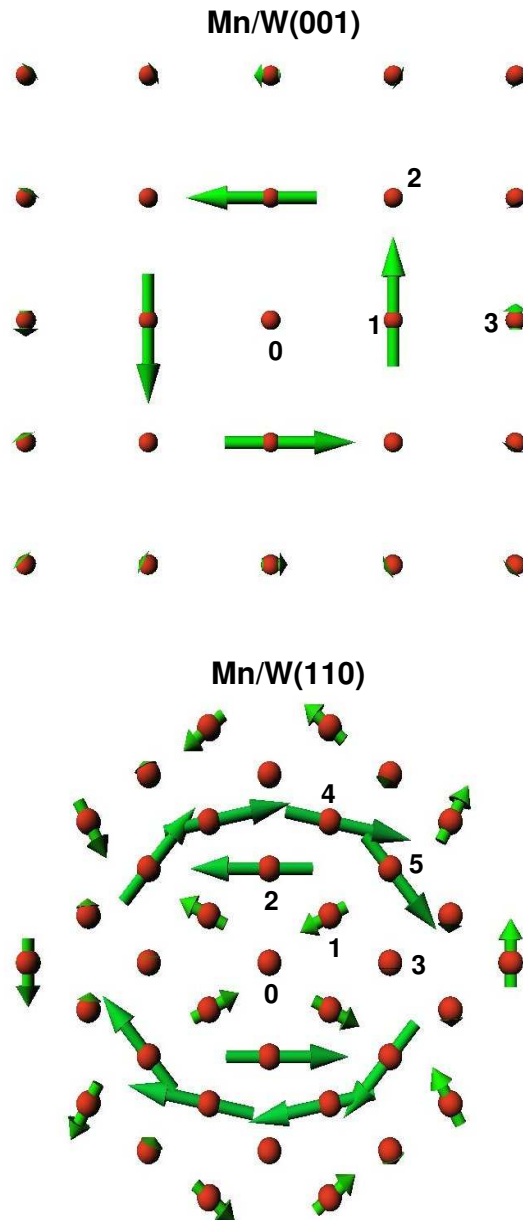
Figure 6.2: Sketch of the Dzaloshinskii-Moriya vectors (green arrows) correspond-
ing to a central atom (labelled by 0) and its nearest neighbors. Selected nearest
neighbors are labelled by the same numbers as in Table 6.1.

system. As can be seen from table (6.1), the leading order exchange interaction are
between site-pairs (0-1) and (0-2) where the indexing is according to Fig.(6.2), and
the largest DM interaction acts between (0-1) and (0-3) therefore the Hamiltonian
can be approximated as

$$E(\{\vec{S}\}) = \sum_R K \, (S_R^z)^2 - \frac{1}{2} \left\{ \sum_{|\mathbf{R}-\mathbf{R'}|=a} J_1 \vec{S}_R \vec{S}_{R'} + \sum_{|\mathbf{R}-\mathbf{R'}|=\sqrt{2}a} J_2 \vec{S}_R \vec{S}_{R'} + \right.$$

$$\left. + \sum_{|\mathbf{R}-\mathbf{R'}|=a} \vec{D}_{\vec{R}-\vec{R'}} \vec{S}_R \times \vec{S}_{R'} + \sum_{|\mathbf{R}-\mathbf{R'}|=2a} \vec{D}_{\vec{R}-\vec{R'}} \vec{S}_R \times \vec{S}_{R'} \right\}, \qquad (6.11)$$

where $\vec{R}$ is the two dimensional square lattice vector

$$\vec{R} = (n_x a, n_y a, 0) \qquad n_x, n_y \in \mathbb{Z}, \qquad (6.12)$$

with lattice parameter a, and $\vec{S}_R$ is the spin vector on site $\vec{R}$. According to the ab initio results of the KKR calculations, the largest DM vectors, which are taken into account (see Fig.(6.2))

$$\vec{D}_{(a00)} = (0, D_1, 0), \quad \vec{D}_{(-a,0,0)} = (0, -D_1, 0), \qquad (6.13)$$

$$\vec{D}_{(0,a,0)} = (-D_1, 0, 0), \quad \vec{D}_{(0,-a,0)} = (D_1, 0, 0),$$

$$\vec{D}_{(2a,0,0)} = (0, D_2, 0), \quad \vec{D}_{(-2a,0,0)} = (0, -D_2, 0),$$

$$\vec{D}_{(0,2a,0)} = (-D_2, 0, 0), \quad \vec{D}_{(0,-2a,0)} = (D_2, 0, 0),$$

where $D_1 = 0.57$ mRyd, $D_2 = 0.24$ mRyd. The on site anisotropy $K = -0.047$ mRyd, and the exchange parameters $J_1 = 3.91$ mRyd , $J_2 = -1.1$ mRyd.

It is easy to see that in the ferromagnetic state, when all $\vec{S}_R \parallel \hat{z}$ the energy per unit cell is

$$E_0 = K - 2(J_1 + J_2). \qquad (6.14)$$

helical spin-spiral state The helical spin-spiral state can be described by the wave vector

$$\vec{q} = (q_x, q_y, 0), \qquad (6.15)$$

and the spin moments perpendicular to it, namely

$$S_{n_x,n_y}^x = \frac{q_y}{\sqrt{q_x^2 + q_y^2}} \sin(q_x n_x a + q_y n_y a), \qquad (6.16)$$

$$S_{n_x,n_y}^y = -\frac{q_x}{\sqrt{q_x^2 + q_y^2}} \sin(q_x n_x a + q_y n_y a), \qquad (6.17)$$

$$S^z_{n_x,n_y} = \cos(q_x n_x a + q_y n_y a). \qquad (6.18)$$

With these forms the terms appearing in Eq.6.11 can be get by lengthy, but straightforward calculations

$$\sum_R K\,(S^z_R)^2 = K \sum_{n_x,n_y} \cos^2(q_x n_x a + q_y n_y a), \qquad (6.19)$$

$$\sum_{|\mathbf{R}-R'|=a} J_1 \vec{S}_R \vec{S}_{R'} = 2J_1 \sum_{n_x,n_y} \{\cos(q_x a) + \cos(q_y a)\}, \qquad (6.20)$$

$$\sum_{|\mathbf{R}-R'|=\sqrt{2}a} J_2 \vec{S}_R \vec{S}_{R'} = 2J_2 \sum_{n_x,n_y} \cos(q_x a)\cos(q_y a), \qquad (6.21)$$

$$\sum_{|\mathbf{R}-R'|=a} \vec{D}_{\vec{R}-\vec{R'}} \vec{S}_R \times \vec{S}_{R'} = \frac{2D_1}{\sqrt{q_x^2+q_y^2}}(q_y \sin(q_x a) - q_x \sin(q_y a)) \qquad (6.22)$$

$$\sum_{|\mathbf{R}-R'|=2a} \vec{D}_{\vec{R}-\vec{R'}} \vec{S}_R \times \vec{S}_{R'} = \frac{2D_2}{\sqrt{q_x^2+q_y^2}}(q_y \sin(2q_x a) - q_x \sin(2q_y a)) \qquad (6.23)$$

therefore the energy per site in the helical spin-spiral state is in case $\mathbf{q} < \infty$:

$$E = \frac{K}{2} - J_1[\cos(q_x a) + \cos(q_y a)] - J_2 \cos(q_x a)\cos(q_y a)-$$

$$-\frac{D_1}{\sqrt{q_x^2+q_y^2}}(q_y \sin(q_x a) - q_x \sin(q_y a)) - \frac{D_2}{\sqrt{q_x^2+q_y^2}}(q_y \sin(2q_x a) - q_x \sin(2q_y a)), \quad (6.24)$$

where we used that for infinite number of sites

$$\frac{1}{N}K \sum_{n_x,n_y} \cos^2(q_x n_x a + q_y n_y a) = \frac{K}{2}.$$

Using a mathematical program like MATLAB we can investigate the the minimum point of Eq.(6.24) in the space of (q_x, q_y). We found that the energy minimum is in $(q_x, q_y) = (0,0)$ i.e. the ferromagnetic state has lower energy than the helical spin-spiral structure.

Cycloidal spin spiral   The spin vector of the cycloidal spin spiral state is given by

$$\vec{S}_{n_x,n_y} = \frac{\vec{q}}{\sqrt{q_x^2+q_y^2}} \sin(q_x n_x a + q_y n_y a) + \vec{e}_z \cos(q_x n_x a + q_y n_y a), \qquad (6.25)$$

and similar calculations as above show that the energy per unit cell can be written as

$$E = \frac{K}{2} - J_1[\cos(q_x a) + \cos(q_y a)] - J_2 \cos(q_x a)\cos(q_y a) -$$

$$-\frac{D_1}{\sqrt{q_x^2 + q_y^2}}(q_x \sin(q_x a) + q_y \sin(q_y a)) - \frac{D_2}{\sqrt{q_x^2 + q_y^2}}(q_x \sin(2q_x a) + q_y \sin(2q_y a)), \quad (6.26)$$

with numerical calculations can be showed that the above expression has minimum at

$$(q_x, q_y) = \frac{1}{a}(0.18, 0.18) \tag{6.27}$$

from which the wave length of the spin-spiral is

$$\lambda = \frac{2\pi}{|\vec{\mathbf{q}}|} = 24.7a. \tag{6.28}$$

This result seemingly doesn't agree perfectly with the results of the MC simulations (see upper part of Fig(6.3)), which gives a helical-like spin spiral ground state with a wavelength of about $11a$, however the propagation direction $(1\bar{1}0)$ is in agreement with the former results. This disagreement probably the effect of the neglected terms in the model Hamiltonian Eq.(6.11). This problem is a subject of further investigations.
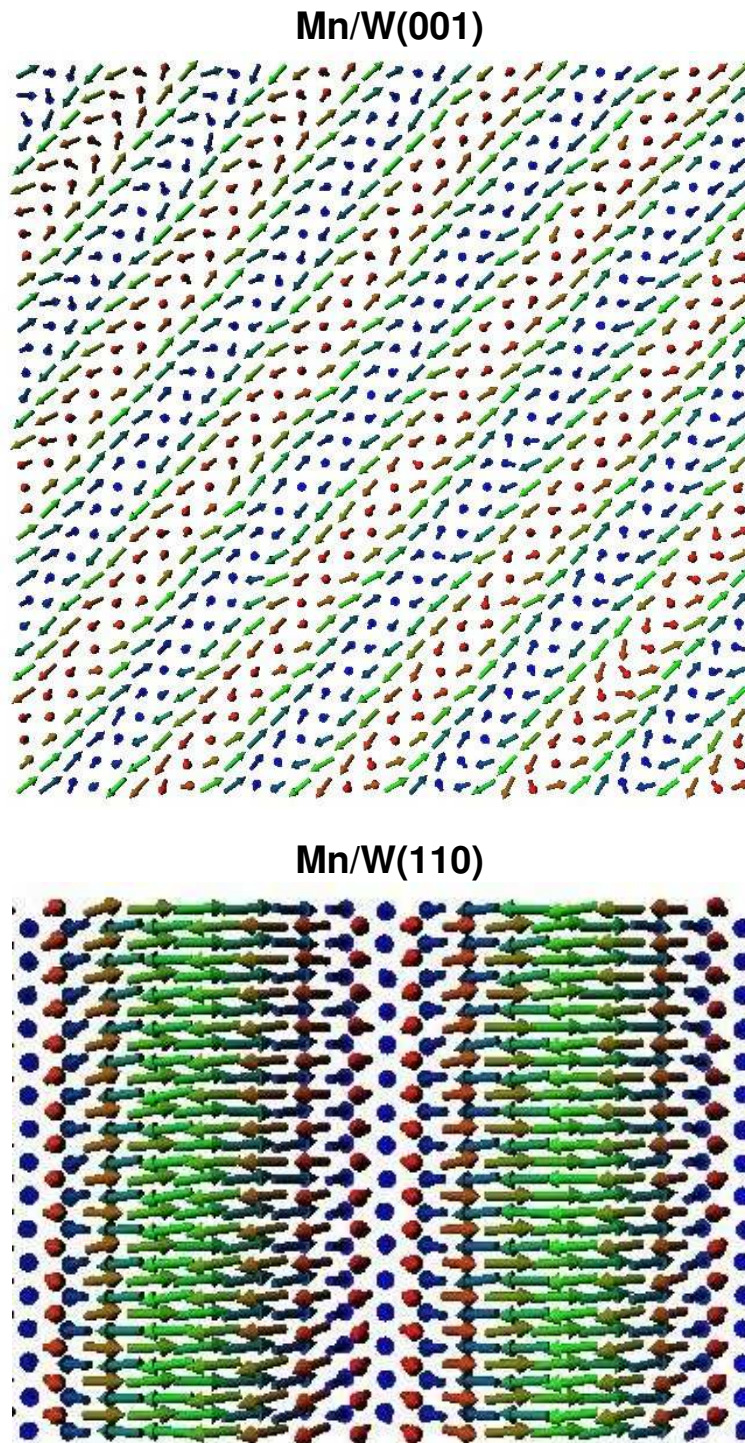
Mn/W(001)

Mn/W(110)

Figure 6.3: Schematic view of the low-temperature spin structures of Mn/W(001) and Mn/W(110) as obtained from the MC simulations. Blue, green and red arrows denote spins pointing downwards, in-plane and upwards, respectively

Chapter 7

Transport results

7.1 Motivation

Spintronics is a new field of electronics, which is not based on the conduction of electrons or holes as in semiconductor devices, but relies on the magnetization dependence of transport properties in magnetic nanostructures, controlled by magnetic field. One of the first and main important topic of spintronics is the giant magnetoresistance (GMR), discovered independently in 1988 in the laboratory of Albert Fert [3] and Peter Grünberg [2]. GMR devices are constructed from multilayers of magnetic and nonmagnetic metals. The GMR is in nutshell the dependence of the resistivity on the parallel or antiparallel alignment of the neighboring magnetic layers. In case of parallel alignment, the scattering in one of the spin channel (let's say spin up) the magnetic scattering is low. In the antiparallel aligning the scattering (and therefore the resistivity) is large for both spin channels. The GMR ratio is defined by [90]

$$\text{GMR} = \frac{R^{\text{AP}} - R^P}{R^P}, \tag{7.1}$$

where $R^{\text{AP}(P)}$ is the resistivity of the anti-parallel (parallel) state. The fact that the IBM started the mass production of GMR based disk drives in 1997 clearly show the fast application of the 10 years earlier discovered phenomena. Today nearly all all disk drives in the industry incorporate the GMR read-head design [8]. In 2007 Fert and Grünberg won the Nobel Prize for their discovery.

The GMR was investigated theoretically by Peter Weinberger and László Szunyogh using the Kubo-Greenwood formalism with the KKR method [29]. They calculated the GMR in

underlayer$[55\dot{A}]$ NiFe$[10\dot{A}]$ CoFe$[10\dot{A}]$ Cu$[y\dot{A}]$ CoFe$[10\dot{A}]$ Ru$[10\dot{A}]$ multilayers on zero temperature.

On larger temperatures the GMR ratio decrease considerably [91]. Assuming that the phonon-electron interaction $(R_{\text{ph}-e})$, impurity scattering (R_i) and magnetic (R_M) part additively contributes to the total resistivity the resistivity on a finite temperature

$$R^{P(\text{AP})}(T) = R_M^{P(\text{AP})}(T) + R_i + R_{\text{ph}-e}(T), \tag{7.2}$$

where the impurity and phonon scattering contribution independent of the parallel or antiparallel alignment. Therefore the temperature dependent GMR

$$\text{GMR}(T) = \frac{R_M^{\text{AP}}(T) - R_M^{P}(T)}{R_M^{P}(T) + R_i + R_{\text{ph}-e}(T)}, \tag{7.3}$$

depends only through the denominator on the temperature dependent phonon-electron coupling contribution. The aim of the current project was to develop a theoretical and computational tool to calculate the magnetic part of the temperature dependent conductivity of ferromagnetic metals, which can be a promising tool to calculate the temperature dependent GMR(T) for realistic magnetic multilayers.

7.2 Computational details

We calculated the magnetic part of the conductivity from the formula Eq.(4.23) using Eq.(4.43). For the $\vec{\mathbf{k}}$ integration in Eq.(4.43) we used a quadrature with 1600 point in the two-dimensional Brillouin zone, which gave converged results. In practice the $\tilde{\sigma}(\varepsilon_F \pm i\delta, \varepsilon_F \pm i\delta)$ in Eq.(4.23) are calculated for some finite imaginary part δ for an intermediate region consists of n atomic layers. The effect of considering a finite number of atomic layers is a $\left(\frac{1}{n}\right)$-like decay [28] in the calculated resistivity

$$\varrho_{\mu\mu}(n, \delta) = \frac{1}{\sigma_{\mu\mu}(n, \delta)} \approx \varrho_{\mu\mu}(\delta) + \frac{\Delta\varrho_{\mu\mu}(\delta)}{n}. \tag{7.4}$$

Therefore plotting $n\varrho_{\mu\mu}(n, \delta)$ versus n the slope of the curve for large n gives $\varrho_{\mu\mu}(\delta)$ which is equal with the $n \to \infty$ bulk resistivity value. It turned out, that $n\varrho_{\mu\mu}(n, \delta)$ is already linear in n for $n \geqslant 50$ layers, so we determined $\varrho_{\mu\mu}(\delta)$ from the slope of the fitted linear curve in the $n \geqslant 50$ regime. For the δ dependence of the resistivity we also found linear dependence, such as described in the literature [92][30] i.e. this

can be obtained from a linear extrapolation

$$\varrho_{\mu\mu} = \lim_{\delta \to 0} \varrho_{\mu\mu}(\delta). \tag{7.5}$$

For this extrapolation we used the $\varrho_{\mu\mu}(\delta)$ values at $\delta =1$ and 2 mRyd. The magnetisation direction was chosen to be perpendicular to the layers ($\hat{z}$ direction). An anisotropy $\varrho_{zz} \neq \varrho_{xx} = \varrho_{yy}$ arise from the relativistic treatment, and from the numerical error. This anisotropy turned out to be very small (smaller than 1 $\mu\Omega cm$) for the whole temperature region. So from now on when we neglect the index μ, and we confine ourselves to the ϱ_{zz} component of the resistivity.

7.3   Results for Fe and Co

First we calculated the temperature dependent Weiss fields, which are needed for the finite temperature thermal averaging in Eq.(4.43). With the experimental lattice parameter (5.4 a.u.) with the DLM we got too large Curie-temperature (T_C) for pure bcc Fe (1670 K), which is 60% larger than the experimental T_C (1040 K). This error is most probably the shortcoming of the mean-field approximation. Using smaller lattice parameter, the T_C is decreasing monotonously and the experimental T_C is obtained at 5.07 a.u.. In Fig. (7.1) we plotted the calculated T_C for Fe versus the lattice parameter used in the calculations. We have to mention that the lattice parameter at the Curie temperature is even larger than at zero temperature because of the heat extension. (According to Ref [93](Chapter 1.1.2.2) it is 5.55 a.u.) LDA gives a smaller lattice parameter than the experiments (5.3 a.u. [94]). Using this lattice parameter and a nonrelativistic DLM Györffy et.al. [20] found 1250 K Curie temperature for Fe from the divergence of paramagnetic spin-susceptibility.

We chose Co as the second test system for our electric transport calculations. Co has a phase transition by about 600-800 K from hcp to fcc structure. We neglected the difference in the resistivity of the two lattice structure, and calculated for every temperature only with the fcc geometry. At zero temperature the experimental and theoretical LDA lattice parameters differ less than 1%, and give 6.69 a.u. (3.53 $\mathring{A}$) [94] . However the lattice parameter at T_c is larger: 6.84 a.u.[93] . The DLM considerably underestimate the Curie temperature of bcc Co, even with the experimental lattice parameter at T_c (6.84 a.u.) we get only 950 K for T_c. The experimental T_c
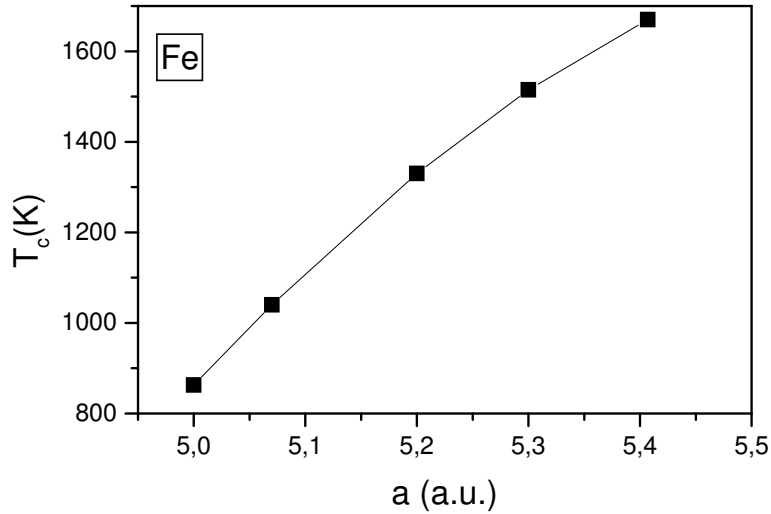
Figure 7.1: Calculated Curie temperature for Fe with different lattice parameters. The experimental zero temperature lattice parameter is 5.4 a.u., the experimental Curie temperature is 1040K.

is 1380 K, which we can reproduce in terms of the DLM using a lattice constant of 7.04 a.u..

With a fixed geometry we calculated selfconsistent potentials for the paramagnetic DLM state. With these potentials we calculated the Weiss fields as described in Chapter (2) for specific temperature points. With these Weiss fields we calculated the temperature dependent electrical conductivity, Eq.(4.23). However, for small temperatures the ferromagnetic potential (what we get solving the KKR equations selfconsistently without DLM) describes the electronic structure better. It turned out, that the difference between the ferromagnetic and paramagnetic potential doesn't influence the conductivity results considerably. In Fig.7.3 the results for pure Fe are plotted. In there we show the results with the experimental lattice parameter corresponding to an overestimated Curie temperature, and those for the reduced lattice parameter, recovering the experimental Curie temperature. For comparison we also show the experimental total resistivity values taken from Ref. [93]. One can approximate the magnetic part for the resistivity similarly to Ref. [95], assuming that well above the Curie temperature only phonon-electron interactions contribute to the resistivity. By using the Bloch-Grüneisen form, we can fit the parameters in Eq.(4.1) to the linear part of the experimental Fe resistivity above T_c. Subtracting this Bloch-Grüneisen term from the total resistivity we get a guess for
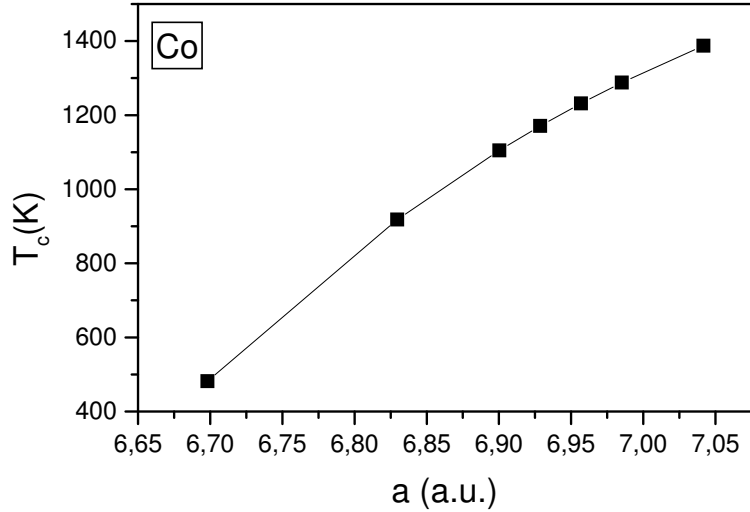
Figure 7.2: DLM results for the Curie temperature of fcc Co with different lattice parameters. The experimental Curie temperature is 1380K, where the lattice parameter is 6.84 a.u.[93].

the magnetic resistivity, also displayed in Fig.(7.3) . We have to stress, that this approximation, however, used by Weiss and Marotta[95] for several magnetic metals, is still not well justified, since using this procedure magnon-phonon interactions are neglected [32]. In fact, the magnetic disorder scattering contribution to the total resistivity is not measurable.

It can be seen in Fig.(7.3) that the DLM gives the right order of magnitude of the magnetic resistivity, however, systematically overestimates that. The deviation between the calculated resistivities with the two different lattice parameters is less than 40% for room temperature, and for temperatures far below the Curie temperature. The DLM result for the experimental lattice parameter fits well to the experimental total resistivity for temperatures below about 700 K, but we have to stress, that the total resistivity is larger than the pure magnetic contribution. We have to mention, that the DLM gives constant magnetic resistivity in the paramagnetic phase since the probability density function is constant (i.e., temperature independent) there.

We also investigated bulk Co. As we mentioned before, for computational reasons we just calculated the fcc structure. We plotted the results in fig 7.5. It can be seen, that the DLM results with different lattice parameters are within 30% difference below 700 K. The common feature of the calculated curves are the bending up
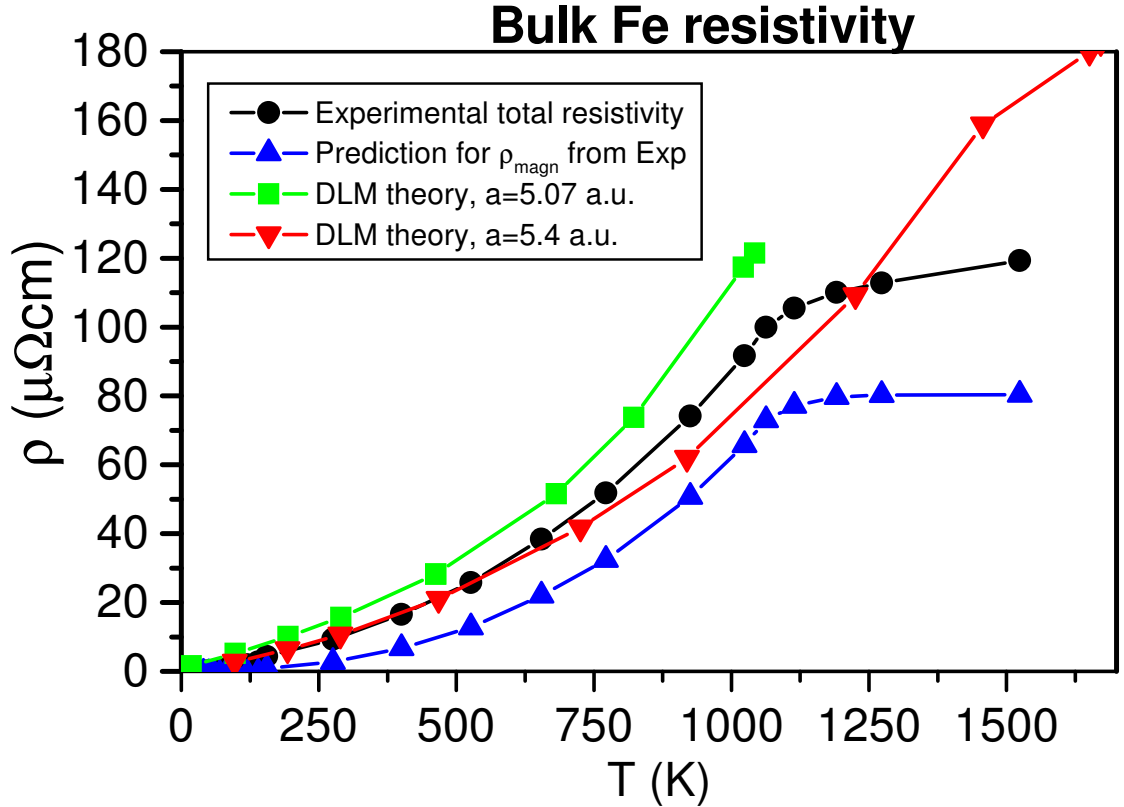
Figure 7.3: Fe resistivity. Black circle: experimental total resistivity from ref [93]. Blue up-triangle: the magnetic part of the resistivity with detaching the phonon-electron contribution assuming Bloch-Grüneisen form. Red down triangle: Our results with the experimental 5.4 a.u. lattice parameter. Green squares: the same with 5.07 a.u. lattice parameter.

right below the Curie temperature. This can be the consequence of the mean field approach that neglects the magnetic short range order above (and right below) the Curie temperature. However the magnetic disorder resistivity still has temperature dependence in the paramagnetic phase following from the smooth vanishing of the short range order [96]. We can see that the computed resistivity curves are above the experimental total resistivity with about 50-100% below 700 K, but we have to stress that the experimental curve shows the total resistivity. Here the above mentioned method to subtract the phonon-electron contribution by fitting the Bloch-Grüneisen formula doesn't work well, because after the subtraction we would get negative value for the magnetic resistivity under 600K as we show in Fig7.4 what is senseless in our opinion.
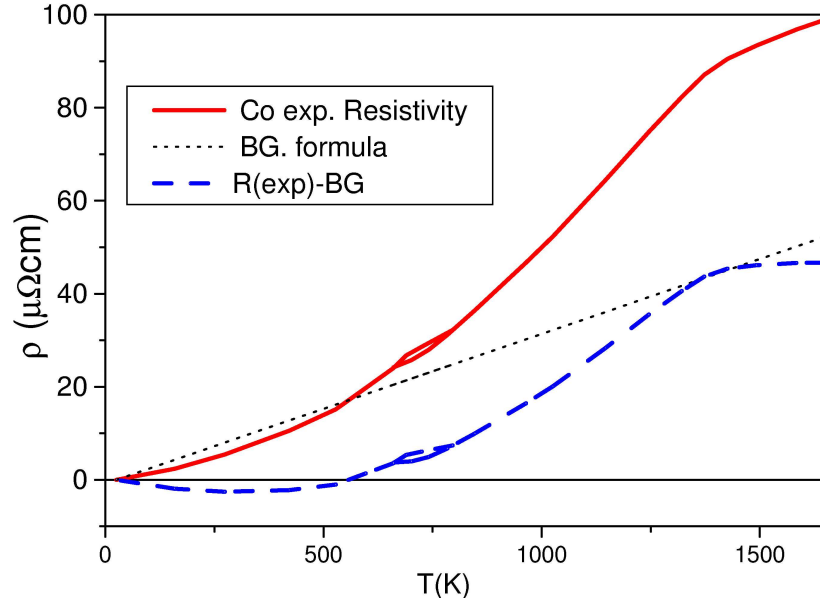
Figure 7.4: Experimental resistivity of Co (red straight curve) ref [93]. The fitted Bloch-Gr*ü*neisen (BG) function (black dotted). The difference of the experimental curve and the BG curve (blue dashed), which is the approximation of the magnetic part of the resistivity is negative under 500 K.

However, Weiss and Marotta[95] used this method to get the high temperature (saturated) magnetic resistivity of Co and gained a value of 50 $\mu\Omega$ cm. The main deficiency of this procedure is probably the consequence of the difference in the phonon-electron contribution in the hcp and fcc phase. From the paramagnetic phase resistivity slope only conclusions for the phonon-electron contribution of the fcc phase can be gained. On the other hand the temperature range between the Curie temperature and the melting point can be too small to saturate the magnetic resistivity, making it difficult to detach the linear phonon-electron contribution. From this reason in Fig (7.5) we just show the experimental total resistivity.

Although our DLM approach overestimates the magnetic part of the resistivity, we have to stress that this is the first parameter-free ab-initio result in the literature. It's failure emerges from the inaccurate determination of the Curie temperature and probably also the inaccurate description of the spin-spin correlation in the mean-field approximation. We have to mention that in case of chemically disordered systems, a more accurate description can be given by taking into account the vertex corrections [67]. Tulip et.al. [97] recently used the nonlocal CPA [98] approximation in the Kubo formalism to investigate the effect of the short range order in the resistivity of
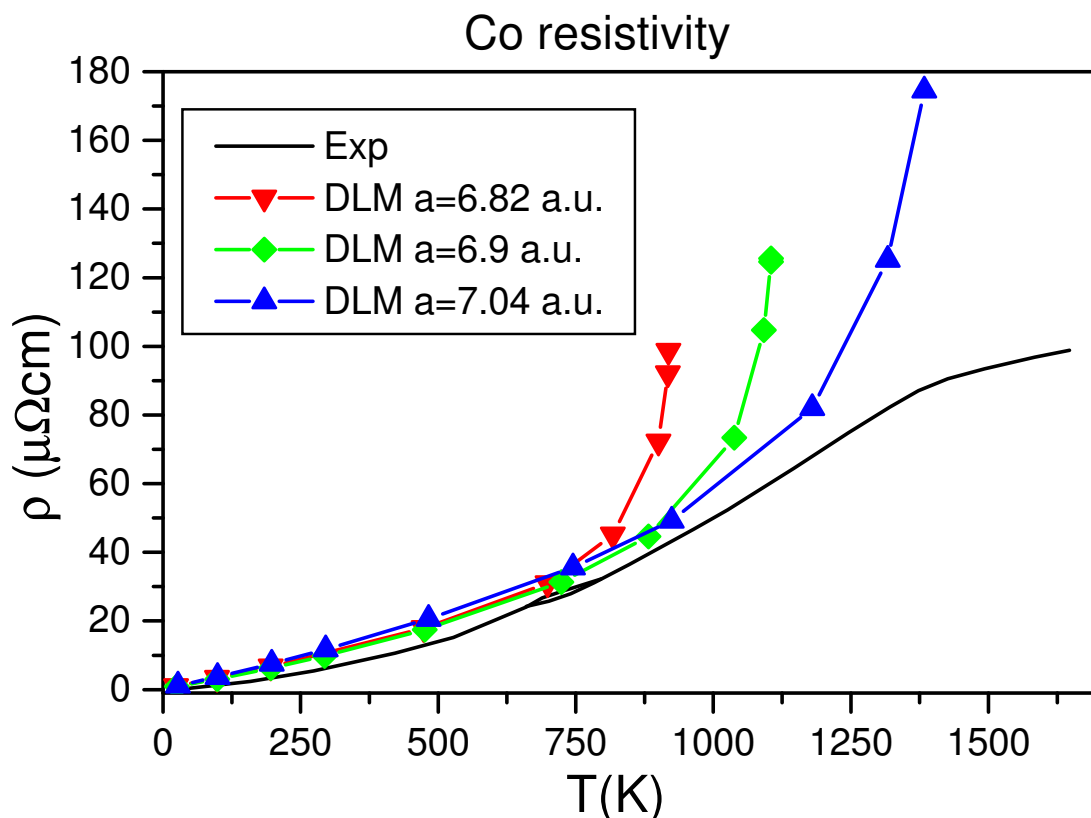
Figure 7.5: Magnetic resistivity of Co. DLM calculations with fcc lattice parameter 6.82 a.u. (red down triangle), 6.9 a.u. (green diamond) 7.04 a.u. (blue upper triangle). Experimental[93] result is is plotted by straight black.

disordered bulk alloys. They chose $Cu_c Zn_{1-c}$ alloy as a test system. In Fig.(2.) of their paper [97] it can be seen, that taking into account the vertex corrections the resistivity is reduced by about a factor of two. The resistivity is further reduced by taking into account the short range order by using the nonlocal CPA method instead of the single-site CPA. Based on the analogy between the "chemical"-CPA and the "spin-disorder"-CPA we expect that the correct calculation of vertex corrections, and a correct description of the short range order in the ferromagnet would reduce our result for the temperature dependent resistivity.

Chapter 8

Conclusion

In this thesis for the first time ever, attempts were made to describe at an ab initio level the temperature dependence of the magnetic anisotropy energy and to extend the formulation to the electrical transport properties. The relativistic version of the disordered local moment scheme were implemented within the screened KKR formalism, which allowed to calculate the temperature dependent magnetic anisotropy of layered structures, and thin films. We tested the developed theory on CoCu(100) structures, and found, that the results can be interpreted with an anisotropic Heisenberg model. We stressed the importance of the anisotropic part of the exchange correlation matrix, which can lead to the unusual temperature dependence of the magnetic anisotropy. In thin films the symmetry allows not only anisotropic symmetric, but antisymmetric part of the Heisenberg exchange matrix, which is responsible for the Dzyaloshinskii-Moriya (DM) interaction. To study this interaction we investigated the Mn monolayer on W surface. We got in agreement with the experiments, that the DM interaction leads to a spin spiral magnetic ground state. We further implemented the DLM scheme in the Kubo-Greenwood equation to calculate the temperature dependence of the magnetic part of the electrical resistivity. My work is the first ab initio approximation for the description of the temperature dependent spin-disorder scattering. To our knowledge no other such attempts have been presented in the literature, although both aspects, magnetic anisotropies and related transport properties are a matter of particular importance in any technological use of "spintronics" and in view of magnetic recording media.

The proposed theoretical methods are easily extendable to alloyed systems, which are commonly used in technical applications. The present applications therefore also

can be viewed as illustrations for the theoretical means applied.

Appendix A

The Density Functional Theory (DFT)

A.1 Hohenberg-Kohn Theorems

The Hamilton operator of an N electron system in the Born-Oppenheimer approximation is given by

$$\hat{H} = \hat{T} + \hat{U} + \hat{W} = -\frac{\hbar^2}{2m} \sum_{i=1}^{N} \nabla_i^2 + \sum_{i=1}^{N} u(\mathbf{r}_i) + \frac{1}{2} \sum_{i \neq j} w(\mathbf{r}_i - \mathbf{r}_j), \tag{A.1}$$

where $\hat{T}$ is the kinetic energy operator, $\hat{U}$ is an external potential containing the electrostatic interaction between the electrons and the nuclei, and $\hat{W}$ is the electron-electron interaction:

$$w(\mathbf{r}_i - \mathbf{r}_j) = \frac{1}{|\mathbf{r}_i - \mathbf{r}_j|} \tag{A.2}$$

The N electron wave functions $\Psi = \Psi(\mathbf{r}_1, \mathbf{r}_2, \ldots, \mathbf{r}_N)$ have to be antisymmetric because of the Pauli exclusion principle . The electron density is then given by

$$n(\mathbf{r}) = \int d^3\mathbf{r}_2 d^3\mathbf{r}_3 \ldots d^3\mathbf{r}_N |\Psi(\mathbf{r}, \mathbf{r}_2, \ldots, \mathbf{r}_N)|^2. \tag{A.3}$$

The Hamiltonian itself is determined by the external potential, Eq.(A.1), $H = \hat{H}[u(\mathbf{r})]$. The ground state energy of the system can be obtained from the variational principle,

$$E_0[u(\mathbf{r})] = \min_{\Psi} \left\langle \Psi \left| \hat{H}[u(\mathbf{r})] \right| \Psi \right\rangle. \tag{A.4}$$

Since the energy functional on the right hand side has a lower bound at the ground state wave function Ψ_0 ,

$$E_0[u(\mathbf{r})] | \Psi_0 \rangle = \hat{H}[u(\mathbf{r})] | \Psi_0 \rangle. \tag{A.5}$$

The Hohenberg-Kohn theorem [99] states the connection between the external potential and the ground state electron density: instead of searching for the whole ground state wave function, the calculation of the expectation value of physical variables only needs the determination of the electron density.

The first Hohenberg-Kohn theorem says that the external potential is a unique function of the ground state density. Two potentials, $u_1(\mathbf{r})$ and $u_2(\mathbf{r})$ are regarded to be different, if $u_1(\mathbf{r}) - u_2(\mathbf{r}) \neq$ const. This theorem states that for two different potentials the ground state electron density is also different, or in other words, for a given electron density $n(\mathbf{r})$ there is only one $u(\mathbf{r})$ potential for which $n(\mathbf{r})$ is the ground state electron density. This can be proven by reductio ad absurdum. Thus $n(\mathbf{r})$ determines the number of particles N and $u(\mathbf{r})$. The ground state energy now can be expressed as

$$E_0[n] = T[n] + U[n] + W[n] = \int d^3r\, n(\mathbf{r})u(\mathbf{r}) + F_{\text{HK}}[n], \qquad \text{(A.6)}$$

where the Hohenberg-Kohn functional is the functional Legendre transformation of the ground state energy, and equals $T[n] + W[n]$, i.e., equals the kinetic energy plus the electron-electron interaction.

The second Hohenberg-Kohn theorem provides the energy variational principle, and states that the exact ground state density $n_0(\mathbf{r})$ minimizes the energy functional $E_0[n]$, such that for any given n, $E_0[n_0] \leq E_0[n]$.

Strictly speaking this theorem stands only for so called v-representable densities (i.e., for a density, for which there exist a potential, for which in turn this density is the correct ground state density). But modifying the definition of the energy functional according to the constrained-search idea of Levy and Lieb [100] as

$$E[n] = \text{Min}_{\Psi \to n} \left\langle \Psi | \hat{H} | \Psi \right\rangle,$$

(i.e., search in the space of the antisymmetric wave functions, yielding the density n), the restriction of v-representable densities can be abandoned, and the Hohenberg-Kohn theorems stands for any N-representable densities.

However, these theorems still don't give explicit forms for the $F_{\text{HK}}[n]$ functional. This was solved by Kohn and Sham [101], who compared the interacting system to a non-interacting reference system, with the same electron density. They assumed,

that for the interacting electron system there exists a non-interacting one with an effective one-particle potential corresponding to the same electron density.

Since for the non-interacting electron gas the wave function can be written as a Slater determinant

$$\Psi^s(\mathbf{r}_1, \mathbf{r}_2, \ldots, \mathbf{r}_N) = \frac{1}{\sqrt{N!}} \det[\phi_i(r_k)],$$

the electron density is therefore given by

$$n^s = \sum_{i=1}^{N} \phi_i^*(r)\phi_i(r) \tag{A.7}$$

and the kinetic energy by

$$T^s = -\frac{\hbar^2}{2m} \sum_{i=1}^{N} \left\langle \phi_i(r) | \nabla^2 | \phi_i(r) \right\rangle. \tag{A.8}$$

The trick of Kohn and Sham was to decompose the energy functional of the interacting electron system into

$$E_0[n] = T[n] + U[n] + W[n] = T^s[n] + U[n] + E_H[n] + E_{\text{xc}}[n], \tag{A.9}$$

where the Hartree energy is given by

$$E_H[n] = \frac{1}{2} \int d^3\mathbf{r} \int d^3\mathbf{r}' \frac{n(\mathbf{r})n(\mathbf{r}')}{|\mathbf{r} - \mathbf{r}'|}, \tag{A.10}$$

and the remaining terms are collected in the so-called exchange-correlation energy:

$$E_{\text{xc}}[n] = T[n] - T^s[n] + W[n] - E_H[n]. \tag{A.11}$$

Using the second Hohenberg-Kohn theorem, which says that the ground state density n_0 minimizes the energy functional, and assuming the form in Eq.(A.7) for an orthonormal basis one gets

$$\frac{\delta(E_0[n] - \varepsilon_i(\int \phi_i^*(r)\phi_i(r) - 1))}{\delta\phi_i^*} = 0.$$

By expressing the derivatives in Eq.(A.9) by means of the equality,

$$(\frac{\delta}{\delta\phi_i^*} = \frac{\delta}{\delta n}\frac{\delta n}{\delta\phi_i^*} = \frac{\delta}{\delta n}\phi_i),$$

we get the Kohn-Sham equation:

$$\left(-\frac{\hbar^2}{2m}\nabla^2 + u(\mathbf{r}) + u_H(\mathbf{r}) + u_{\text{xc}}(\mathbf{r})\right)\phi_i(r) = \varepsilon_i\phi_i(r), \tag{A.12}$$

where the Hartree potential is given by

$$u_H(\mathbf{r}) = \int d^3\mathbf{r}' \frac{n(\mathbf{r}')}{|\mathbf{r}-\mathbf{r}'|}$$

and the exchange correlation potential by

$$u_{\text{xc}}(\mathbf{r}) = \frac{\delta E_{\text{xc}}[n]}{\delta n}. \tag{A.13}$$

Since the exact form of this functional derivative is not known, further approximations are needed such as the so-called Local Density Approximation (LDA),

$$E_{\text{xc}}[n] = \int d^3\mathbf{r}\,\varepsilon_{\text{xc}}(n(\mathbf{r}))n(\mathbf{r}), \tag{A.14}$$

in which $\varepsilon_{\text{xc}}[n]$ is the exchange correlation energy density of a homogeneous electron gas of density n. The exchange-correlation potential is then given by

$$u_{\text{xc}}(\mathbf{r}) = \varepsilon_{\text{xc}}(n(\mathbf{r})) + \frac{d\varepsilon_{\text{xc}}(n(\mathbf{r}))}{dn(\mathbf{r})}n(\mathbf{r}).$$

In the spinpolarized calculations we used the local spin density approximation (LSDA), where the spin up and spin down electrons have different density ($n_\uparrow(\mathbf{r})$ and $n_\downarrow(\mathbf{r})$ respectively), and for the exchange-correlation potential $\varepsilon_{\text{xc}}(n_\uparrow(\mathbf{r}), n_\downarrow(\mathbf{r}))$ as parametrized by Perdew and Zunger [102], based on the results of Monte Carlo simulations of Ceperley and Alder for the correlation energy of a homogenous electron gas [103].

A.1.1 Relativistic DFT

To include in particular spin-orbit effects a relativistic generalization of the DFT is needed. In the presence of a magnetic field (corresponding to a vector potential **A**) the Dirac Hamiltonian is given by

$$\hat{H} = c\hat{\alpha}\left(\frac{\hbar}{i}\nabla - e\mathbf{A}(\mathbf{r})\right) + \hat{\beta}\,\text{mc}^2 + V(\mathbf{r}) = -\text{ic}\,\hat{\alpha}\hbar\nabla + \hat{\beta}\,\text{mc}^2 - \text{ce}\,\hat{\beta}\gamma_\mu A_\mu, \tag{A.15}$$

where

$$\hat{\alpha}_i = \begin{pmatrix} 0 & \sigma_i \\ \sigma_i & 0 \end{pmatrix}, \quad \hat{\beta} = \begin{pmatrix} I_2 & 0 \\ 0 & -I_2 \end{pmatrix}, \quad \gamma_i = \hat{\beta}\hat{\alpha}_i(i=1,2,3), \quad \gamma_4 = \hat{\beta},$$

are the Dirac matrices, and

$$\sigma_1 = \begin{pmatrix} 0 & 1 \\ 1 & 0 \end{pmatrix}, \quad \sigma_2 = \begin{pmatrix} 0 & -i \\ i & 0 \end{pmatrix}, \quad \sigma_3 = \begin{pmatrix} 1 & 0 \\ 0 & -1 \end{pmatrix} \tag{A.16}$$

are the well known Pauli matrices. In Eq.(A.15) $A_\mu = (A_1, A_2, A_3, V)$ is the four component vector potential. In case of N electrons the Hamiltonian is of the following form:

$$H = T + W_{\text{ee}} + V_{\text{ext}},$$

where the kinetic term is defined by

$$T = \int \psi^+(\mathbf{r})(c\hat{\alpha} \cdot \hat{\mathbf{p}} + \hat{\beta}\, \text{mc}^2)\psi(\mathbf{r})d\mathbf{r},$$

with

$$\hat{\mathbf{p}} = \frac{\hbar}{i}\nabla$$

being the momentum operator, the electron-electron interaction by

$$W_{\text{ee}} = \frac{1}{2}\int d^3\mathbf{r}\int d^3\mathbf{r}'\frac{\varphi^+(\mathbf{r})\varphi^+(\mathbf{r}')\varphi(\mathbf{r})\varphi(\mathbf{r}')}{|\mathbf{r} - \mathbf{r}'|},$$

and the interaction of electrons with the external electromagnetic potential by

$$V_{\text{ext}} = -e\int J_\mu(\mathbf{r})A_\mu(\mathbf{r})d\mathbf{r}. \tag{A.17}$$

Here $J_\mu = \Psi^+\hat{\beta}\gamma_\mu\Psi$ is the relativistic four current.

In the relativistic density functional theory the four current takes up the role of the electron density. The Hohenberg-Kohn theorem can be proved similarly as in the nonrelativistic case: The ground state energy is a unique functional of the four component current. Expanding Eq.(A.17) in terms of the Gordon decomposition ([104], [105]) (using $\bar{\psi}^+ = \psi^+\hat{\beta}$ notation):

$$\mathbf{J} = \frac{1}{2m}\{\bar{\psi}^+(\mathbf{r})\hat{\mathbf{p}}\psi(\mathbf{r}) - \hat{\mathbf{p}}\bar{\psi}^+(\mathbf{r})\psi(\mathbf{r}) - 2e\mathbf{A}\bar{\psi}^+(\mathbf{r})\psi(\mathbf{r}) + \hbar\nabla \times \bar{\psi}^+(\mathbf{r})\sigma\psi(\mathbf{r})\},$$

which can be written in the form $\mathbf{J} = \nabla \times (\mathbf{L} + 2\mathbf{S})$. Neglecting $\mathbf{L}$ (i.e. the first 3 terms on rhs in the above equation), we get for the energy functional

$$E[J_\mu(\mathbf{r})] = T[J_\mu(\mathbf{r})] + W[J_\mu(\mathbf{r})] + \int (n(\mathbf{r})V(\mathbf{r}) - m(\mathbf{r})B(\mathbf{r}))\, d\mathbf{r},$$

with the magnetisation density

$$m(\mathbf{r}) = \frac{e\hbar}{2m}\psi^+(\mathbf{r})\hat{\beta}\sigma\psi(\mathbf{r}).$$

Assuming a non-interacting Kohn-Sham reference system, similarly to the non-relativistic case, the Dirac Kohn-Sham equation can be derived:

$$(c\hat{\alpha} \cdot \hat{\mathbf{p}} + \hat{\beta}\,\mathrm{mc}^2 + v_{\mathrm{eff}}(\mathbf{r}) - m(\mathbf{r})\mathbf{B}_{\mathrm{eff}}(\mathbf{r}))\psi_i = \varepsilon_i \psi_i \qquad (A.18)$$

with

$$v_{\mathrm{eff}}(\mathbf{r}) = V(\mathbf{r}) + \int d^3\mathbf{r}' \frac{n(\mathbf{r}')}{|\mathbf{r} - \mathbf{r}'|} + \frac{\delta E_{\mathrm{xc}}[n(\mathbf{r}), \mathbf{m}(\mathbf{r})]}{\delta n(\mathbf{r})},$$

$$\mathbf{B}_{\mathrm{eff}}(\mathbf{r}) = \mathbf{B}_{\mathrm{ext}}(\mathbf{r}) + \mathbf{B}_{\mathrm{exc}}(\mathbf{r}),$$

$$\mathbf{B}_{\mathrm{exc}}(\mathbf{r}) = \frac{\delta E_{\mathrm{xc}}[n(\mathbf{r}), \mathbf{m}(\mathbf{r})]}{\delta \mathbf{m}(\mathbf{r})},$$

$$n(\mathbf{r}) = \sum_{i=1}^{N} \psi_i^+(\mathbf{r})\psi_i(\mathbf{r}), \qquad m(\mathbf{r}) = \frac{e\hbar}{2m} \sum_{i=1}^{N} \psi_i^+(\mathbf{r})\hat{\beta}\sigma\psi_i(\mathbf{r}).$$

This equation has to be solved self-consistently for the electron and magnetisation density. As a first attempt to treat the exchange-correlation functional, the Local-Spin Density approximation (LSDA) was developed in order to approximate the exchange field $\mathbf{B}_{\mathrm{exc}}(\mathbf{r})$ by MacDonald et. al. [106].

Appendix A

KKR Scattering theory

A.1 The formal theory

The key quantity in the scattering theory is the Green's function, which is formally defined as the representation of the resolvent operator

$$\hat{G}(z) = (z - \hat{H})^{-1}, \tag{A.1}$$

where $\hat{H}$ is the Hamilton operator of the system, $z \in \mathfrak{C} \backslash \sigma(\hat{H})$ and $\sigma(\hat{H})$ is the spectrum of $\hat{H}$. In the spectral representation the Green's function reads as

$$G(z, \mathbf{r}, \mathbf{r}') = \sum_n \frac{\psi_n(\mathbf{r})\psi_n^*(\mathbf{r}')}{z - \varepsilon_n}. \tag{A.2}$$

It is also useful to define the side limits

$$G^{\pm}(\varepsilon) = G(\varepsilon^{\pm}) = \lim_{\delta \to +0} G(\varepsilon \pm i\delta). \tag{A.3}$$

If the system Hamiltonian is split into a reference (unperturbed) Hamiltonian plus a perturbation potential:

$$\hat{H} = \hat{H}_0 + \hat{V}, \tag{A.4}$$

then the resolvent can be expressed in terms of the unperturbed resolvent $G_0(z) = (z - H_0)^{-1}$ as

$$\hat{G}(z) = \hat{G}_0(z)(\hat{I} + \hat{V}\hat{G}(z)). \tag{A.5}$$

This equation is called the Dyson equation. Introducing the so-called transition operators (T-operators)

$$\hat{T}(z) = \hat{V} + \hat{V}\hat{G}(z)\hat{V}, \tag{A.6}$$

the Dyson equation reads

$$\hat{G}(z) = \hat{G}_0(z) + \hat{G}_0(z)\hat{T}(z)\hat{G}_0(z). \tag{A.7}$$

Thus knowing a representation of the free electron Green's function, the determination of the T-operator is practically equivalent with the determination of the Green's function. From the Green's function an expectation value of a physical quantity defined by a Hermitian one-particle operator $\hat{A}$ over the energy range $(\varepsilon_A, \varepsilon_B)$ is defined by the contour integral [12]:

$$A_{\mathrm{ab}} = -\frac{1}{\pi} \operatorname{Im} \int_{\curvearrowright} dz \operatorname{Tr}(\hat{A}\hat{G}(z)),$$

where $\curvearrowright$ means the integration over a semi circle contour in the upper complex semi-plane with the lower and upper limits ε_A and ε_B, respectively, e.g. the electron density is given by

$$\varrho(\mathbf{r}) = -\frac{e}{\pi} \operatorname{Im} \int_{\curvearrowright} dz \operatorname{Tr}(\hat{G}(z, \mathbf{r}, \mathbf{r})). \tag{A.8}$$

In terms of the side limits of the resolvent operator (A.3) the density of states DOS can be expressed as

$$n(\varepsilon) = \sum_n \operatorname{Tr}\{\delta(\varepsilon - \varepsilon_n)|n\rangle\langle n|\} = \mp\frac{1}{\pi} \operatorname{Tr}(\operatorname{Im}G^{\pm}(\varepsilon)). \tag{A.9}$$

Using the resolvent with the T-operator from this equation the Lloyd's formula for the integrated DOS can be derived [12]:

$$N(\varepsilon) = \int_{-\infty}^{\varepsilon} d\varepsilon' n(\varepsilon') = N_0(\varepsilon) + \frac{1}{\pi} \operatorname{Im} \operatorname{Tr}(\ln T^{\pm}(\varepsilon)). \tag{A.10}$$

A.2 Multiple scattering (KKR)

In the simple version of the Korringa-Kohn-Rostoker theory an ensemble of N atom is modeled by a set of individual scattering potentials. In this model the spherically symmetric potentials are centered at the lattice positions $\mathbf{R}_i (i = 1, \ldots, N)$.

$$V(\mathbf{r}) = \sum_{i=1}^N V_i(\mathbf{r}_i) \quad (\mathbf{r}_i = r - \mathbf{R}_i)$$

$$V_i(\mathbf{r}_i) = \begin{cases} V_i(r_i) & \text{if } |\mathbf{r}_i| < S_i \\ 0 & \text{otherwise} \end{cases} \tag{A.11}$$

In case of the so called muffin-tin approach the atomic spheres (with radius S_i) do not overlap. In the atomic sphere approximation (ASA) the radius is equal with the Wigner Seitz radius. In case of zero effective field the Dirac equation Eq.(A.18) can be written as

$$\hat{H}|\psi\rangle = \begin{pmatrix} (V(r) + \text{mc}^2)\hat{I}_2 & c\hat{\sigma}_r(\frac{\partial}{\partial r} + \frac{1}{r} - \frac{1}{r}\hat{\beta}\hat{K}) \\ c\hat{\sigma}_r(\frac{\partial}{\partial r} + \frac{1}{r} - \frac{1}{r}\hat{\beta}\hat{K}) & (V(r) - \text{mc}^2)\hat{I}_2 \end{pmatrix} |\psi\rangle = W|\psi\rangle, \qquad \text{(A.12)}$$

where $\hat{\sigma}_r = \hat{\mathbf{r}}\hat{\sigma}$ and we introduced the operator $\hat{K} = \hat{\sigma}\hat{\mathbf{L}} + \hbar\hat{I}_2$, which commutes with the Hamilton operator just as well as the square and z component of the total angular momentum operator $\hat{J}^2$ and $\hat{J}_z$. The common basis functions $\chi_{\kappa\mu}(\mathbf{r})$ are called the *spin spherical harmonics*.

$$\hat{J}^2|\chi_{\kappa\mu}\rangle = \hbar^2 j(j+1)|\chi_{\kappa\mu}\rangle \quad j = l \pm 1/2,$$

$$\widehat{J}_z|\chi_{\kappa\mu}\rangle = \hbar\mu|\chi_{\kappa\mu}\rangle \quad \mu = -j, \ldots j,$$

$$\hat{K}|\chi_{\kappa\mu}\rangle = -\hbar\kappa|\chi_{\kappa\mu}\rangle \quad \kappa = \begin{cases} l & \text{if } j = l - 1/2 \\ -l - 1 & \text{if } j = l + 1/2 \end{cases}.$$

The spin spherical harmonics can be expressed with the complex spherical harmonics $Y_l^{\mu-s}(\hat{r})$, and bispinor basis functions as

$$|\chi_{\kappa\mu}\rangle = \sum_{s=\pm 1/2} C(l, \kappa, 1/2|\mu - s, s)Y_l^{\mu-s}(\hat{r})\Phi_s, \qquad \text{(A.13)}$$

where $C(l, \kappa, 1/2|\mu - s, s)$ are the Clebsch-Gordan coefficients [12]. The relativistic free Green's function can then be written as [12]

$$G_0^r(\varepsilon, \mathbf{r}, \mathbf{r}') = -\text{ip}\frac{W + \text{mc}^2}{2\,\text{mc}^2}\sum_Q (h_Q^+(\varepsilon, \mathbf{r})j_Q(\varepsilon, \mathbf{r}')^\times\Theta(r-r') + j_Q(\varepsilon, \mathbf{r})h_Q^+(\varepsilon, \mathbf{r}')^\times\Theta(r'-r)),$$

$$\text{(A.14)}$$

where the relativistic quantum number $Q = (\kappa, \mu)$ and $\bar{Q} = (-\kappa, \mu)$, and the solutions of the free particle Dirac equation,

$$f_{\kappa\mu} = \begin{bmatrix} f_l(\frac{\text{pr}}{\hbar})\chi_{\kappa\mu}(\mathbf{r}) \\ \frac{\text{iS}_\kappa\,\text{pc}}{W+\text{mc}^2}f_{\bar{l}}(\frac{\text{pr}}{\hbar})\chi_{-\kappa\mu}(\mathbf{r}) \end{bmatrix} \qquad \text{(A.15)}$$

with $S_\kappa = \frac{\kappa}{|\kappa|}$, $\bar{l} = l - S_\kappa$ and $f_l = j_l, n_l, h_l$ being spherical Bessel, Neumann, and Hankel functions respectively, while

$$f_{\kappa\mu}(\varepsilon, \mathbf{r})^\times = \left[\; f_l(\tfrac{\mathrm{pr}}{\hbar})\chi_{\kappa\mu}(\mathbf{r})^+, \quad \tfrac{-\mathrm{i}S_\kappa\,\mathrm{pc}}{W+\mathrm{mc}^2} f_{\bar{l}}(\tfrac{\mathrm{pr}}{\hbar})\chi_{-\kappa\mu}(\mathbf{r})^+ \; \right]. \tag{A.16}$$

A general solution of Eq. (A.12) is of the form,

$$R_Q(\varepsilon, \mathbf{r}) = \sum_{Q'} \left[\begin{matrix} g_{Q'Q}(r)\chi_{Q'}(\mathbf{r}) \\ if_{Q'Q}(r)\chi_{\bar{Q}'}(\mathbf{r}) \end{matrix} \right]. \tag{A.17}$$

Inside the muffin-tin sphere the functions $g(r)$ and $f(r)$ are determined numerically by solving Eq. (A.12). Outside the muffin-tin sphere, where the potential is zero, the solutions can be expressed using the matrix elements of the single-site T operator, $t_{\mathrm{QQ}'}$ as

$$R_Q(\varepsilon, \mathbf{r}) = j_Q(\varepsilon, \mathbf{r}) - \mathrm{ip} \sum_Q h^+(\varepsilon, \mathbf{r})t_{\mathrm{QQ}'}(\varepsilon). \tag{A.18}$$

By using the condition that the solution of Eq.(A.17) and Eq.(A.18) smoothly join at the muffin-tin sphere S, we can get the single-site t matrix, $t_{\mathrm{QQ}'}(\varepsilon)$ [107].

For more scattering centers, the potential is the sum of the individual site potentials, Eq.(A.11), and the transition operator Eq.(A.6) is given by

$$\hat{T}(\varepsilon) = \sum_i V_i + \sum_{i,j} V_i \hat{G}_0(\varepsilon) V_j + \sum_{i,j,k} V_i \hat{G}_0(\varepsilon) V_j \hat{G}_0(\varepsilon) V_k + \ldots, \tag{A.19}$$

which can be expressed with the single-site t operators as

$$\hat{T}(\varepsilon) = \sum_i \hat{t}_i(\varepsilon) + \sum_{i \neq j} \hat{t}_i(\varepsilon)\hat{G}_0(\varepsilon)\hat{t}_j(\varepsilon) + \sum_{i \neq j, j \neq k} \hat{t}_i(\varepsilon)\hat{G}_0(\varepsilon)\hat{t}_j(\varepsilon)\hat{G}_0(\varepsilon)\hat{t}_k(\varepsilon) + \ldots. \tag{A.20}$$

Introducing the so-called scattering path operator (SPO), $\hat{\tau}_{\mathrm{ij}}(\varepsilon)$, as

$$\hat{\tau}_{\mathrm{ij}}(\varepsilon) = \hat{t}_i(\varepsilon)\delta_{\mathrm{ij}} + \hat{t}_i(\varepsilon)\hat{G}_0(\varepsilon) \sum_{k \neq j} \hat{\tau}_{\mathrm{ij}}(\varepsilon) \tag{A.21}$$

the transition operator and the resolvent can be expressed as

$$\hat{T}(\varepsilon) = \sum_{i,j} \hat{\tau}_{\mathrm{ij}}(\varepsilon), \tag{A.22}$$

and

$$\hat{G}(\varepsilon) = \hat{G}_0(\varepsilon) + \hat{G}_0(\varepsilon) \sum_{i,j} \hat{\tau}_{\mathrm{ij}}(\varepsilon)\hat{G}_0(\varepsilon). \tag{A.23}$$

Expressing these quantities in the basis of Bessel functions, Eq.(A.15), centered at the lattice positions, Eq (A.21) can be written in a supermatrix formalism as

$$\underline{\underline{\tau}}(\varepsilon) = \left(\underline{\underline{t}}(\varepsilon) - \underline{\underline{G}}_0(\varepsilon)\right)^{-1},\tag{A.24}$$

where double underline means matrices with site and angular momentum indices,

$$\underline{\underline{t}}(\varepsilon) = \{\underline{t}^i(\varepsilon)\delta_{\mathrm{ij}}\}, \quad \underline{\underline{\tau}}(\varepsilon) = \{\underline{\tau}^{\mathrm{ij}}(\varepsilon)\}, \quad \underline{\underline{G}}_0(\varepsilon) = \{\underline{G}_0^{\mathrm{ij}}(\varepsilon)\}\tag{A.25}$$

and single underlined quantities are matrices with momentum indices (Q,Q'). The matrix related to the Green's function is then given by

$$\underline{\underline{G}}(\varepsilon) = \underline{\underline{G}}_0(\varepsilon)(\underline{\underline{I}} - \underline{\underline{t}}(\varepsilon)\underline{\underline{G}}_0(\varepsilon))^{-1}.\tag{A.26}$$

Eqs.(A.24) and (A.26) are the fundamental equations of the Multiple Scattering Theory. The geometrical property of the system is contained in the so called bare structure constant $\underline{\underline{G}}_0(\varepsilon)$, and the (chemical) properties of the individual scatterers are comprised in $\underline{\underline{t}}(\varepsilon)$. The Green's function, Eq.(A.31), can then be written as [108]

$$G(\varepsilon, \mathbf{r}_i + \mathbf{R}_i, \mathbf{r}'_j + \mathbf{R}_j) = \sum_{Q,Q'}[Z_Q^i(\varepsilon, \mathbf{r}_i)\tau_{\mathrm{QQ'}}^{\mathrm{ij}}(\varepsilon)Z_{Q'}^j(\varepsilon, \mathbf{r}'_j)^+ -$$
$$-\delta_{\mathrm{ij}}(\Theta(\mathbf{r}_i - \mathbf{r}'_i)J_Q^i(\varepsilon, \mathbf{r}_i)Z_{Q'}^i(\varepsilon, \mathbf{r}'_i)^+ + \Theta(\mathbf{r}'_i - \mathbf{r}_i)Z_Q^i(\varepsilon, \mathbf{r}'_i)J_{Q'}^i(\varepsilon, \mathbf{r}_i)^+)],\tag{A.27}$$

where the regular and irregular scattering solutions are defined out of the muffin-tin sphere as

$$Z_Q^i(\varepsilon, \mathbf{r}_i) = \sum_{Q'}(t^i)_{\mathrm{QQ'}}^{-1}j_{Q'}^i(\varepsilon, \mathbf{r}_i) - \mathrm{iph}_Q^+(\varepsilon, \mathbf{r}_i),\tag{A.28}$$

and

$$J_Q^i(\varepsilon, \mathbf{r}_i) = j_Q^i(\varepsilon, \mathbf{r}_i)\tag{A.29}$$

respectively.

A.3 Screened KKR

The difficulty in the KKR theory is the long range character of the structure constants $\underline{\underline{G}}_0(\varepsilon)$. To overcome this computational difficulty Szunyogh et.al. introduced [11] the so-called Screened KKR method for layered systems. In this method first the structure constant of a reference system with a repulsive potential is calculated.

This reference system has a constant potential within the muffin-tin spheres by about 1-2 Ry above the valence band, which gives rise to an exponential fast decay of the structure constants [109].

The structural Green's function matrix for the reference (screened) system can be written as

$$\underline{\underline{G}}^r(\varepsilon) = \underline{\underline{G}}_0(\varepsilon)(\underline{\underline{I}} - \underline{\underline{t}}^r(\varepsilon)\underline{\underline{G}}_0(\varepsilon))^{-1}, \tag{A.30}$$

and that for the original system by Eq.(A.26). It can be seen that the original Green's function matrix of the system can be expressed by the screened one as

$$\underline{\underline{G}}(\varepsilon) = \underline{\underline{G}}^r(\varepsilon)(\underline{\underline{I}} - \Delta\underline{\underline{t}}(\varepsilon)\underline{\underline{G}}^r(\varepsilon))^{-1}, \tag{A.31}$$

where $\underline{\underline{\Delta t}}(\varepsilon) = \underline{\underline{t}}(\varepsilon) - \underline{\underline{t}}^r(\varepsilon)$, and the screened t^r matrices can be calculated analytically. Introducing the screened scattering path operator as

$$\underline{\underline{\tau}}_\Delta(\varepsilon) = (\Delta\underline{\underline{t}}(\varepsilon)^{-1} - \underline{\underline{G}}^r(\varepsilon))^{-1}, \tag{A.32}$$

Eq.(A.31) can further be expressed as

$$\underline{\underline{G}}(\varepsilon) = \Delta\underline{\underline{t}}(\varepsilon)^{-1}\underline{\underline{\tau}}_\Delta(\varepsilon)\Delta\underline{\underline{t}}(\varepsilon)^{-1} - \Delta\underline{\underline{t}}(\varepsilon)^{-1}. \tag{A.33}$$

From a similar equation for the physical quantities follows the equality between the screened and non-screened SPO-s,

$$\underline{\underline{\tau}}(\varepsilon) = \underline{\underline{t}}(\varepsilon)[\Delta\underline{\underline{t}}(\varepsilon)^{-1}\underline{\underline{\tau}}_\Delta(\varepsilon)\Delta\underline{\underline{t}}(\varepsilon)^{-1} + (\underline{\underline{t}}(\varepsilon)^{-1} - \Delta\underline{\underline{t}}(\varepsilon)^{-1})]\underline{\underline{t}}(\varepsilon). \tag{A.34}$$

Thus the SPO of the real system can be calculated from the screened SPO using the appropriate t matricies. Szunyogh et.al. used the screened KKR method for 2 dimensional translation invariant systems (first for free surfaces [11], later for thin multilayers [15]). In this case the atomic position vectors $\mathbf{R}_i$ can be written as

$$\mathbf{R}_{\mathrm{pi}} = \mathbf{C}_p + \mathbf{R}_{i\|}, \tag{A.35}$$

where $\mathbf{R}_{i\|} \in L_2$, and L_2 is the two dimensional translation group. C_p is the spanning vector of the layer p. Because of the two-dimensional translation invariance, it is straightforward to use a lattice Fourier transformation of the structure constant

$$\underline{\underline{G}}_0^{\mathrm{pq}}(\varepsilon, \mathbf{k}_\|) = \sum_{\mathbf{R}_{i\|}\in L_2} \underline{\underline{G}}_0(\varepsilon, \mathbf{C}_p - \mathbf{C}_q + \mathbf{R}_{i\|})e^{i\mathbf{k}_\|\mathbf{R}_{i\|}}, \tag{A.36}$$

$$\underline{\underline{\tau}}_{\Delta}(\varepsilon, \mathbf{k}_{\parallel}) = (\Delta \underline{\underline{t}}(\varepsilon)^{-1} - \underline{\underline{G}}^{r}(\varepsilon, \mathbf{k}_{\parallel}))^{-1}. \tag{A.37}$$

Because of the fast decay of the screened structure constant, it can be truncated for large layer-layer distances (usually truncated beyond 3 layers), and regarded as a block tridiagonal matrix, where the blocks are related to the so-called principal layers. The system can be partitioned into a semi-infinite left (L) and right part (R), and an in-between intermediate part (I), which is in the focus of interest. According to this grouping the inverse SPO matrix also split to blocks,

$$(\underline{\underline{\tau}}_{\Delta}(\varepsilon, \mathbf{k}_{\parallel}))^{-1} = \begin{pmatrix} (\underline{\underline{\tau}}_{\Delta}(\varepsilon, \mathbf{k}_{\parallel}))_{\mathrm{LL}}^{-1} & (\underline{\underline{\tau}}_{\Delta}(\varepsilon, \mathbf{k}_{\parallel}))_{\mathrm{LI}}^{-1} & \mathbf{0} \\ (\underline{\underline{\tau}}_{\Delta}(\varepsilon, \mathbf{k}_{\parallel}))_{\mathrm{IL}}^{-1} & (\underline{\underline{\tau}}_{\Delta}(\varepsilon, \mathbf{k}_{\parallel}))_{\mathrm{II}}^{-1} & (\underline{\underline{\tau}}_{\Delta}(\varepsilon, \mathbf{k}_{\parallel}))_{\mathrm{IR}}^{-1} \\ \mathbf{0} & (\underline{\underline{\tau}}_{\Delta}(\varepsilon, \mathbf{k}_{\parallel}))_{\mathrm{RI}}^{-1} & (\underline{\underline{\tau}}_{\Delta}(\varepsilon, \mathbf{k}_{\parallel}))_{\mathrm{RR}}^{-1} \end{pmatrix}, \tag{A.38}$$

where using the block-tridiagonal property of the above matrix, the inversion can be efficiently performed by using the method proposed by Godfrin [110]. The computation time of this inversion method scales linearly with the number of layers N. Compared to other methods, which show a N^3 scaling, this method saves a considerable computer time especially for large systems. The real space screened SPO can then be obtained in terms of an inverse Fourier transformation,

$$\underline{\underline{\tau}}_{\Delta}(\varepsilon, \mathbf{R}_{\mathrm{pi}} - \mathbf{R}_{\mathrm{qj}}) = \frac{1}{\Omega_{\mathrm{BZ}}} \int d\mathbf{k}_{\parallel}^2 \underline{\underline{\tau}}_{\Delta}(\varepsilon, \mathbf{k}_{\parallel}) e^{-i\mathbf{k}_{\parallel}(\mathbf{R}_{i\parallel} - \mathbf{R}_{j\parallel})}. \tag{A.39}$$

Appendix B

Coherent potential approximation (CPA)

The CPA is commonly used calculate configurational averaged quantities of chemically disordered systems. A good description of the single-site CPA impemented in the KKR formalism can be found in the paper of Butler [67]. In the present work we extended the single-site CPA formalism to the averaging for the continous variable of the local moment directions. In this appendix we describe this formalism. In the "direction"-CPA the probability density functional replaces the concentrations of the components in the original "chemical"-CPA.

The main idea of the CPA, is to regard a reference coherent (translational invariant) system, where the Green's fuction (and other physical quantities which are derived from it) are equal with the configurational average of the disordered system, i.e.

$$G_c = \langle G \rangle = \left(\prod_i \int d\hat{e}_i \right) P(\{\hat{e}\}) G(\{\hat{e}\}) \qquad (B.1)$$

equality holds, where $G(\{\hat{e}\})$ is the Green's function of a system in a configuration specified by $\{\hat{e}\}$. This equation can be formulated with the scattering path operators:

$$\tau_c = \prod_i \int d\hat{e}_i P(\{\hat{e}\}) \tau(\{\hat{e}\}) \qquad (B.2)$$

τ is regarded to be the scattering path operator (SPO) of a system, where the i-th site occupied by the local moment $\hat{e}_i$.

$$\underline{\tau}(\{\hat{e}\}) = (\underline{m}(\{\hat{e}\}) - G_0)^{-1}$$

where $\underline{m}(\{\hat{e}\})_{ij} = \delta_{ij} t(\hat{e}_i)^{-1}$.

$$\underline{\tau}(\{\hat{e}\}) = (\underline{m}_c - G_0 + \Delta\underline{m}(\{\hat{e}\}))^{-1}$$

where $\Delta\underline{m}(\{\hat{e}\})_{ij} = \delta_{ij}(t_i^{-1} - t_c^{-1})$. using that $\tau_c = (\underline{m}_c - G_0)^{-1}$

$$\underline{\tau}(\{\hat{e}\}) = \tau_c(1 + \Delta\underline{m}(\{\hat{e}\})\tau_c)^{-1}$$

splitting $\tau_c = \tau_c^d + \tau_c^o$ to diagonal and offdiagonal part:

$$\underline{\tau}(\{\hat{e}\}) = \tau_c\{\underline{1} + (1 + \Delta\underline{m}(\{\hat{e}\})\tau_c^d)^{-1}\Delta\underline{m}(\{\hat{e}\})\tau_c^o\}^{-1}(1 + \Delta\underline{m}(\{\hat{e}\})\tau_c^d)^{-1} \quad \text{(B.3)}$$

let's denote the diagonal matrix $(1 + \Delta\underline{m}(\{\hat{e}\})\tau_c^d)^{-1} = \underline{D}(\{\hat{e}\})$, where the diagonal elements $(\underline{D})_{ij} = \delta_{ij}D_i$

$$D_i = (1 + (t_i^{-1} - t_c^{-1})\tau_c^{ii})^{-1} \quad \text{(B.4)}$$

it is easy to see, that the expansion of $\underline{D}(\{\hat{e}\})$ is

$$\underline{D}(\{\hat{e}\}) = 1 - \Delta\underline{m}(\{\hat{e}\})\tau_c^d + \Delta\underline{m}(\{\hat{e}\})\tau_c^d\Delta\underline{m}(\{\hat{e}\})\tau_c^d - \ldots..$$

We can introduce the so called excess scattering matrix,

$$X(\{\hat{e}\}) = \underline{D}(\{\hat{e}\})\Delta m(\{\hat{e}\}) = \quad \Delta\underline{m}(\{\hat{e}\}) - \Delta\underline{m}(\{\hat{e}\})\tau_c^d\Delta\underline{m}(\{\hat{e}\}) +$$

$$+\Delta\underline{m}(\{\hat{e}\})\tau_c^d\Delta\underline{m}(\{\hat{e}\})\tau_c^d\Delta\underline{m}(\{\hat{e}\}) - \ldots . = \quad (D(\{\hat{e}\}) - 1)(\tau_c^d)^{-1} \quad \text{(B.5)}$$

What is also diagonal: $(\underline{X})_{ij} = \delta_{ij}X_i$ with

$$X_i = -((t_i^{-1} - t_c^{-1}) + \tau_c^{ii})^{-1}$$

so Eq.(B.3) reads:

$$\underline{\tau}(\{\hat{e}\}) = \tau_c\{\underline{1} + X(\{\hat{e}\})\tau_c^o\}^{-1}D(\{\hat{e}\})$$

what can be expanded as

$$\underline{\tau}(\{\hat{e}\}) = \tau_c\{D(\{\hat{e}\}) + X(\{\hat{e}\})\tau_c^o D(\{\hat{e}\}) + X(\{\hat{e}\})\tau_c^o X(\{\hat{e}\})\tau_c^o D(\{\hat{e}\}) + \ldots\} \quad \text{(B.6)}$$

In the single-site CPA the sites regarded to be independent, i.e. the probability splits to site-independent quantities, i.e.

$$P(\{\hat{e}\}) = \prod_i P(\hat{e}_i)$$

The essence of the singleCPA is demanding that

$$\int d\hat{e}_i X_i(\hat{e}_i)P(\hat{e}_i) = \underline{0} \quad \text{(B.7)}$$

i.e. $\langle X_i \rangle = 0$. From Eq.(B.5) follows, that this is equivalent with

$$\langle D_i \rangle = \underline{1}.$$

In this case writing back Eq.(B.6) to Eq.(B.2) we can average the terms separately, and we get, that beside the remaining zero order term, the terms from 1. up to 4. order in X dissappear through the averaging i.e.

$$\int \tau_c D(\{\hat{e}\}) P(\{\hat{e}\}) = \tau_c$$
$$\int \tau_c X(\{\hat{e}\}) \tau_c^o D(\{\hat{e}\}) P(\{\hat{e}\}) = \int \tau_c^{ij} X_j (1 - \delta_{jk}) \tau_c^{jk} D_k P(\{\hat{e}\}) = 0 \qquad \text{(B.8)}$$
$$\int \tau_c^{ij} X_j (1 - \delta_{jk}) \tau_c^{jk} X_k (1 - \delta_{kl}) \tau_c^{kl} D_l P(\{\hat{e}\}) = 0 \qquad \ldots.$$

from Eq.(B.7), but the fourth order term (and higher even order terms) don't disappear because terms containing $\langle X_i^2 \rangle \neq 0$ remains. With these terms the diagonals of Eq.(B.2) in this case reads

$$\tau_c^{ii} = \int d\hat{e}_i P(\hat{e}_i) \left\langle \tau^{ii} \right\rangle_{\hat{e}_i} \qquad \text{(B.9)}$$

where the restricted average of quantity A is defined as

$$\langle A \rangle_{\hat{e}_i} = \frac{\int \ldots \int A(\{\hat{e}\}) P_0(\{\hat{e}\}) \, d\hat{e}_1 \ldots d\hat{e}_{i-1} d\hat{e}_{i+1} \ldots d\hat{e}_N}{P_i(\hat{e}_i)}, \qquad \text{(B.10)}$$

and using Eq.(B.6) and (B.8) up to fourth order in X the restricted average of the SPO can be written as

$$\left\langle \tau^{ii} \right\rangle_{\hat{e}_i} = \tau_c^{ii} D_i(\hat{e}_i). \qquad \text{(B.11)}$$

Similarly can be seen, after a longer derivation, that if we restrict the local moment on two different sites, the restricted average is

$$\left\langle \tau^{ij} \right\rangle_{\hat{e}_i, \hat{e}_j} = D_i^t(\hat{e}_i) \tau_c^{ij} D_j(\hat{e}_j). \qquad \text{(B.12)}$$

where the t upper index means matrix transpose.

The use of single-site (mean-field) approximation is a weakness of the single-site CPA, it neglects the correlations between sites. The first attempts to go beyond the single-site CPA is given by Rowlands et.al. who give a cluster generalization of the CPA (so called Nonlocal-CPA) which takes into account the correlations (short range order) within a cluster [111][98].

Appendix C

Onsager Reaction Field approximation

As we wrote earlier, the DLM uses the mean-field approximation, and it is known, that it is exact only in the limit of the infinitely large coordination number. J. Staunton and B. Györffy [112] used the so-called Onsager Reaction Field (ORF) approximation to go beyond the mean-field approximation within the DLM. They successfully got a 1015K Curie temperature for Fe, which is a large improvement compared to the mean-field DLM results.

We demonstrate now the idea of the Onsager Reaction Field approximation on a simple 3 dimensional Heisenberg model. Starting from a Hamiltonian

$$H = \sum_{i \neq j} \frac{1}{2} \hat{s}_i J_{ij} \hat{s}_j + \sum_i B_i \hat{s}_i \qquad \text{(C.1)}$$

where J_{ij} are the exchange parameters, and B_i is the external magnetic field on site i. In the mean-field approximation the total Hamiltonian is constructed from independent one-site Hamiltonians:

$$H = \sum_i H_i,$$

with the $\hat{m}_j = \langle \hat{s}_j \rangle$ notation for the average moment using the approximation

$$\hat{s}_i J_{ij} \hat{s}_j = (\hat{m}_i + \hat{s}_i - \hat{m}_i) J_{ij} (\hat{m}_j + \hat{s}_j - \hat{m}_j) =$$

$$= \hat{s}_i J_{ij} \hat{m}_j + \hat{m}_i J_{ij} \hat{s}_j - \hat{m}_i J_{ij} \hat{m}_j + (\hat{s}_i - \hat{m}_i) J_{ij} (\hat{s}_j - \hat{m}_j)$$

and neglecting the last term we get for the one-site Hamiltonian:

$$H_i^{\mathrm{MF}} = \hat{s}_i \hat{h}_i - \frac{1}{2} \sum_j \hat{m}_i J_{ij} \hat{m}_j = \hat{s}_i \left(\sum_j J_{ij} \hat{m}_j + B_i \right) - \frac{1}{2} \hat{m}_i \sum_j J_{ij} \hat{m}_j \qquad \text{(C.2)}$$

The idea of the ORF is to add a correction term to the Weiss field

$$H_i^{\text{ORF}} = \hat{s}_i \hat{h}_i - \frac{1}{2} \sum_j \hat{m}_i J_{ij} \hat{m}_j = \hat{s}_i \left(\sum_j J_{ij} \hat{m}_j - \lambda_i \hat{m}_i + B_i \right) - \frac{1}{2} \hat{m}_i \sum_j J_{ij} \hat{m}_j$$

with a yet unknown parameter λ_i, which is the strength of the reaction field. In this case the average magnetisation (not writing out the $1/2 \hat{m}_i J_{ij} \hat{m}_j$ so called double counting term, which is just a constant shift)

$$m_i = \langle \hat{s}_i \rangle = \frac{\int \hat{s}_i e^{-\beta \hat{s}_i \hat{h}_i} d\hat{s}_i}{\int e^{-\beta \hat{s}_i \hat{h}_i} d\hat{s}_i} = -L(\beta h_i) \tag{C.3}$$

with $\beta = 1/\,\text{kT}$ and $L(x) = \frac{1}{x} - \coth(x)$ the ORF Weiss-field

$$m_i = -L\left(\beta \left[\sum_j J_{ij} m_j - \lambda m_i + B_i \right] \right) \tag{C.4}$$

From this the paramagnetic susceptibilty can be given as

$$\chi_{i,j} = \frac{\partial m_i}{\partial B_j} = -L'(x) \left(\beta \sum_k (J_{ik} - \lambda_i \delta_{ik}) \chi_{k,j} + \beta \delta_{ij} \right) \tag{C.5}$$

where $x = \beta \sum_j (J_{ij} - \lambda_i \delta_{ij}) m_j + \beta B_i$. In the paramagnetic state $m_i = 0$, therefore from the identity

$$\lim_{x \to o} L'(x) = -\lim_{x \to o}(\frac{1}{x^2} + 1 - \coth^2(x)) = -1/3$$

we get for the susceptibility

$$\chi_{i,j} = \frac{\beta}{3} \sum_k (J_{ik} - \lambda_i \delta_{ik}) \chi_{k,j} + \beta \delta_{ij}$$

In 3 dimensional translational invarinant system we can take the lattice Fourier transform:

$$\chi(\mathbf{q}) = \frac{1}{N} \sum_{i,j} \chi_{i,j} e^{i\underline{\mathbf{q}}(\underline{R}_i - \underline{R}_j)} \tag{C.6}$$

and using that

$$\frac{1}{N} \sum_{i,j} \left(\sum_k A_{ik} \chi_{k,j} \right) e^{i\mathbf{q}(\underline{\mathbf{R}}_i - \underline{\mathbf{R}}_j)} = A(\mathbf{q})\chi(\mathbf{q})$$

we get

$$\chi(\mathbf{q}) = \frac{\beta}{3}(J(\mathbf{q}) - \bar{\lambda})\chi(\mathbf{q}) + \beta, \tag{C.7}$$

where

$$\bar{\lambda} = \frac{1}{N} \sum_i \lambda_i. \tag{C.8}$$

Or reorganizing

$$\chi(\mathbf{q}) = 3 \left(\frac{3}{\beta} + \bar{\lambda} - J(\mathbf{q}) \right)^{-1}. \tag{C.9}$$

On the other hand, using Eq.C.3 we can calculate the diagonal part of the susceptibility from deriving the integral ratio, using that in case of neglecting the offdiagonal $\frac{\partial m_j}{\partial B_i}(i \neq j)$ terms

$$\frac{\partial(-\beta \hat{s}_i \hat{h}_i)}{\partial B_i} = -\beta \hat{s}_i \tag{C.10}$$

therefore

$$\chi_{\text{ii}} = \frac{\partial m_i}{\partial B_i} = \frac{-\beta \int \hat{s}_i \hat{s}_i e^{-\beta \hat{s}_i \hat{h}_i} d\hat{s}_i - \int \hat{s}_i e^{-\beta \hat{s}_i \hat{h}_i} d\hat{s}_i * \int \hat{s}_i e^{-\beta \hat{s}_i \hat{h}_i} d\hat{s}_i}{\left(\int e^{-\beta \hat{s}_i \hat{h}_i} d\hat{s}_i \right)^2} = -\beta[\langle \hat{s}_i \hat{s}_i \rangle - \langle \hat{s}_i \rangle \langle \hat{s}_i \rangle]$$

In the paramagnetc phase $\langle \hat{s}_i \rangle = 0$ and the first term is 1, because $\hat{s}_i$ unitary vector, therefore

$$\chi_{\text{ii}} = -\beta.$$

On the other hand from the inverse Fourier transformation

$$\chi_{\text{ii}} = \int \chi(\mathbf{q}) d\mathbf{q}$$

so from Eq.C.9 we get:

$$\int 3 \left(\frac{3}{\beta} + \bar{\lambda} - J(\mathbf{q}) \right)^{-1} d\mathbf{q} = -\beta. \tag{C.11}$$

The value of $\bar{\lambda}$ is still not determined yet. We get it from the condition, that at the Curie temperature (T_c) the $\mathbf{q} = 0$ susceptibility diverge

$$\lim_{T \to T_c} \chi(\mathbf{q} = 0) = \infty,$$

i.e., from Eq.C.9

$$\frac{3}{\beta} + \bar{\lambda} - J(\mathbf{0}) = 0. \tag{C.12}$$

writing this back to Eq.C.11 we get the Curie temperature:

$$\int \frac{1}{J(\mathbf{q}) - J(0)} d\mathbf{q} = \frac{\beta_c}{3}. \tag{C.13}$$

This formula is the same as the result of Random Phase Approximation (RPA) [113]. The RPA describes much better the magnetic structure than the mean field approximation. It was proven that the result of the RPA approximation for the magnetization-temperature dependence is very close to the exact solution of the Heisenberg model [114]. A similar derivation can be given for 2 dimensional Hesinberg model, where the i, j indices run over the two dimensional lattice sites, and $\mathbf{q}$ is a two dimensional Brillouin zone vector. The integral in Eq.C.13 diverge for 2 dimension, which would mean zero T_c which is in agreement with the Mermin-Wagner theorem, what says that there is no phase transition in the 2 dimensional isotropic Heisenberg model (notice that the Mean-field approximation gives finite Curie temperature, which is a large mistake). However taking into account the anisotropy energy as an addittive parameter to $J(\mathbf{q}) - J(0)$ the integral will be non divergent, and gives the inverse Curie temperature. This method was used by Pajda et.al. [115] to determine the T_c of magnetic overlayers on Cu(001) surface.

The ORF method sounds promising for the first sight, but if we want to use it to describe the magnetisation (or anisotropy) temperature dependence in magnetic thin films, we have serious problems

- The effect of the anisotropy is not solved yet.

- The result for $n = \infty$ and 1 layer is clear, but not for an intermediate n.

- How can we describe the ferromagnetic region ($T < T_c$) ? Is the λ temperature dependent?

Appendix D

Mean-field solution of the anisotropic Heisenberg model

Starting from an anisotropic Heisenberg Hamiltonian

$$H = -\frac{1}{2} \sum_{pq} \hat{e}_p \underline{J}_{pq} \hat{e}_q - \sum_p K_p \left(e_p^z \right)^2, \tag{D.1}$$

where $\hat{e}_p$ are the unitary spin vectors. The anisotropy of this Hamiltonian arise not only from the on-site anisotropy K_p, but also from the anisotropy of the exchange matrix $\underline{J}_{pq}$ which is no longer proportional to the unitary matrix for fix p and q layer index. For uniaxial anisotropy

$$\hat{x} \underline{J}_{pq} \hat{x} := J_{pq}^{\mathrm{xx}} = \hat{y} \underline{J}_{pq} \hat{y} := J_{pq}^{\mathrm{yy}} \neq J_{pq}^{\mathrm{zz}} := \hat{z} \underline{J}_{pq} \hat{z}. \tag{D.2}$$

In the mean field approximation the probability of a configuration splits to a product of site independent probabilities:

$$P(\{\hat{e}_i\}) = \prod_i P_i^{(\hat{n})} \left(\hat{e}_i \right) \tag{D.3}$$

The magnetisation of the p layer is:

$$m_p^z = \int e_z P_p^{(\hat{z})} \left(\hat{e} \right) d\hat{e} = L \left(-\beta h_p^{(\hat{z})} \right) \tag{D.4}$$

Beside this, for a first approximation neglecting the anisotropy the Weiss field can be given by (see appendix C) :

$$h_p^{(\hat{n})} = \sum_q J_{pq}^{\mathrm{nn}} m_q^n. \tag{D.5}$$

Therefore in order to get the magnetisation, the equation:

$$m_p^z = L\left(-\beta \sum_q J_{pq}^{zz} m_q^z\right) \tag{D.6}$$

should be solved self consistently for the layer dependent magnetisations, which on this level regarded to be direction independent, i.e. from Eq.D.6 the z index can be abandoned, and the averaged J_{pq} used as the Heisenberg exchange matrix.

The magnetic anisotropy i.e. the free-energy difference between the two different orientation of the averaged magnetisation ($\hat{m}_p \parallel \hat{x}$ and $\hat{m}_p \parallel \hat{z}$) can be expressed as

$$F_x - F_z = \langle H \rangle_x - \langle H \rangle_z - (TS_x - TS_z). \tag{D.7}$$

From the assumption of the orientation independent Weiss fields follows that the entropy difference vanish: $S_x - S_z = 0$. Thus the average of the Hamiltonian function (Eq. D.1) can be written as

$$\langle H_x \rangle = -\frac{1}{2} \sum_{pq} m_p^x J_{pq}^{xx} m_q^x - \sum_p K_p \left\langle \left(e_p^z\right)^2\right\rangle_x. \tag{D.8}$$

Here

$$\left\langle \left(e_p^z\right)^2 \right\rangle_z = 2\pi \int \cos^2 \vartheta \frac{\beta h_p^{\hat{z}}}{4\pi \sinh \beta h_p^{(\hat{z})}} \exp\left(-\beta h_p^{\hat{z}} \cos \vartheta\right) \sin \vartheta d\vartheta = \tag{D.9}$$

$$= \frac{2}{\left(\beta h_p^{\hat{z}}\right)^2} \quad -\frac{2}{\beta h_p^{\hat{z}}} \coth(\beta h_p^{\hat{z}}) + 1 = \frac{2}{\beta h_p^{\hat{z}}} L(-\beta h_p^{\hat{z}}) + 1 = \frac{2}{\beta h_p^{\hat{z}}} m_p^z + 1$$

and from symmetry considerations

$$\left\langle \left(e_p^z\right)^2 \right\rangle_x = \left\langle \left(e_p^x\right)^2 \right\rangle_z = \int \int \sin^2 \vartheta \cos^2 \varphi \frac{\beta h_p^{\hat{z}}}{4\pi \sinh \beta h_p^{(\hat{z})}} \exp\left(-\beta h_p^{\hat{z}} \cos \vartheta\right) \sin \vartheta d\vartheta d\varphi = \tag{D.10}$$

$$= \pi \int (1 - \cos^2 \vartheta) \frac{\beta h_p^{\hat{z}}}{4\pi \sinh \beta h_p^{(\hat{z})}} \exp\left(-\beta h_p^{\hat{z}} \cos \vartheta\right) \sin \vartheta d\vartheta = \frac{1}{2}\left(1 - \left\langle \left(e_p^z\right)^2\right\rangle_z\right), \tag{D.11}$$

therefore

$$\left\langle \left(e_p^z\right)^2 \right\rangle_z - \left\langle \left(e_p^z\right)^2 \right\rangle_x = \frac{3}{\beta h_p^{\hat{z}}} m_p^z + 1. \tag{D.12}$$

The magnetisation difference cause only a second order term, therefore as a first approximation the $m_p^x = m_p^z = m_p$ can be used, and we get for the magnetic

anisotropy:

$$F_x - F_z = \langle H_x \rangle - \langle H_z \rangle = -\frac{1}{2} \sum_{pq} m_p \left(J_{pq}^{xx} - J_{pq}^{zz} \right) m_q + \sum_p K_p \left(\frac{3}{\beta h_p} m_p + 1 \right) \quad \text{(D.13)}$$

where m_p is the soultion of Eq.D.6, and h_p can be get from Eq.D.5.

Bibliography

[1] E. Grochowski and R. Halem, "Technological impact of magnetic hard disk drives on storage systems," *IBM Systems Journal*, vol. 42, p. 338, 2003.

[2] G. Binasch, P. Grünberg, F. Saurenbach, and W. Zinn *Phys. Rev. B*, vol. 39, p. 4828, 1989.

[3] M. N. Baibich, J. M. Broto, A. Fert, F. N. Van Dau, F. Petroff, P. Eitenne, G. Creuzet, A. Friederich, and J. Chazelas, "Giant magnetoresistance of (001)fe/(001)cr magnetic superlattices," *Phys. Rev. Lett.*, vol. 61, pp. 2472–2475, Nov 1988.

[4] D. Weller, A. Moser, L. Folks, M. E. Best, W. Lee, M. Toney, M. Schwickert, U. Thiele, and M. Doerner *IEEE Trans. Magn.*, vol. 36, p. 10, 2000.

[5] E. Fullerton, D. Marguiles, M. Schabes, M. Carey, B. Gurney, and A. Moser, "Antiferromagnetically coupled magnetic media layers for thermally stable high-density recording," *Appl. Phys. Lett.*, vol. 77, p. 3806, 2000.

[6] T. McDaniel, W. Challener, and K. Sendur, "Issues of heat assisted perpendicular recording," *IEEE trans. Magn.*, vol. 39, p. 1972, 2003.

[7] H. Harmann, Y. C. Martin, and H. K. Wickramasinghe, "Thermally assisted recording beyond traditional limits," *Appl. Phys. Lett.*, vol. 84, p. 810, 2004.

[8] S. Wolf, A. Chtchelkanova, and D. Treger *IBM J. Res. and Dev.*, vol. 50, p. 101, 2006.

[9] W. Gallagher and S. Parkin, "Development of the magnetic tunnel junction mram at ibm," *IBM J. Res. and Dev.*, vol. 50, p. 5, 2006.

[10] R. Bez and A. Pirovano *Mat. Sci. Sem. Proc.*, vol. 7, p. 349, 2004.

[11] L. Szunyogh, B. Újfalussy, P. Weinberger, and J. Kollár, "Self-consistent localized kkr scheme for surfaces and interfaces," *Phys. Rev. B*, vol. 49, p. 2721, 1994.

[12] J. Zabloudil, R. Hammerling, L. Szunyogh, and P. Weinberger, *Electron scattering in solid matter*. Springer, 2004.

[13] P. Weinberger and L. Szunyogh *Comput. Mater. Sci.*, vol. 17, p. 414, 2000.

[14] C. Uiberacker, L. Szunyogh, B. Újfalussy, P. Weinberger, E. A., and P. Dederichs *Phil. Mag. B*, vol. 78, p. 423, 1998.

[15] L. Szunyogh, B. Újfalussy, and P. Weinberger *Phys. Rev. B*, vol. 51, p. 9552, 1995.

[16] L. Szunyogh, B. Újfalussy, C. Blaas, U. Pustogowa, C. Sommers, and P. Weinberger, "Oscillatory behavior of the magnetic anisotropy energy in $cu(100)/con$ multilayer systems," *Phys. Rev. B*, vol. 56, pp. 14036–14044, 1997.

[17] B. Lazarovits, L. Szunyogh, and P. Weinberger, "Fully relativistic calculation of magnetic properties of fe, co, and ni adclusters on ag(100)," *Phys. Rev. B*, vol. 65, p. 104441, 2002.

[18] B. Lazarovits, L. Szunyogh, and P. Weinberger, "Magnetic properties of finite co chains on pt(111)," *Phys. Rev. B*, vol. 67, p. 024415, 2003.

[19] C. Etz, B. Lazarovits, J. Zabloudil, R. Hammerling, B. Ujfalussy, L. Szunyogh, G. M. Stocks, and P. Weinberger, "Magnetic properties of feco nanoclusters on cu(100): Ab initio calculations," *Physical Review B (Condensed Matter and Materials Physics)*, vol. 75, p. 245432, 2007.

[20] B. L. Györffy, A. J. Pindor, J. B. Staunton, G. M. Stocks, and H. Winter *J. Phys. F*, vol. 15, p. 1337, 1985.

[21] J. Staunton, B. L. Györffy, G. M. Stocks, and J. Wadsworth *J. Phys.F: Met. Phys*, vol. 16, p. 1761, 1986.

[22] S. S. A. Razee, J. B. Staunton, L. Szunyogh, and B. L. Gyorffy, "Onset of magnetic order in fcc-fe films on cu(100)," *Phys. Rev. Lett.*, vol. 88, no. 14, p. 147201, 2002.

[23] S. S. A. Razee, J. B. Staunton, L. Szunyogh, and B. L. Györffy, "Local moments and magnetic correlations above the curie temperature in thin films on and embedded in nonmagnetic substrates: fe/cu(100), co/cu(100), and fe/w(100)," *Phys. Rev. B*, vol. 66, no. 9, p. 094415, 2002.

[24] J. Staunton, S. Razee, L. Szunyogh, and B. Györffy *Physica B.*, vol. 318, p. 316, 2002.

[25] L. Szunyogh and L. Udvardi *Phil. Mag. B.*, vol. 78, p. 617, 1998.

[26] P. Bruno, "Tight-binding approach to the orbital magnetic moment and magnetocrystalline anisotropy of transition-metal monolayers," *Phys. Rev. B*, vol. 39, pp. 865–868, 1989.

[27] P. Weinberger, P. Levy, J. Banhardt, L. Szunyogh, and B. Újfalussy *J.Phys.: Condens. Matter*, vol. 8, p. 7677, 1996.

[28] C. Blaas, P. Weinberger, L. Szunyogh, P. Levy, and C. Sommers *Phys. Rev. B*, vol. 60, p. 492, 1999.

[29] P. Weinberger and L. Szunyogh, "Ab initio characterization of the giant magnetoresistance in realistic spin valves," *Phys. Rev. B*, vol. 66, no. 14, p. 144427, 2002.

[30] S. Khmelevskyi, K. Palotás, L. Szunyogh, and P. Weinberger *Phys. Rev. B*, vol. 68, p. 012402, 2003.

[31] K. Palotás, B. Lazarovits, L. Szunyogh, and P. Weinberger, "Ab initio study of the electric transport in gold nanocontacts containing single impurities," *Phys. Rev. B*, vol. 70, p. 134421, 2004.

[32] D. A. Goodings *Physical Review*, vol. 132, p. 542, 1963.

[33] B. Raquet, M. Viret, E. Sondergard, O. Cespedes, and R. Mamy *Phys. Rev. B*, vol. 66, p. 024433, 2002.

[34] N. Mermin *Phys. Rev.*, vol. 137, p. A1441, 1965.

[35] U. Gupta and A. K. Rajagopal *Phys. Rev. A*, vol. 21, p. 20641, 1980.

[36] J. Hubbard *Phys. Rev. B*, vol. 19, p. 2626, 1979.

[37] H. Hasewaga *J. Phys. Soc. Japan*, vol. 46, p. 1504, 1979.

[38] R. P. Feynman *Phys. Rev.*, vol. 97, p. 660, 1955.

[39] B. Ginatempo and J. B. Staunton *J. Phy. F:Met. Phys.*, vol. 18, p. 1827, 1988.

[40] R. Mills, L. Gray, and T. Kaplan *Phys. Rev. B*, vol. 27, p. 3252, 1983.

[41] P. Lloyd *Proc. Phys. Soc.*, vol. 90, p. 207, 1967.

[42] L. Udvardi, L. Szunyogh, K. Palotás, and P. Weinberger, "First-principles relativistic study of spin waves in thin magnetic films," *Phys. Rev. B*, vol. 68, no. 10, p. 104436, 2003.

[43] H. Jansen *Phys. Rev. B*, vol. 59, p. 4699, 1999.

[44] G. Daalderop, P. Kelly, and M. Schuurmans *Phys. Rev. B*, vol. 41, p. 11919, 1990.

[45] X. D. Wang, R. Wu, D. Wang, and A. Freeman *PRB*, vol. 54, p. 61, 1996.

[46] A. Gonis, *Green Functions for Ordered and Disordered Systems*. North Holland, 1990.

[47] J. Kondo *Prog. Theor. Phys.*, vol. 32, p. 37, 1964.

[48] J. Ziman, *Electrons and Phonons*. Oxford University Press, 1960.

[49] G. K. White and S. Woods *Phil. Trans. Roy. Soc. London*, vol. A251, p. 273, 1958.

[50] B. Raquet, M. Viret, J. Broto, E. Sondergard, O. Cespedes, and R. Mamy *J. Appl. Phys.*, vol. 91, p. 8129, 2002.

[51] A. Fert and I. Campbell *Phys. Rev. Lett.*, vol. 21, p. 1190, 1968.

[52] A. Fert and I. Campbell *J. Phys. F: Metal Phys*, vol. 6, p. 849, 1976.

[53] A. Fert *J. Phys. F: Met. Phys*, vol. 1, p. L42, 1971.

[54] A. Fert *J. Phys. C: Solid St. Phys*, vol. 2, p. 1784, 1969.

[55] D.L.Mills, A. Fert, and I. Campbell *Phys. Rev. B*, vol. 4, p. 196, 1971.

[56] A. Vernes, H. Ebert, and J. Banhart *Computational Materials Science*, vol. 10, p. 221, 1998.

[57] P. de Gennes and J. Friedel *J. Phys. Chem. Solids*, vol. 4, p. 71, 1958.

[58] P. Craig, W. Goldburg, T. Kitchens, and J. Budnick *Phys. Rev. Lett.*, vol. 19, p. 1334, 1967.

[59] M. Fisher and J. Langer *Phys. Rev. Lett.*, vol. 20, p. 665, 1968.

[60] C. Haas *Phys. Rev.*, vol. 168, p. 531, 1968.

[61] Y. Nishino, S. Inoue, S. Asano, and N. Kawamiya *Phys. Rev. B*, vol. 48, p. 13607, 1993.

[62] F. Matsakura, H. Ohno, A. Shen, and Y. Sugawara *Phys. Rev. B*, vol. 57, p. R2037, 1998.

[63] A. Esch, L. Bockstal, J. Boeck, G. V. A. Steenbergen, P. Wellmann, and G. Borghs *Phys. Rev. B*, vol. 56, p. 13103, 1997.

[64] M. Kataoka *Phys. Rev. B*, vol. 63, p. 134435, 2001.

[65] R. Kubo *j. Phys. Soc. Japan*, vol. 12, p. 570, 1957.

[66] R. Kubo *Rep. Prog. Phys*, vol. 29, p. 255, 1966.

[67] W. H. Butler *Phys. Rev. B*, vol. 34, p. 3260, 1985.

[68] H. B. Callen and E. Callen *J. Phys. Chem. Solids*, vol. 27, p. 1271, 1966.

[69] L. W. S.H. Vosko and M. Nusair *Can. J. Phys.*, vol. 58, p. 1200, 1980.

[70] D. Johnson *Phys. Rev. B*, vol. 38, p. 12807, 1988.

[71] J. B. Staunton, S. Ostanin, S. S. A. Razee, B. L. Gyorffy, L. Szunyogh, B. Ginatempo, and E. Bruno, "Temperature dependent magnetic anisotropy in metallic magnets from an ab initio electronic structure theory: $l1$-ordered fept," *Phys. Rev. Lett.*, vol. 93, p. 257204, 2004.

[72] O. Mryasov, U. Nowak, K. Guslienko, and R. Chantrell *Europhys. Lett.*, vol. 69, p. 805, 2005.

[73] S. Okamoto, N. Kikuchi, O. Kitakami, T. Miyazaki, Y. Shimada, and K. Fukamichi, "Chemical-order-dependent magnetic anisotropy and exchange stiffness constant of fept (001) epitaxial films," *Phys. Rev. B*, vol. 66, p. 024413, 2002.

[74] J. B. Staunton, L. Szunyogh, A. Buruzs, B. L. Gyorffy, S. Ostanin, and L. Udvardi, "Temperature dependence of magnetic anisotropy: An ab initio approach," *Physical Review B*, vol. 74, p. 144411, 2006.

[75] H. Shima, K. Oikawa, A. Fujita, K. Fukamichi, K. Ishida, and A. Sakuma, "Lattice axial ratio and large uniaxial magnetocrystalline anisotropy in $l1$ -type fepd single crystals prepared under compressive stress," *Phys. Rev. B*, vol. 70, no. 22, p. 224408, 2004.

[76] P.Bruno, "Physical origins and theoretical models of magnetic anisotropy," in *Magnetismus von Festkörpern und grenzflächen, 24. IFF-Ferienkurs* (P. Dederichs, P. Gru ́nberg, and W. Zinn, eds.), pp. 24.1–24.28, Forschungszentrum Julich, 1993.

[77] F. Huang, M. T. Kief, G. J. Mankey, and R. F. Willis *Phys. Rev. B*, vol. 49, p. 3962, 1994.

[78] G. J. Mankey, S. Wu, F. O. Schumann, F. Huang, M. T. Kief, and R. Willis *J. Vac. Sci. Technol.*, vol. 13(3), p. 1531, 1995.

[79] L. Szunyogh and L. Udvardi *J. Magn. Magn. Mater.*, vol. 198-199, p. 537, 1999.

[80] S. Wu, G. J. Mankey, F. O. Schumann, and R. Willis *J. Vac. Sci. Technol. B.*, vol. 14(4), p. 3189, 1996.

[81] P.Bruno *Phys. Rev. B*, vol. 43, p. 6015, 1991.

[82] M. Pajda, J. Kudrnovský, I. Turek, V. Drchal, and P. Bruno, "Oscillatory curie temperature of two-dimensional ferromagnets," *Phys. Rev. Lett.*, vol. 85, pp. 5424–5427, 2000.

[83] P. Jensen and K. Bennemann *Surf. Sci. Rep.*, vol. 61, p. 129, 2006.

[84] L. Udvardi, L. Szunyogh, A. Vernes, and P. Weinberger *Philos. Mag. B.*, vol. 81, p. 613, 2001.

[85] L. Dzyaloshinskii *J. Phys. Chem. Solids*, vol. 4, p. 241, 1958.

[86] T. Moriya, "Anisotropic superexchange interaction and weak ferromagnetism," *Phys. Rev.*, vol. 120, pp. 91–98, 1960.

[87] M. Bode, M. Heide, K. von Bergmann, P. Ferriani, S. Heinze1, G. Bihlmayer2, A. Kubetzka1, O. Pietzsch, S. Blgel, and R. Wiesendanger, "Chiral magnetic order at surfaces driven by inversion asymmetry," *Nature*, vol. 447, p. 190, 2007.

[88] T. Moriya, "New mechanism of anisotropic superexchange interaction," *Phys. Rev. Lett.*, vol. 4, p. 228, 1960.

[89] A. Liechtenstein, M. Katsnelson, V. P. Antropov, and V. Gubanov *J. Magn. Magn. Mat.*, vol. 67, p. 65, 1987.

[90] A. Barthelemy, A. Fert, J. Contour, and M. Bowen *J. Magn. Magn. Mat.*, vol. 242, p. 68, 2002.

[91] D. Tripathy, A. O. Adeyeye, and S. Shannigrahi *Phys. Rev. B*, vol. 75, p. 012403, 2007.

[92] K. Palotás, B. Lazarovits, L. Szunyogh, and P. Weinberger *Phys. Rev. B*, vol. 67, p. 174404, 2003.

[93] M. Stearns, *Landolt-Bornstein New Series - Group III Condensed Matter - 19A*. Springer, 1986.

[94] M. Lezaic, P. Mavropoulos, and S. Blügel *Appl. Phys. Lett.*, vol. 90, p. 082504, 2007.

[95] R. Weiss and A. Marotta *J. Phys. Chem. Solids*, vol. 9, p. 302, 1959.

[96] W. Borgiel, D. Stysiak, M. Gonsion, and M. Lipowczan *Journal of Alloys and Compounds*, vol. 442, p. 139, 2007.

[97] P. R. Tulip, J. B. Staunton, S. Lowitzer, D. Kodderitzsch, and H. Ebert, "Theory of electronic transport in random alloys with short-range order: Korringa-kohn-rostoker nonlocal coherent potential approximation," *Physical Review B (Condensed Matter and Materials Physics)*, vol. 77, no. 16, p. 165116, 2008.

[98] D. A. Rowlands, J. B. Staunton, and B. L. Györffy, "Korringa-kohn-rostoker nonlocal coherent-potential approximation," *Phys. Rev. B*, vol. 67, no. 11, p. 115109, 2003.

[99] P. Hohenberg and W. Kohn *Phys. Rev.*, vol. 136, p. B864, 1964.

[100] M. Levy *Phys. Rev. A*, vol. 26, p. 1200, 1982.

[101] W. Kohn and L. J. Sham *Phys. Rev.*, vol. 140, p. A1133, 1965.

[102] J. P. Perdew and A. Zunger *Phys. Rev. B*, vol. 23, p. 5048, 1981.

[103] D. Ceperley and B. Alder *Phys. Rev. Lett.*, vol. 45, p. 566, 1980.

[104] P. Strange, *Relativistic Quantum mechanics*. Cambridge University Press, 1998.

[105] A. K. Rajagopal and J. Callaway *Phys. Rev. B*, vol. 7, p. 1912, 1973.

[106] A. MacDonald, J. Daams, S. H. Vosko, and D. D. Koelling *Phys. Rev. B*, vol. 25, p. 713, 1981.

[107] P. Weinberger, *Electron Scattering Theory for Ordered and Disordered Matter*. Clarendon Press, Oxford, 1990.

[108] J. Faulkner and G. Stocks *Phys. Rev. B*, vol. 21, p. 3222, 1980.

[109] R. Zeller, P. Dederics, B. Újfalussy, L. Szunyogh, and P. Weinberger *Phys. Rev. B*, vol. 52, p. 8807, 1995.

[110] E. Godfrin *J. Phys.:Condens. Matter*, vol. 3, p. 7843, 1991.

[111] D. A. Rowlands, A. Ernst, B. L. Györffy, and J. B. Staunton, "Density functional theory for disordered alloys with short-range order: Systematic inclusion of charge-correlation effects," *Physical Review B (Condensed Matter and Materials Physics)*, vol. 73, no. 16, p. 165122, 2006.

[112] J. Staunton and B. L. Györffy *Phys. Rev. Lett.*, vol. 69, p. 371, 1992.

[113] R. Tahir-Kheli and D. T. Haar *Phys. Rev.*, vol. 127, p. 88, 1962.

[114] A. Ecker, P. Fröbrich, P. Jensen, and P. Kuntz *J. Phys.: Condens. Matter*, vol. 11, p. 1557, 1999.

[115] M. Pajda, J. Kudrnovský, I. Turek, V. Drchal, and P. Bruno, "Ab initio calculations of exchange interactions, spin-wave stiffness constants, and curie temperatures of fe, co, and ni," *Phys. Rev. B*, vol. 64, no. 17, p. 174402, 2001.

Acknowledgement

that I could achieve the PhD studies.

Publications

Publications connected to my PhD work

1. A. Buruzs, L. Szunyogh, L. Udvardi, P. Weinberger and J.B. Staunton ,
   Temperature dependent magneto-crystalline anisotropy of thin films: A relativistic disordered local moment approach
   Journal of Magnetism and Magnetic Materials, **316**, (2007) e371-e373

2. J.B. Staunton, L. Szunyogh, A. Buruzs, B.L. Györffy, S. Ostanin, L. Udvardi,
   Temperature dependence of magnetic anisotropy: An ab initio approach
   Phys. Rev. B **74**, 144411 (2006)

3. L. Udvardi, A. Antal, L. Szunyogh, A. Buruzs and P. Weinberger,
   Magnetic pattern formation on the nanoscale due to relativistic exchange interactions
   Physica B: Condensed Matter, **403** , 402 (2007)

4. A. Buruzs, P. Weinberger, L. Szunyogh, L. Udvardi, P. I. Chleboun, A. M. Fischer, and J. B. Staunton,
   Ab initio theory of temperature dependence of magnetic anisotropy in layered systems: Applications to thin Co films on Cu(100)
   Phys. Rev. B **76**, 064417. (2007)

5. A. Buruzs, L. Szunyogh and P. Weinberger,
   Ab initio theory of temperature dependent magneto-resistivity
   sent to Phil. Mag. B.

Further publications

6. Peter Deák, Adam Gali, A. Sólyom, Adam Buruzs and Thomas Frauenheim
   Electronic structure of boron-interstitial clusters in silicon
   J. Phys.: Condens. Matter **17** 2141-2153 (2005)

7. P. Deák, A. Buruzs, A. Gali, and T. Frauenheim,
   Strain-Free Polarization Superlattice in Silicon Carbide: A Theoretical Investigation
   Phys. Rev. Lett. **96**, 236803 (2006)

Conference presentations and seminars

8. Talk *'Determination of electronic properties of layer defects in SiC using quantum mechanical calculations'* (in hungarian language)
   Scientific Student's Conference at Technical University of Budapest (2.place on the championship), November 9. 2004 Budapest

9. Poster *'Temperature dependent magneto-crystalline anisotropy of thin films: a relativistic Disordered Local Moment approach'*
   JEMS conference, June 26.-30. 2006, San Sebastian, Spain

10. Talk *'Temperature dependent magnetic anisotropy of nanostructures: Theoretical study with Relativistic Disordered Local Moments theory'*
    "New Developments in Surface Science" seminar (CMS), May 31. 2007, Technical University of Vienna, Austria

11. Talk *'Temperature dependent magnetic anisotropy and electrical conductivity of thin films and bulk ferromagnets, Theoretical study with the Relativistic Disordered Local Moments theory'*
    International Conference on Computational Materials Science Febr 4. 2008, Cocoyoc , Mexico

Curriculum Vitae

Personal data:

name:	Ádám Buruzs
address:	Institut fuer Allgemeine Physik, Technische Universitaet Wien, Getreidemarkt 9/134, A-1060 Vienna, Austria
born:	November 28, 1981 in Szeged, Hungary
nationality:	Hungary
marital status:	unmarried, no children yet
languages:	Hungarian, English, German

Basic Education:

1988-1992	elementary school in Szeged
Sep 1992 – Jun 2000	grammar-school in Szeged

Studies:

Undergraduate studies:

Sept 2000 - Jun 2005	Technical Physics at the Technical University of Budapest, Hungary
Sept 2003 - Sept 2004	Assistent at "Department of Differential equations"
Jan 2004 - June 2005	diploma thesis "Investigation of electronic properties of layer defects in SiC semiconductors with ab initio computer simulations"
July 2004 & Febr. 2005	Stay at University of Paderborn (Germany) Fachbereit der theoretische Physik work on computer simulations of SiC.
August 2004	Stay at EPFL (Lausanne) in group of László Forró work on superconductor transport measurements
July 2005	diploma degree

Postgraduate studies:

since Oct 2005	doctoral study of Technical Sciences-physics, member of the Science College at CMS supervisor Prof. Dr. Laszlo Szunyogh and Univ.-Prof. Dr. Peter Weinberger, Institut für Allgemeine Physik